Algorithmes de traitement d'image pour l'estimation des caractéristiques locales de la diffusion.

Orateur : **D. Tschumperlé**

Travail en collaboration avec **Haz-Edine Assemlal** and **Luc Brun**

GREYC-ENSICAEN (CNRS UMR 6072), CAEN, FRANCE

JIRNFI'2009,
Septembre 2009

Outline

1. Context
2. DTI model : Diffusion Tensor Imaging
3. QBI model : Q-Ball Imaging
4. Measuring the PDF : DSI and Multi Q-Ball
5. Conclusions & Perspectives

Diffusion MRI: Brownian Motion

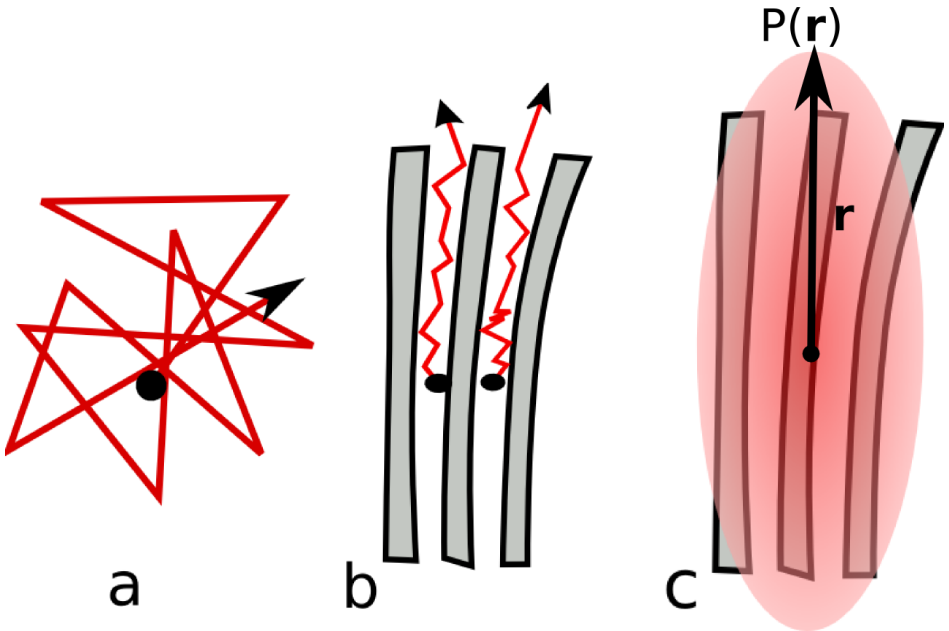

a: Brownian motion of water molecules
b: Constraints due to body internal structures
c: Signal = Local macroscopic diffusion

Objective

To estimate the probability P of the macroscopic displacement $\mathbf{p}$ during a diffusion time dt.

Signal acquisition

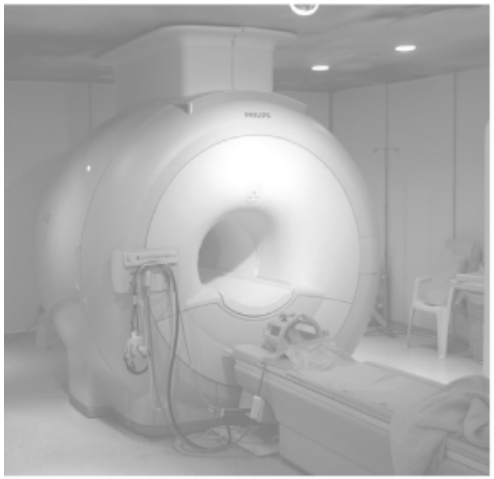

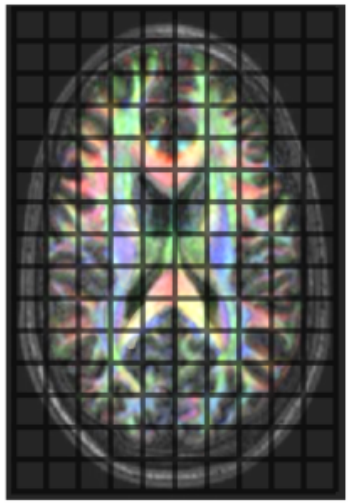

Figure: Diffusion MRI acquisition steps.

Signal acquisition

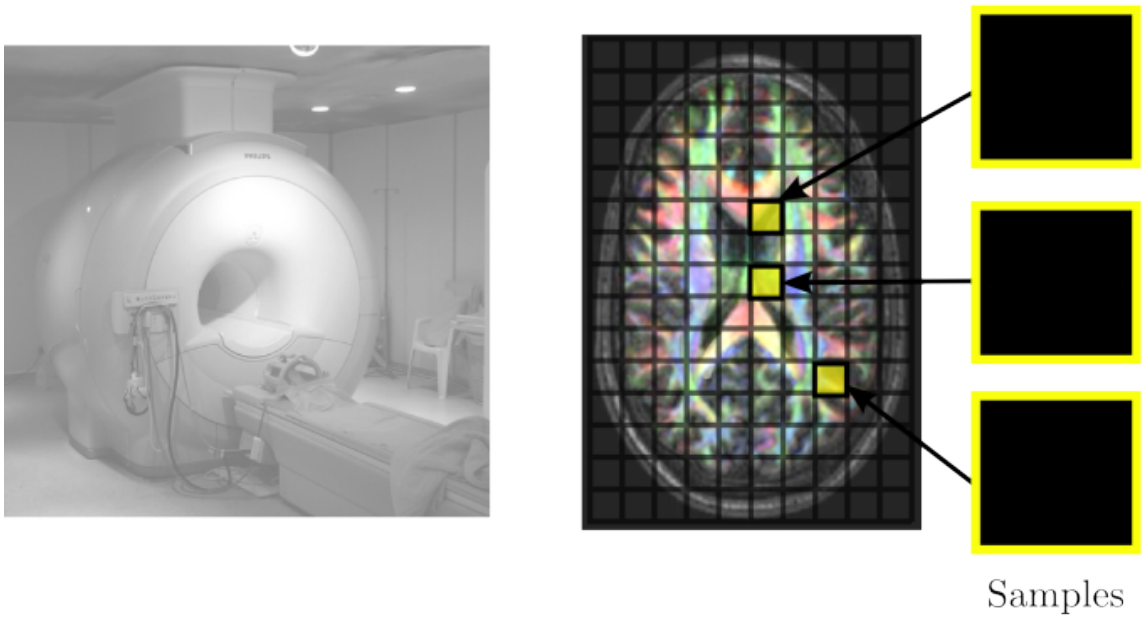

Figure: Diffusion MRI acquisition steps.

Signal acquisition

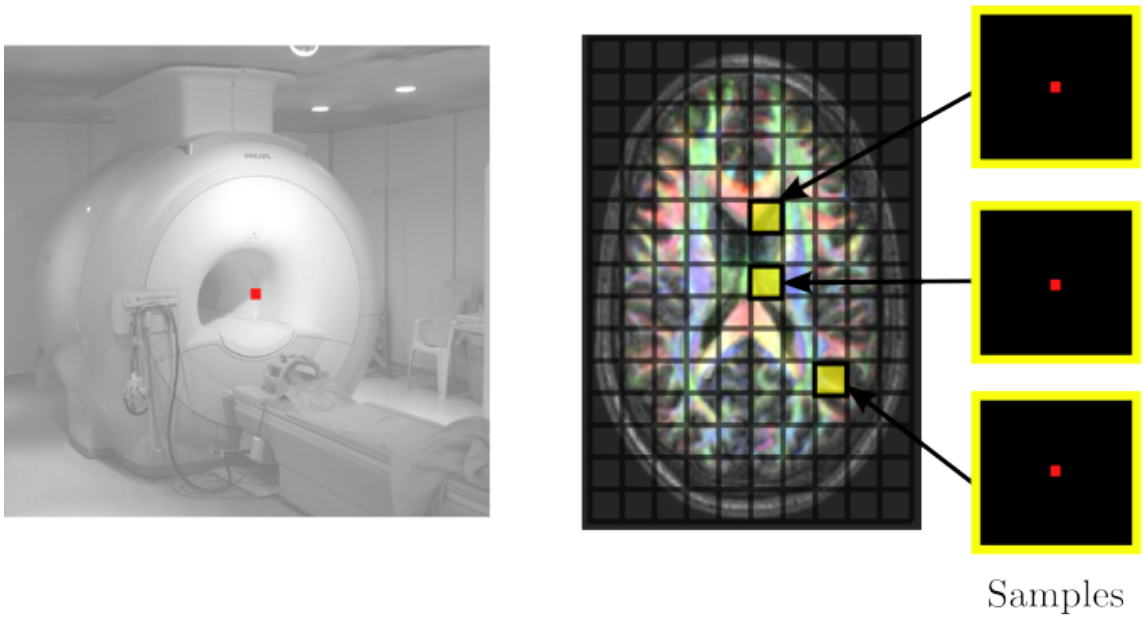

Figure: Diffusion MRI acquisition steps.

Signal acquisition

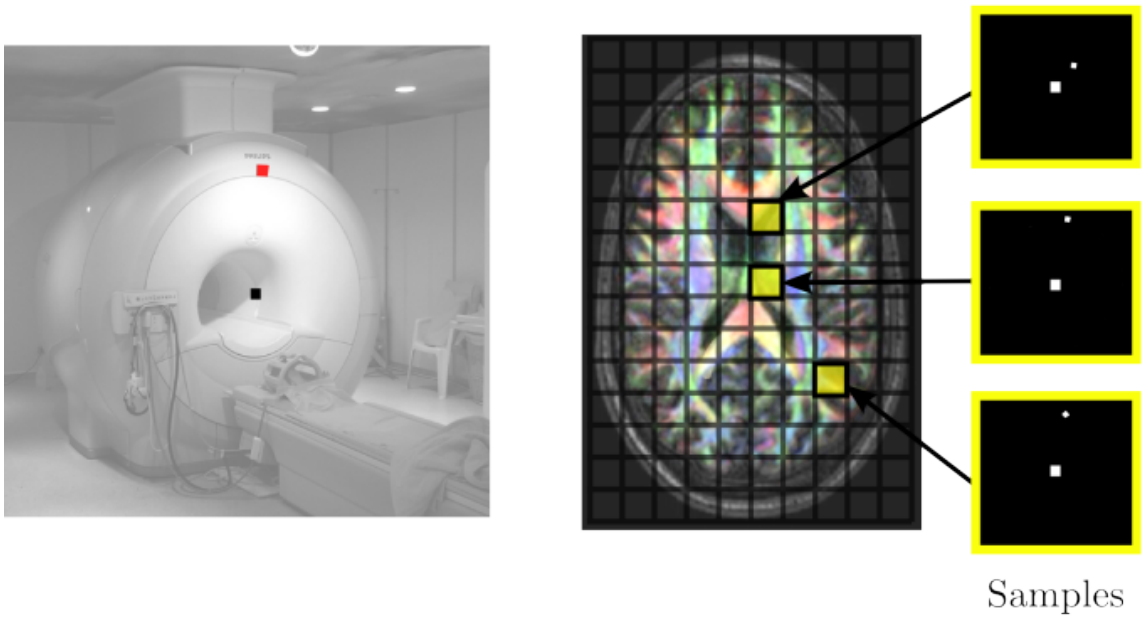

Figure: Diffusion MRI acquisition steps.

Signal acquisition

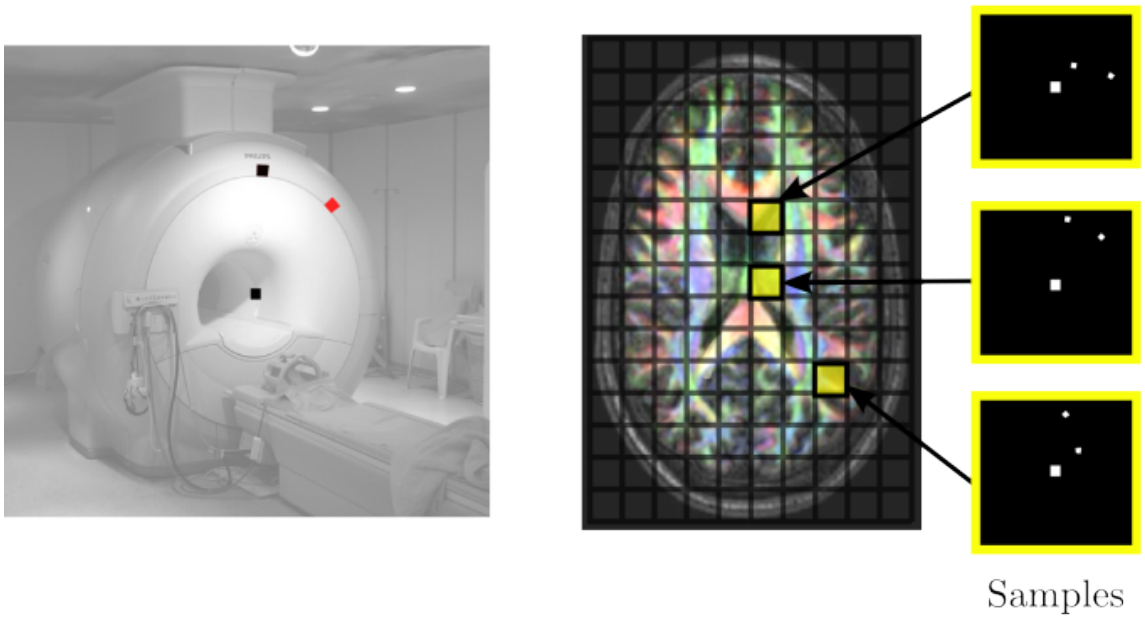

Figure: Diffusion MRI acquisition steps.

Signal acquisition

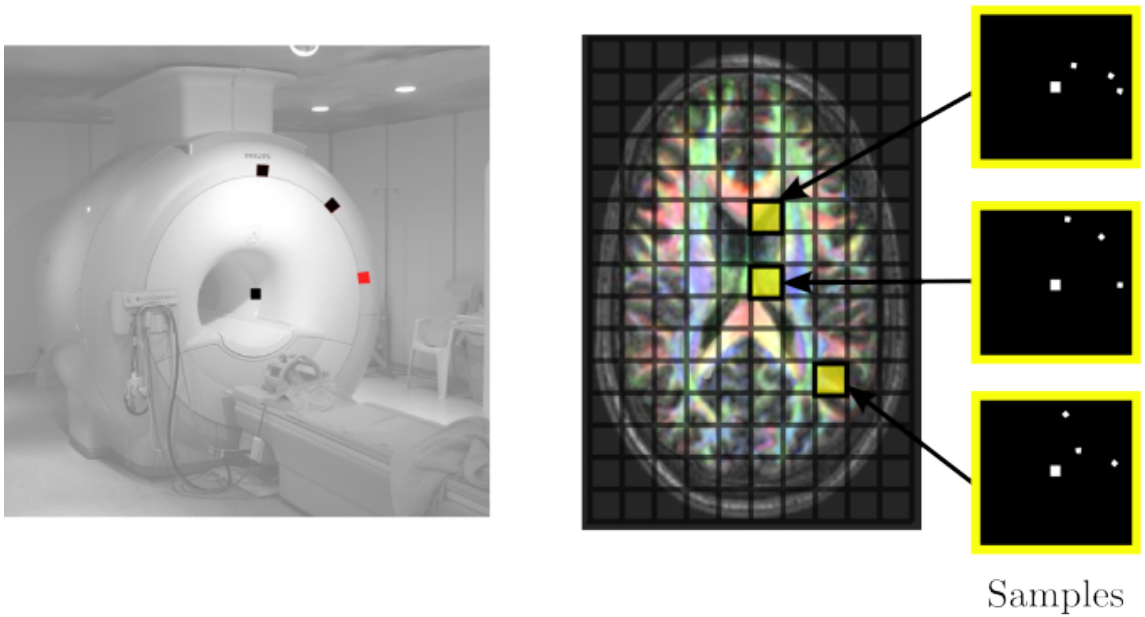

Figure: Diffusion MRI acquisition steps.

Signal acquisition

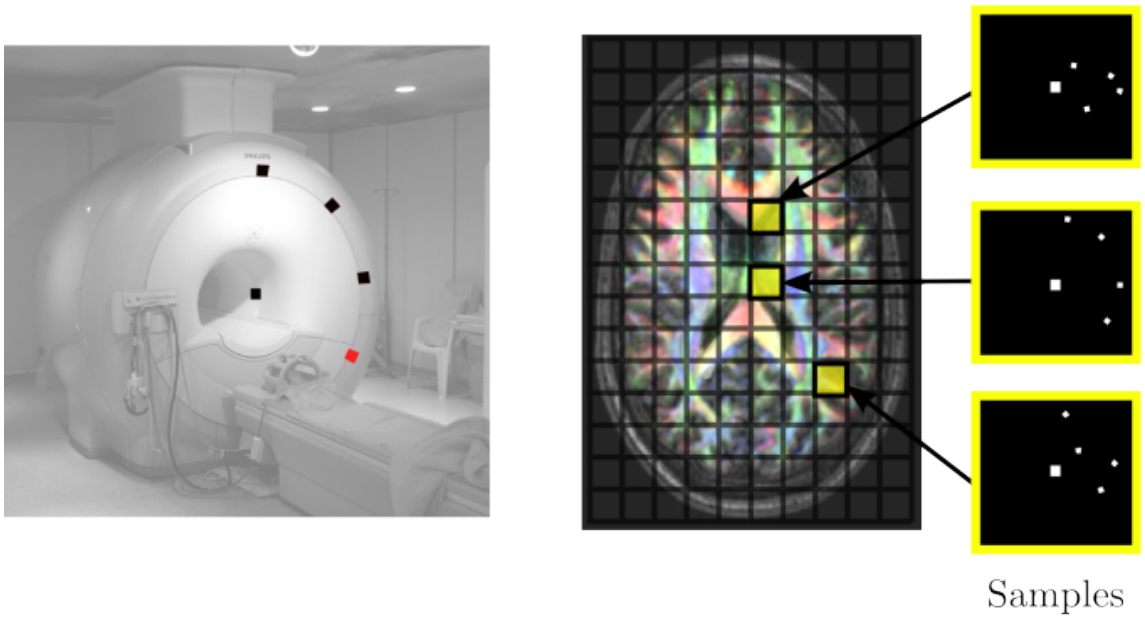

Figure: Diffusion MRI acquisition steps.

Signal acquisition

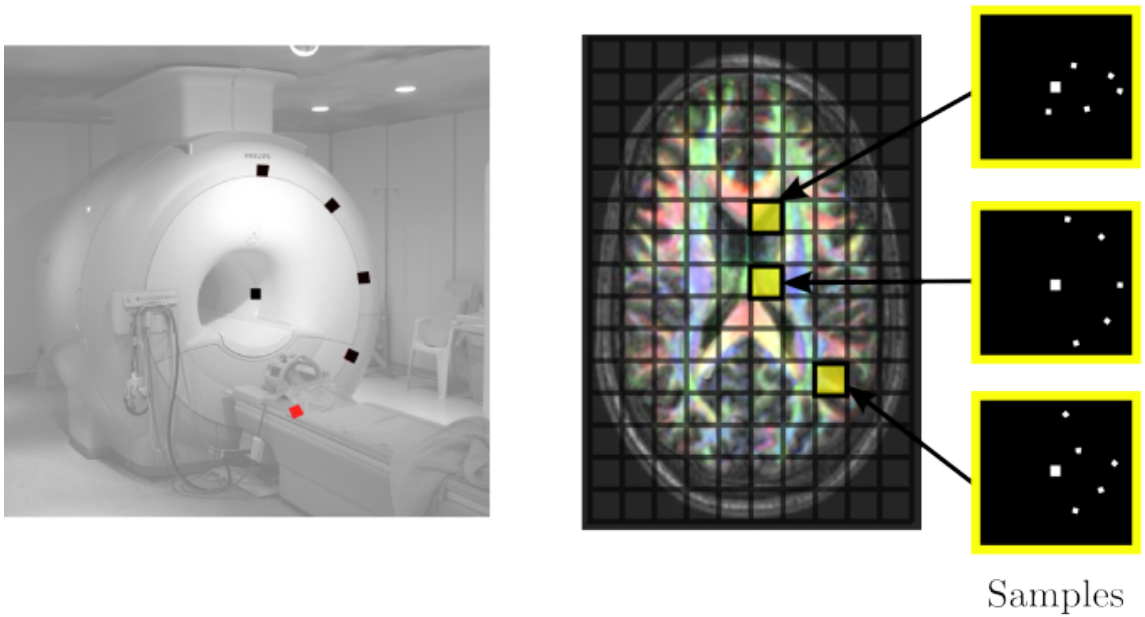

Figure: Diffusion MRI acquisition steps.

Signal acquisition

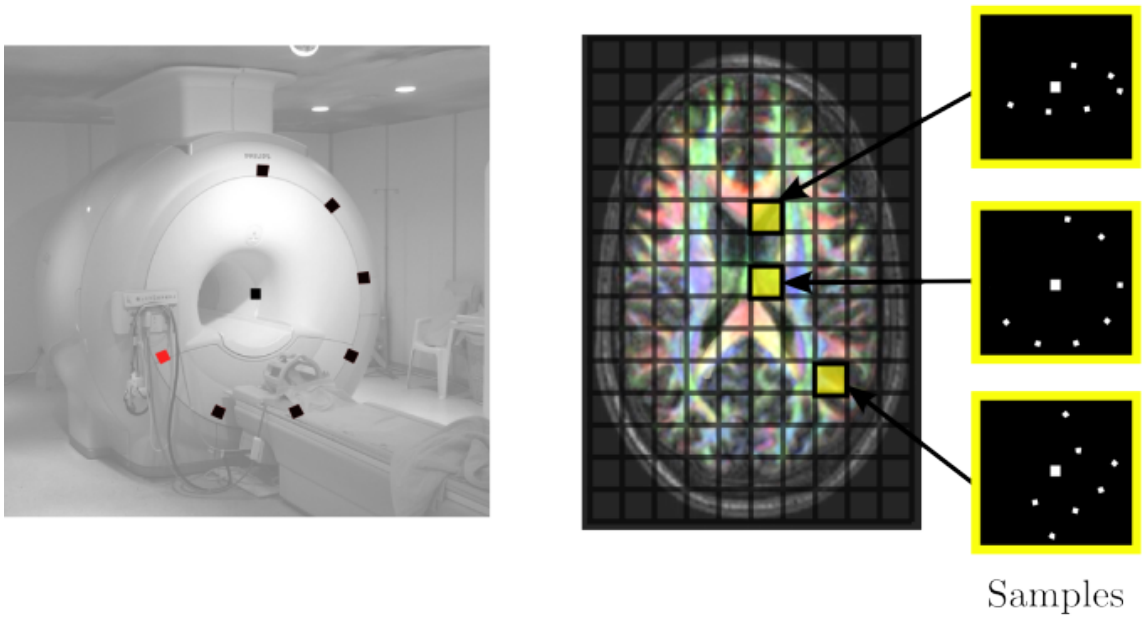

Figure: Diffusion MRI acquisition steps.

Signal acquisition

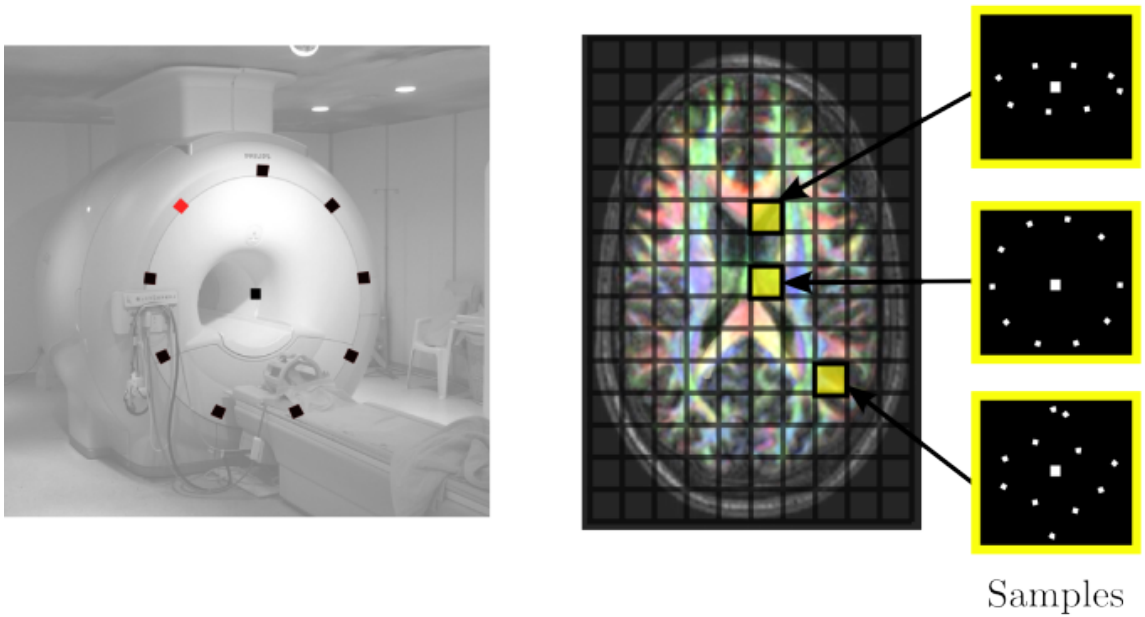

Figure: Diffusion MRI acquisition steps.

Signal acquisition

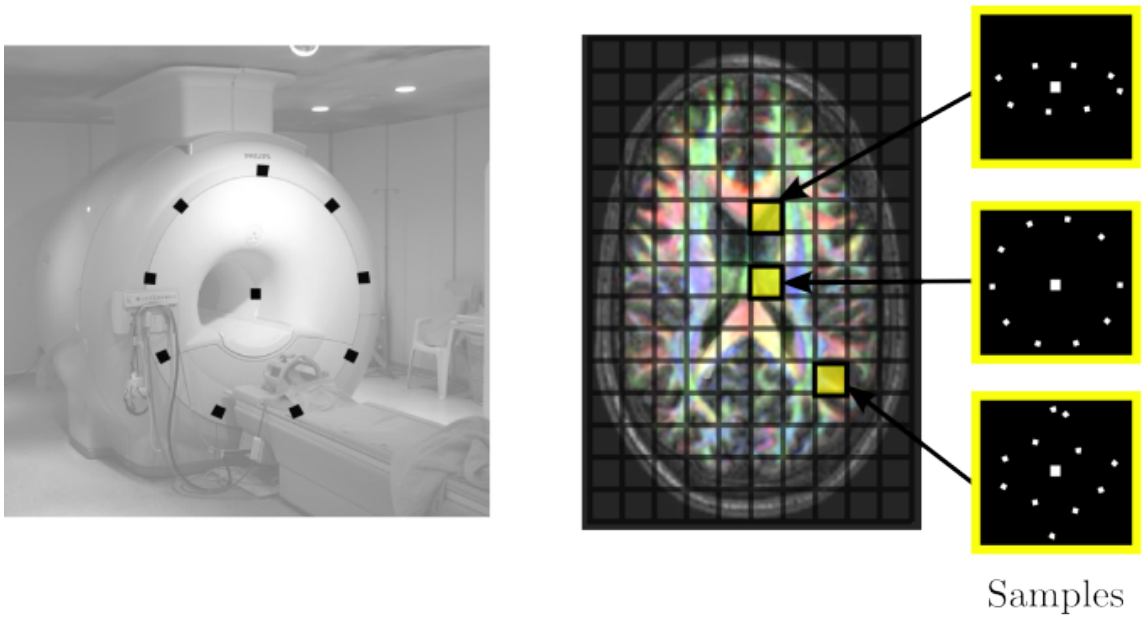

Figure: Diffusion MRI acquisition steps.

Signal acquisition

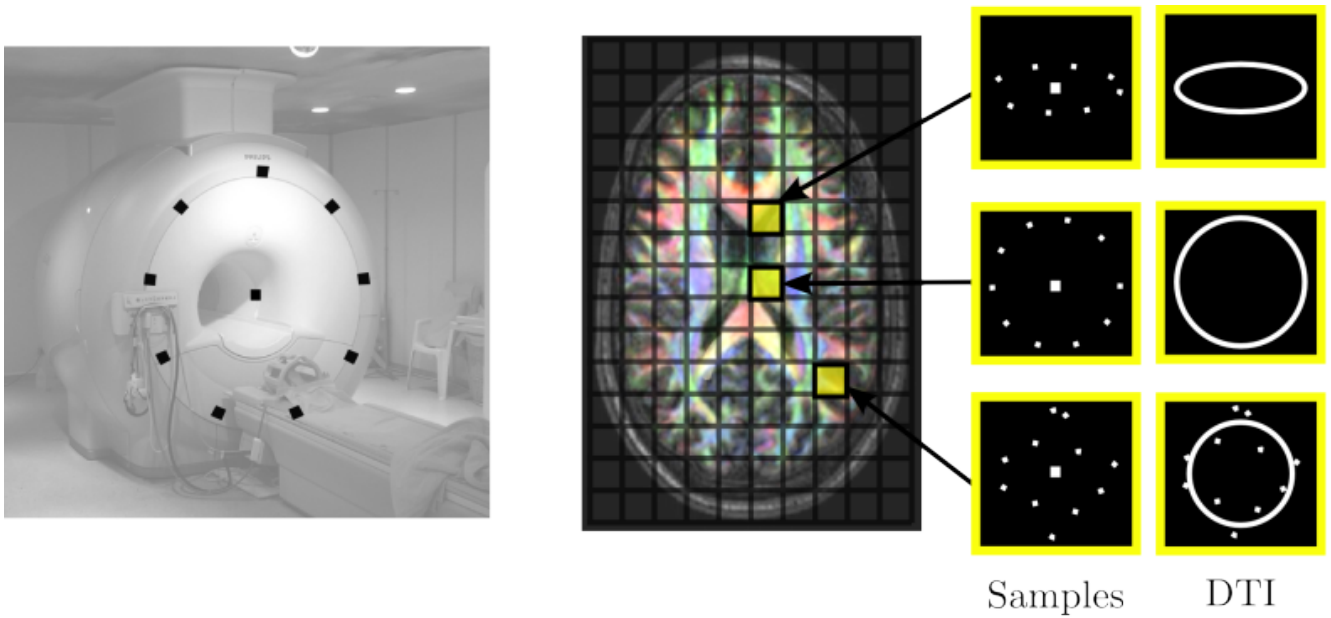

Figure: Diffusion MRI acquisition steps.

Signal acquisition

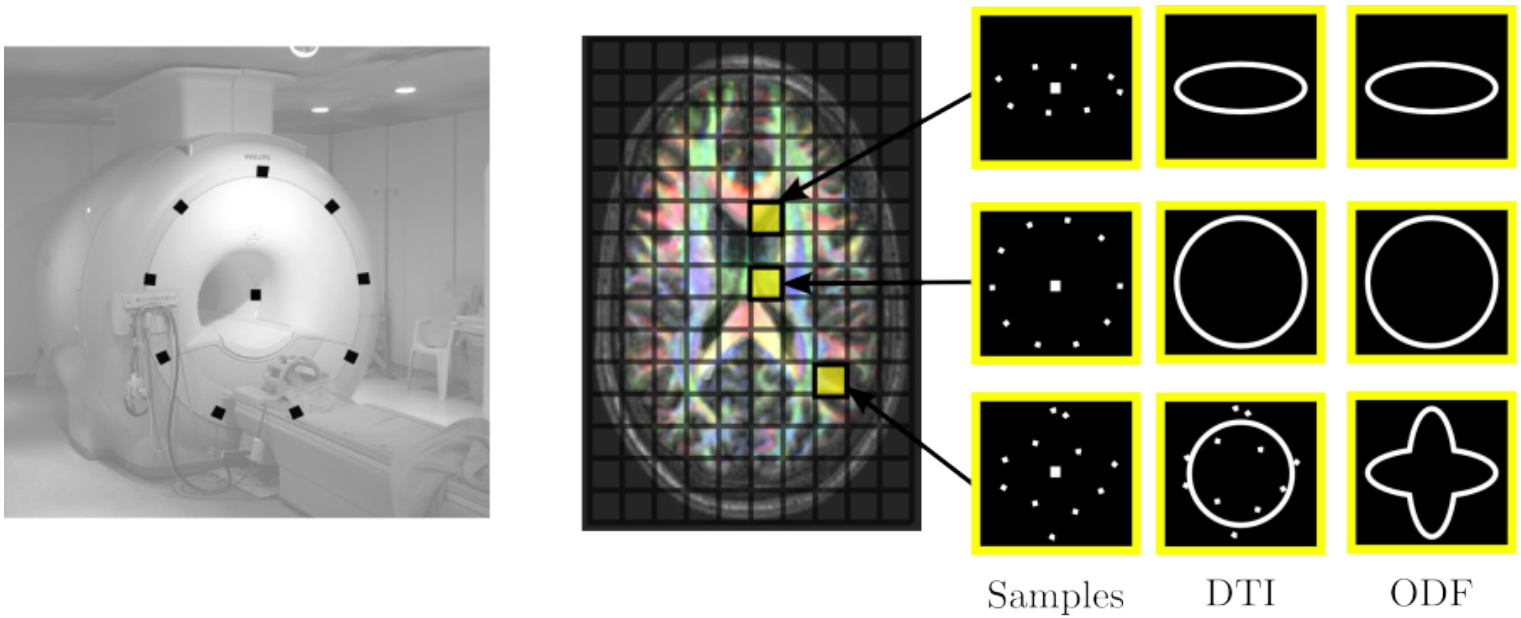

Figure: Diffusion MRI acquisition steps.

Signal acquisition

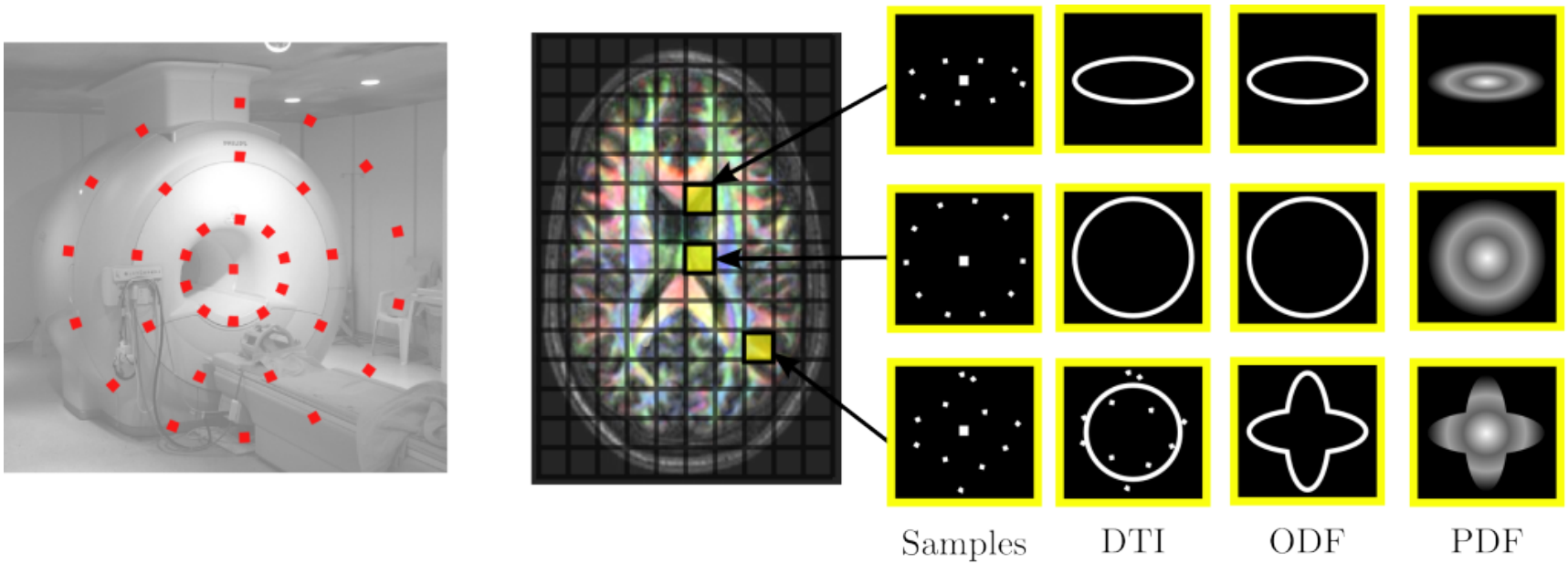

Figure: Diffusion MRI acquisition steps.

Q-Space

- MRI-based image modality is able to measure water diffusion within tissues.
- Acquisition of several raw images under different magnetic field magnitudes and orientations (Q-space).

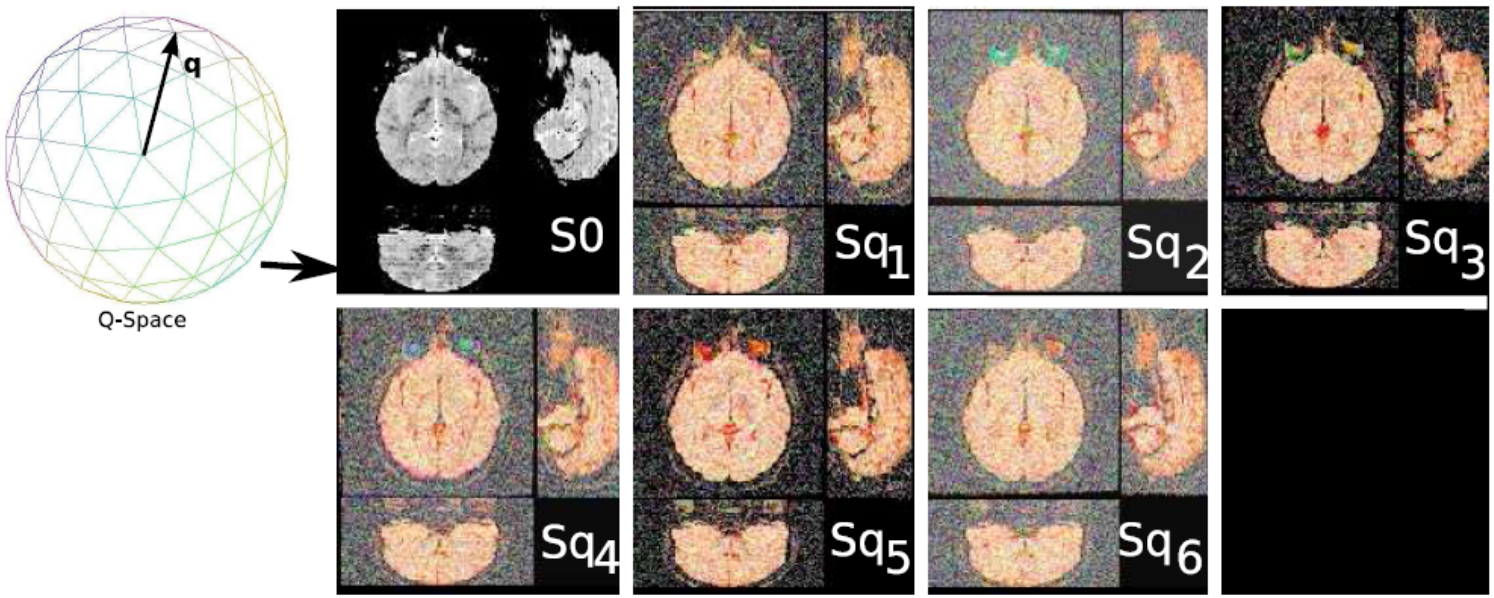

(a) Acquisition in $\mathbf{q}$-space on a sphere of radius $||\mathbf{q}||$: a baseline image S_0 and several other gradients images $S(\mathbf{q})$.

1 Context

2 DTI model : Diffusion Tensor Imaging

3 QBI model : Q-Ball Imaging

4 Measuring the PDF : DSI and Multi Q-Ball

5 Conclusions & Perspectives

Signal acquisition

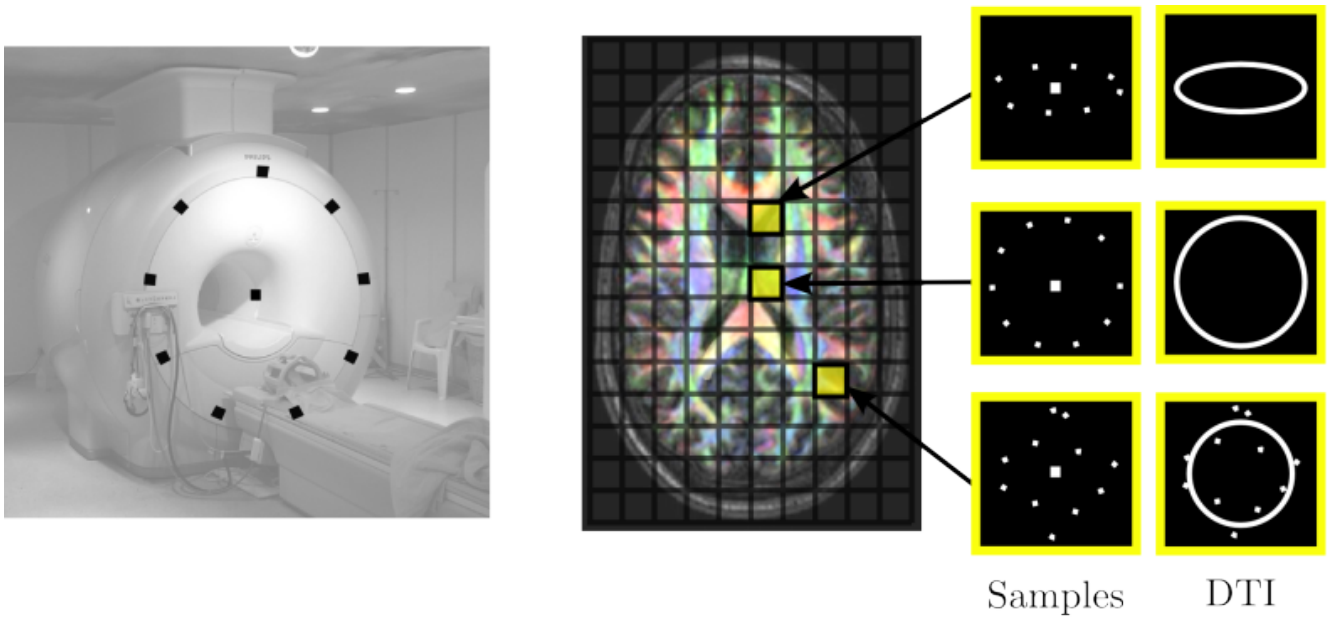

Figure: Diffusion MRI acquisition steps.

2nd-order Diffusion tensors

- A volume of **Diffusion Tensors** can be estimated from these raw images.
- Diffusion tensors represents Gaussian models of the water diffusion in the voxels, and are **3x3 symmetric and positive-definite matrices**.
- Representation of a DTI reconstructed image with a **volume of ellipsoids** :

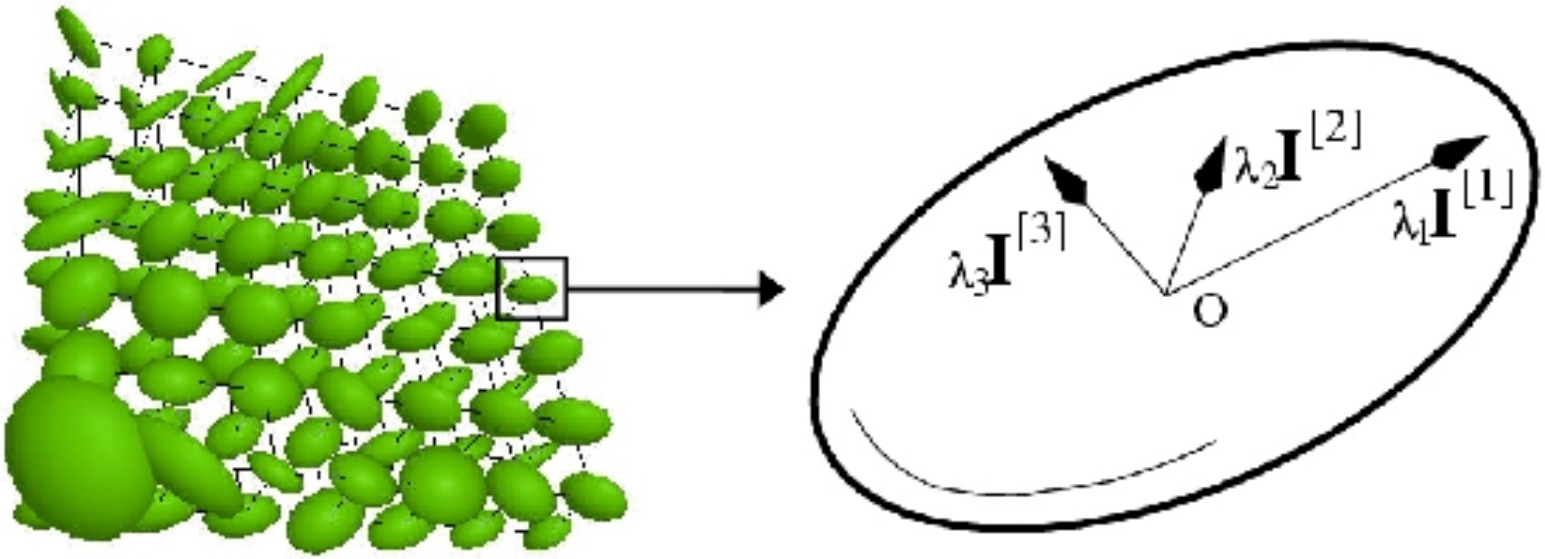

(a) Diffusion tensor field, giving a Gaussian diffusion model on each voxel.

Diffusion tensors for fibertracking

- Diffusion MRI images give **structural informations** about fiber networks within tissues.
- Fiber tractography can be performed by tracking the **principal diffusion directions**.

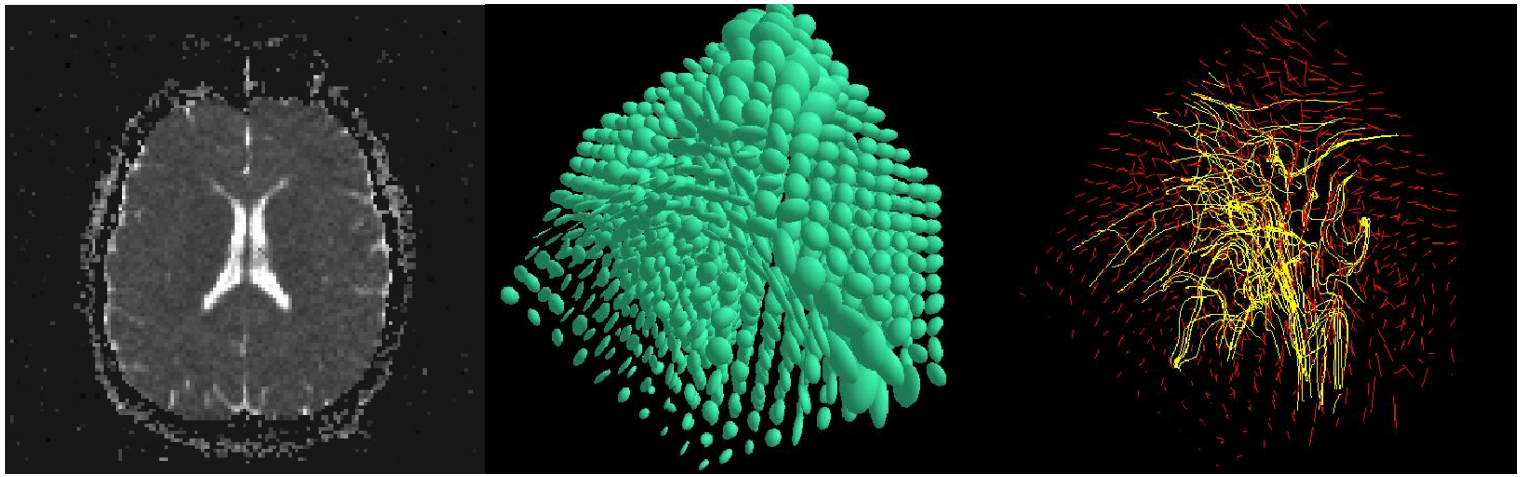

Raise a lot of image processing problems : Estimation of diffusion profiles, Regularization (Raw images are noisy), Visualization.

Diffusion MRI: fiber-tracking

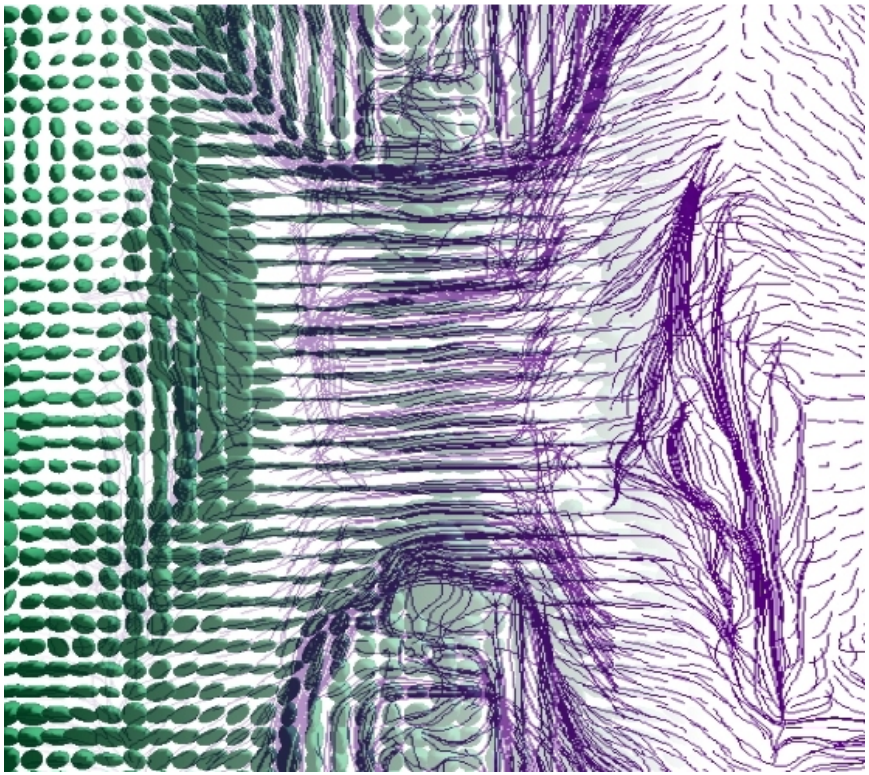

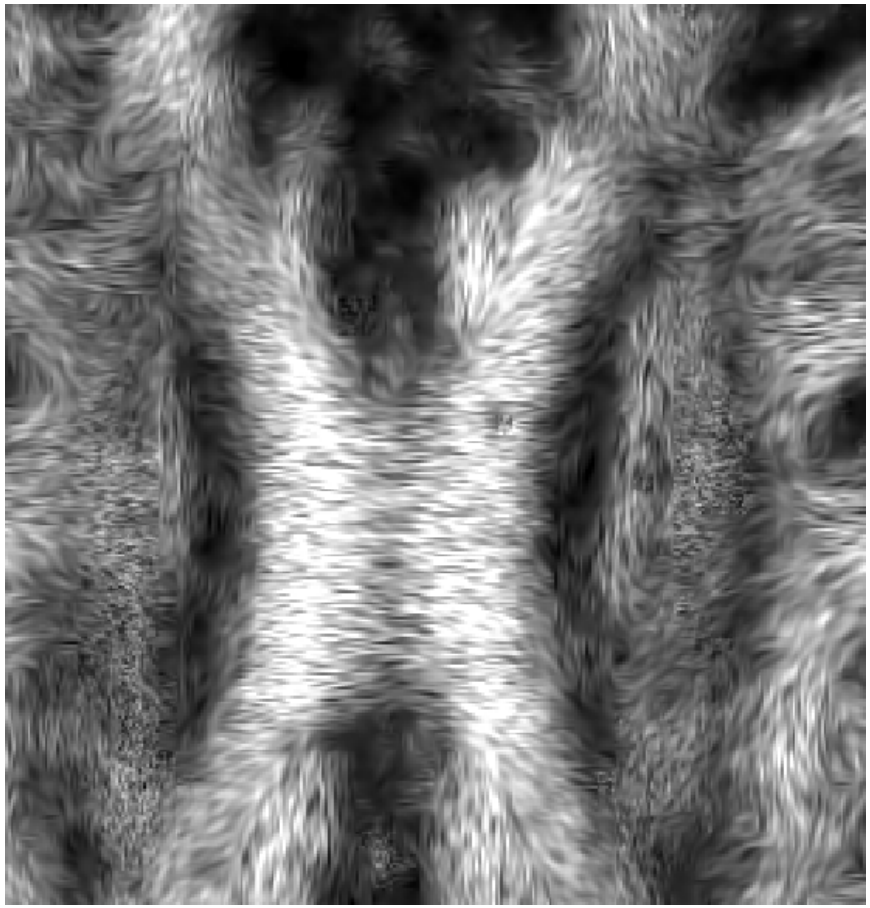

Fiber-tracking through human tissues (brain white matter) is usually done by following the principal eigen vector of tensors

DTI : The Stejskal-Tanner Equation

- Consider $\mathbf{D}_{(x,y,z)} = \begin{pmatrix} a & b & c \\ b & d & e \\ c & e & f \end{pmatrix}$, the diffusion tensor modeling the local Gaussian diffusion at voxel (x, y, z).
- Measured (raw) images S_k are related to the projection of the tensors $\mathbf{D}_{(x,y,z)}$ along a particular gradient orientation $\mathbf{q}_k$:

$$\forall (x, y, z), \qquad S_{k_{(x,y,z)}} = S_{0_{(x,y,z)}} \; e^{-b \, \mathbf{q}_k^T \, \mathbf{D}_{(x,y,z)} \, \mathbf{q}_k}$$

At least **7 images** are needed to get an estimation of $\mathbf{D}$.

DTI Estimation : A Direct Approach

- Method proposed by [Westin:2002], using a dual tensor basis.

Direct estimation :

$$\mathbf{D} = \sum_{k=1}^{6} < \mathbf{D}, g_k g_k^T > \; g_k g_k^T = \sum_{k=1}^{6} -\frac{1}{b} \ln\left(\frac{S_k}{S_0}\right) \; g_k g_k^T$$

- ⊕ At least six non-colinear diffusion gradient directions, i.e **7 images** are then theoretically sufficient.
- ⊕ Real-time.
- ⊖ Positive definiteness of the tensors is not insured.
- ⊖ Not robust to noise.

DTI Estimation : Minimizing Least Square Error

- When $n > 7$ raw images are available, $\mathbf{D}$ can be retrieved by a least square minimization method :

$$\min_{\mathbf{D}} \sum_{k=1}^{n} \left(-\frac{1}{b} \ln \left(\frac{S_k}{S_0} \right) - g_k^T \mathbf{D} g_k \right)^2 \quad \Rightarrow \quad \begin{cases} \min_X \|AX - b\|^2 \\ \hat{X} = (A^T A)^{-1} A^T b \end{cases}$$

- $\oplus$ Least square methods are more robust to noise, by using all the raw image informations.
- $\ominus$ Positive definiteness of the tensors is not insured.
- $\Rightarrow$ **Reprojection** of the tensors into the positive tensor space is needed by both estimation methods.

DTI Estimation : Variational Approach

- Minimizing the following criterion, in the **constrained positive tensor space :**

$$\min_{\mathbf{D}\in \mathrm{P}(3)} \int_{\Omega} \sum_{k=1}^{n} \psi\left(\left|\ln\left(\frac{S_0}{S_k}\right) - g_k^T \mathbf{D} g_k\right|\right) + \alpha\, \phi(\|\nabla \mathbf{D}\|)\, d\Omega$$

- The corresponding gradient descent that respect the positive-definite property of the tensors is (Euler-Lagrange) :

$$\begin{cases} \mathbf{T}_{(t=0)} = \mathbf{Id} \\ \\ \frac{\partial \mathbf{T}}{\partial t} = (\mathbf{G} + \mathbf{G}^T)\mathbf{T}^2 + \mathbf{T}^2(\mathbf{G} + \mathbf{G}^T) \end{cases}$$

where $\mathbf{G}$ corresponds to the unconstrained velocity matrix defined as :

$$G_{i,j} = \sum_{k=1}^{n} \psi'(|v_k|)\mathrm{sign}(v_k)\left(g_k g_k^T\right)_{i,j} + \alpha \mathrm{div}\left(\frac{\phi'(\|\nabla \mathbf{T}\|)}{\|\nabla \mathbf{T}\|}\, \nabla T_{i,j}\right),$$

DTI Estimation : Variational Approach

- Comparison results with synthetic datasets :

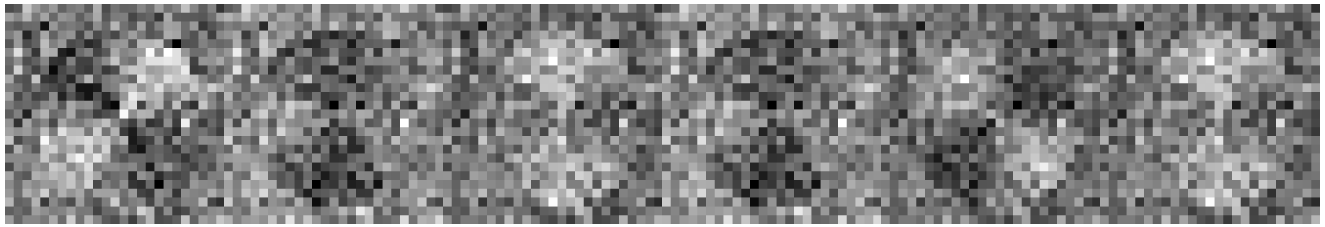

(a) Partial set of noisy raw images S_k (in 6 different gradient directions)

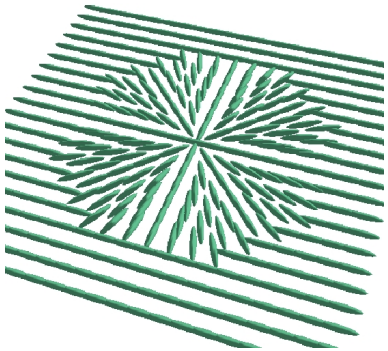

(b) True tensor field

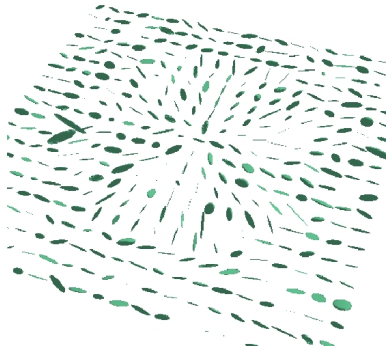

(c) Direct estimation

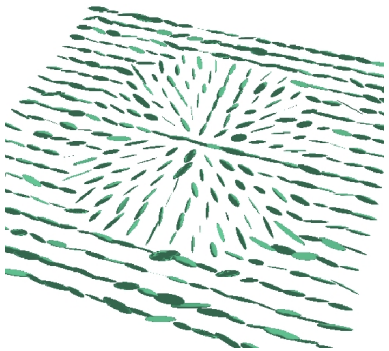

(d) LS estimation

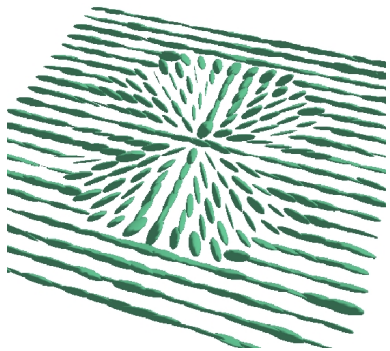

(e) Variational method

Effect on fiber-tracking

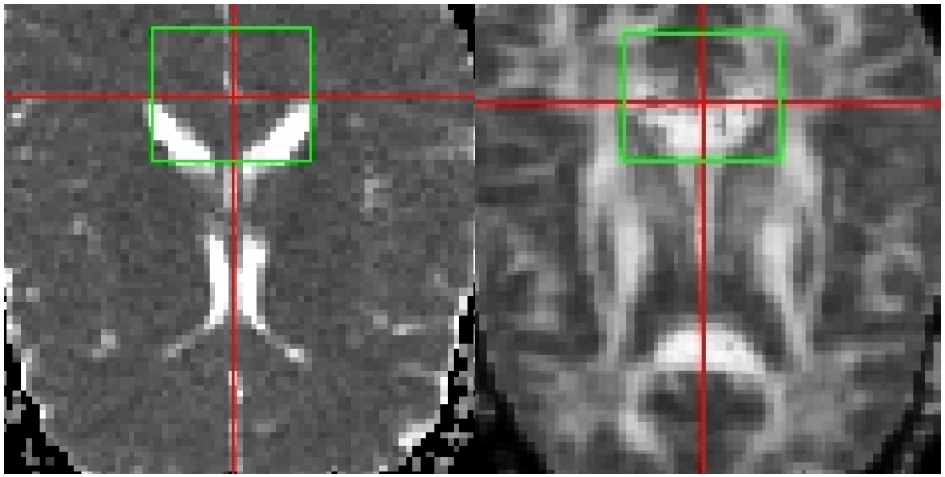

(a) Mean diffusivity (left) and Fractional Anisotropy (right)

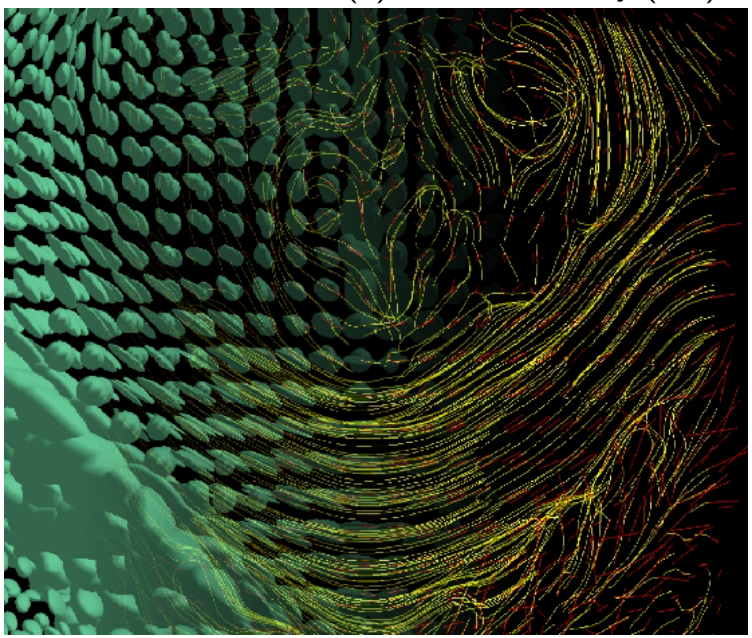

(b) LS estimation + fibers

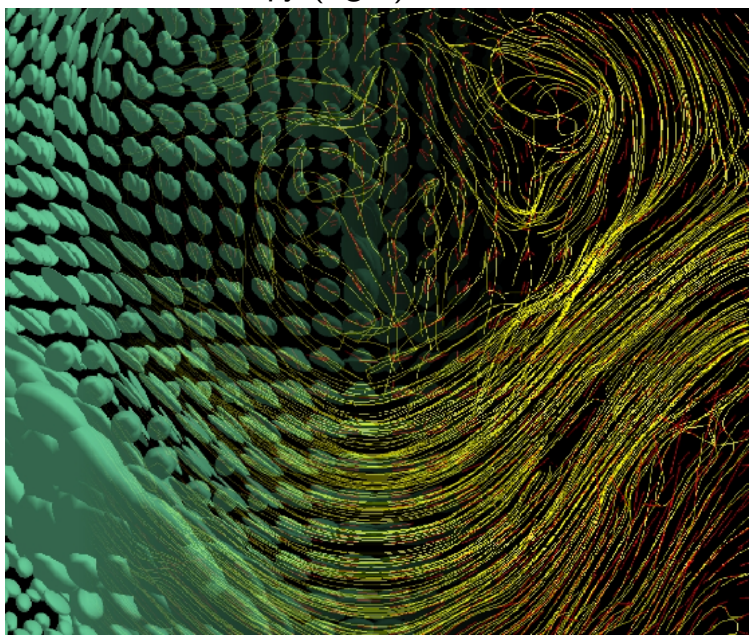

(c) Variational estimation + fibers

Fiber scale space

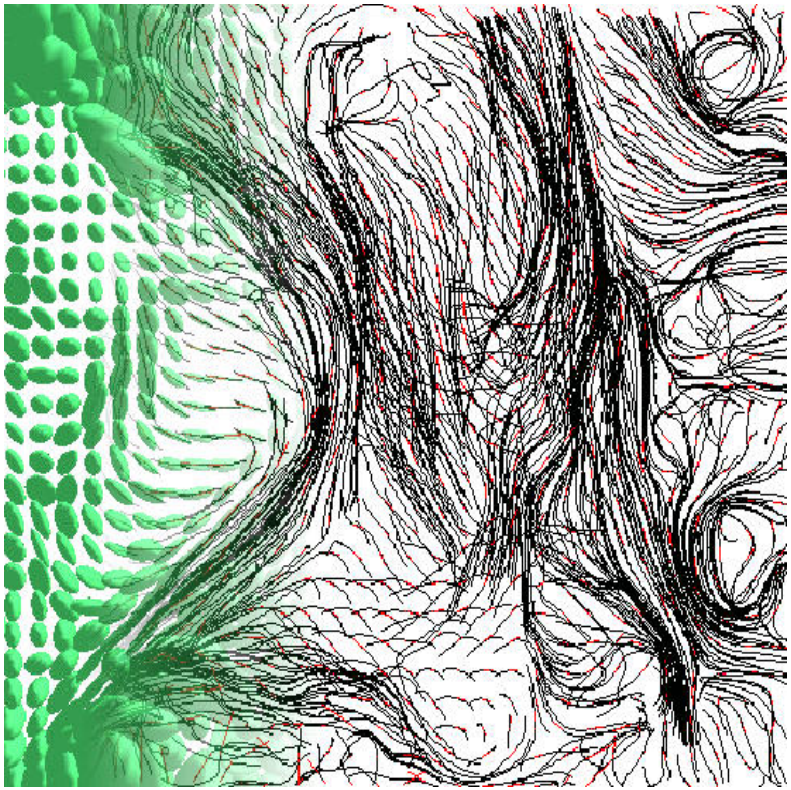

Tensor (left) & Fibers (right)
Variational estimation with $\alpha = 0.1$

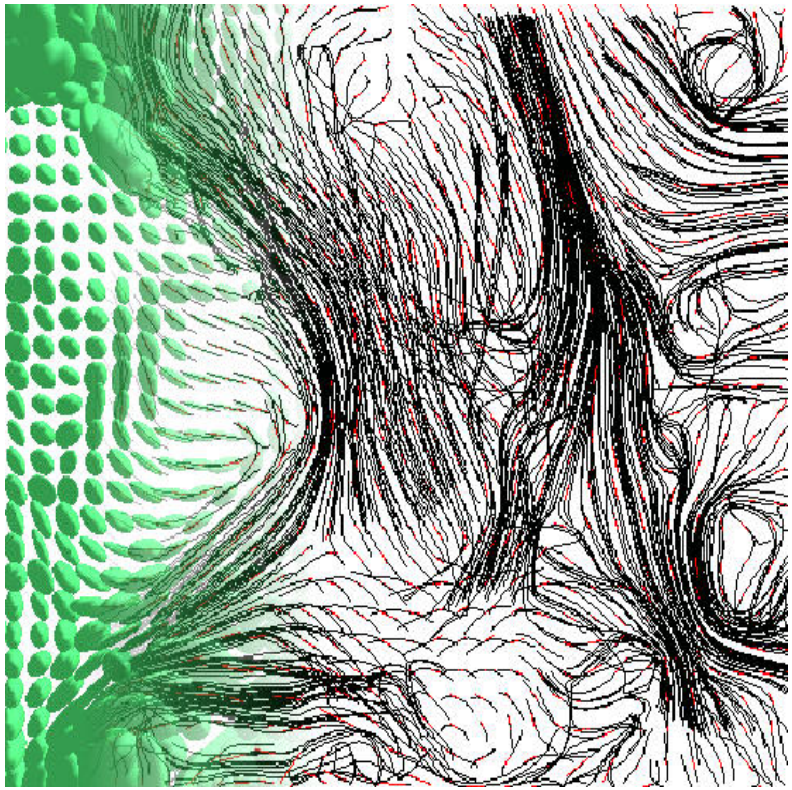

Variational estimation with $\alpha = 0.3$.

Fiber scale space

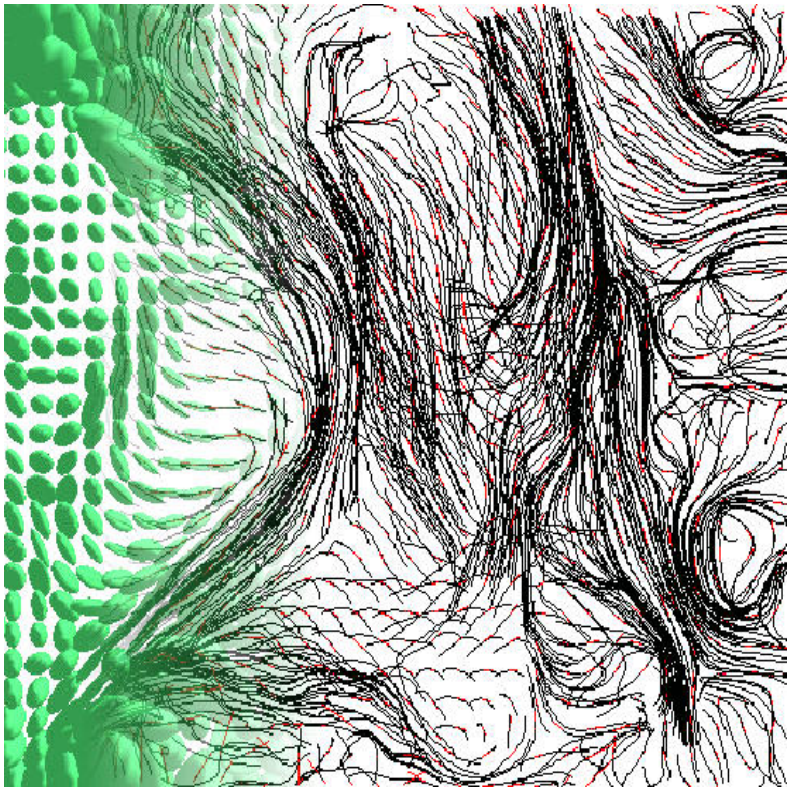

Tensor (left) & Fibers (right)
Variational estimation with $\alpha = 0.1$

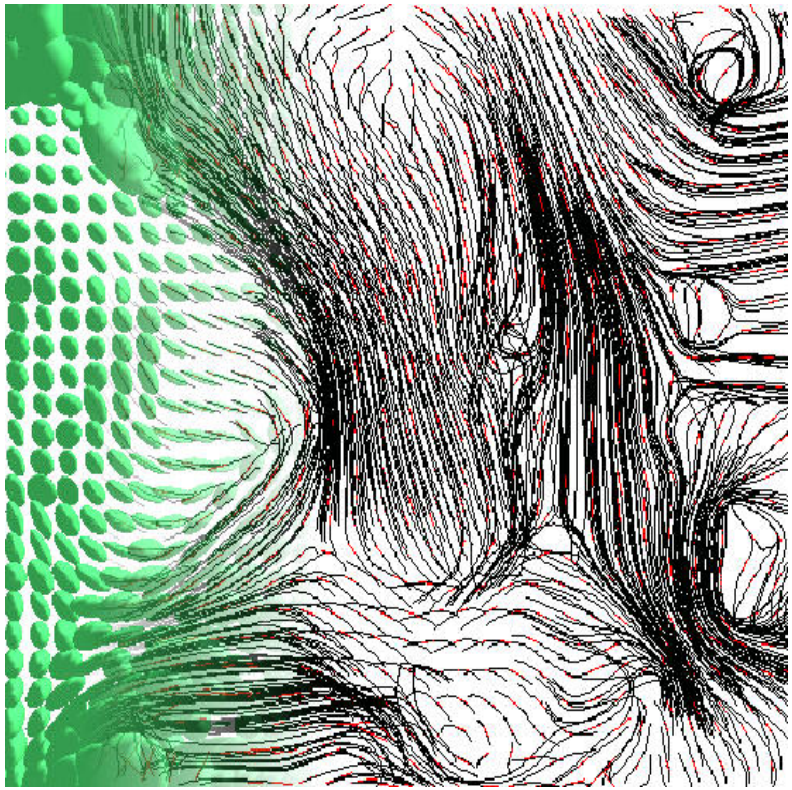

Variational estimation with $\alpha = 1$.

Limits of Tensor Models

- When $n >> 7$ images are available, there is an **average of diffusion orientations** for each voxel.
- Gaussian diffusion models cannot handle **the crossing problem**.

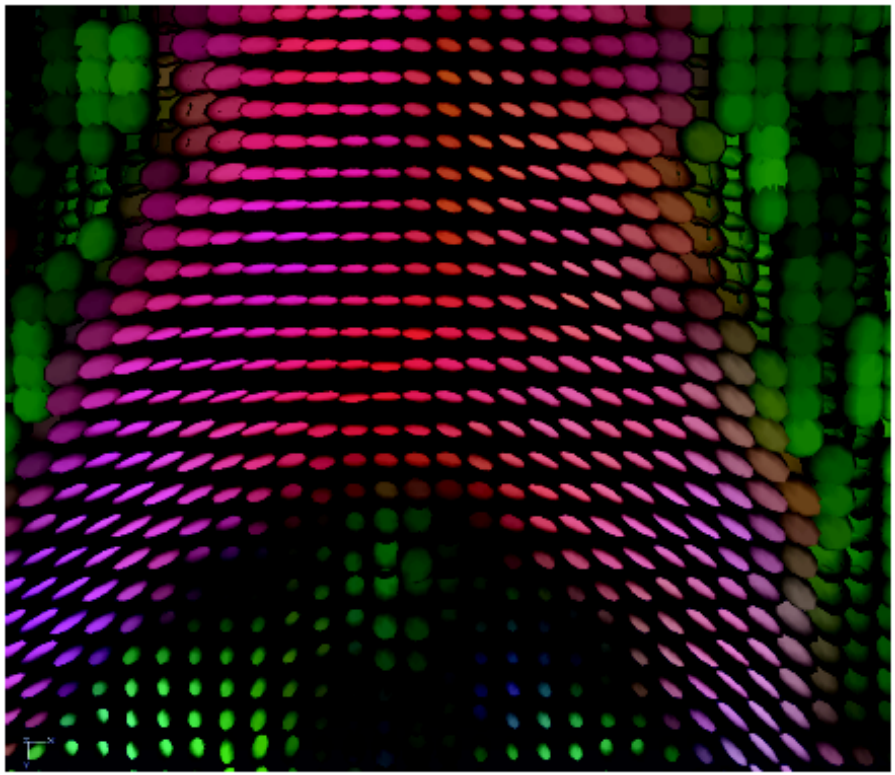

(a) DTI are sufficient when fibers are mainly monodirectional

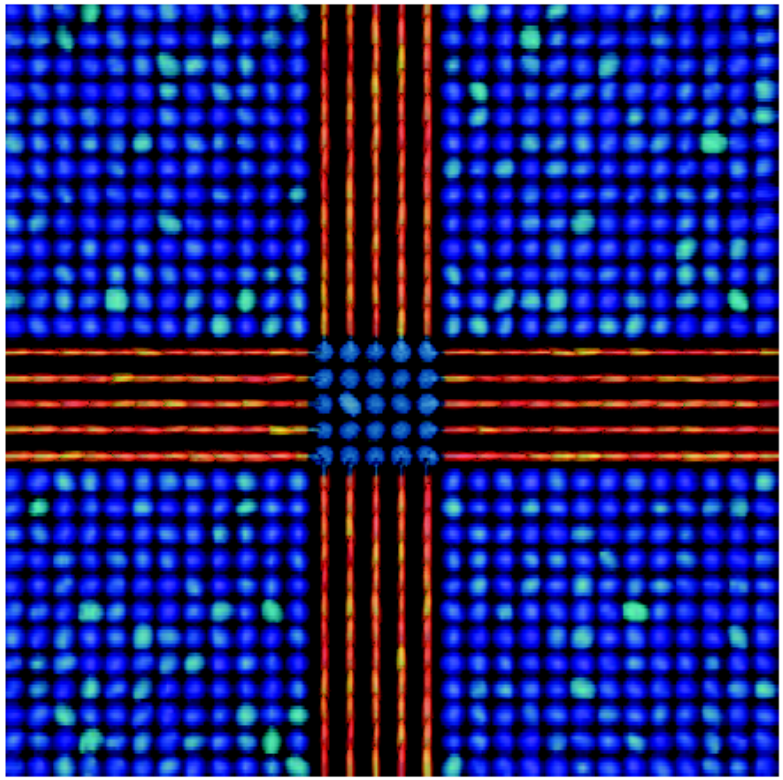

(b) DTI fails at modeling fiber crossing

Limits of Tensor Models

- In case of crossing, the "best" case happens when the directions are orthogonals, so the fibertracking algorithm may stop.
- When crossing directions are more close, **fibertracking directions just go wrong**.

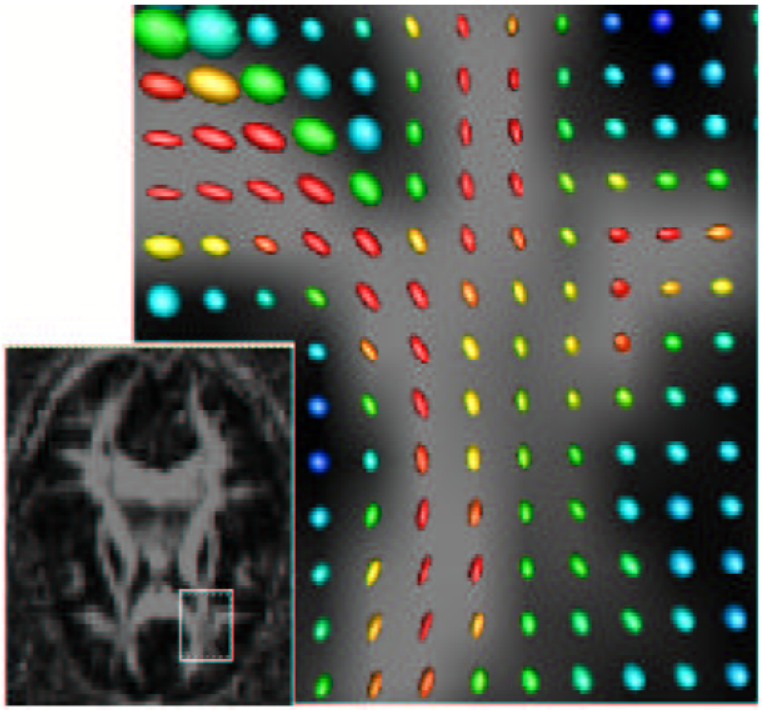

(b) DTI fails at modeling fiber crossing (from Descoteaux-etal:05)

1 Context

2 DTI model : Diffusion Tensor Imaging

3 QBI model : Q-Ball Imaging

4 Measuring the PDF : DSI and Multi Q-Ball

5 Conclusions & Perspectives

Signal acquisition

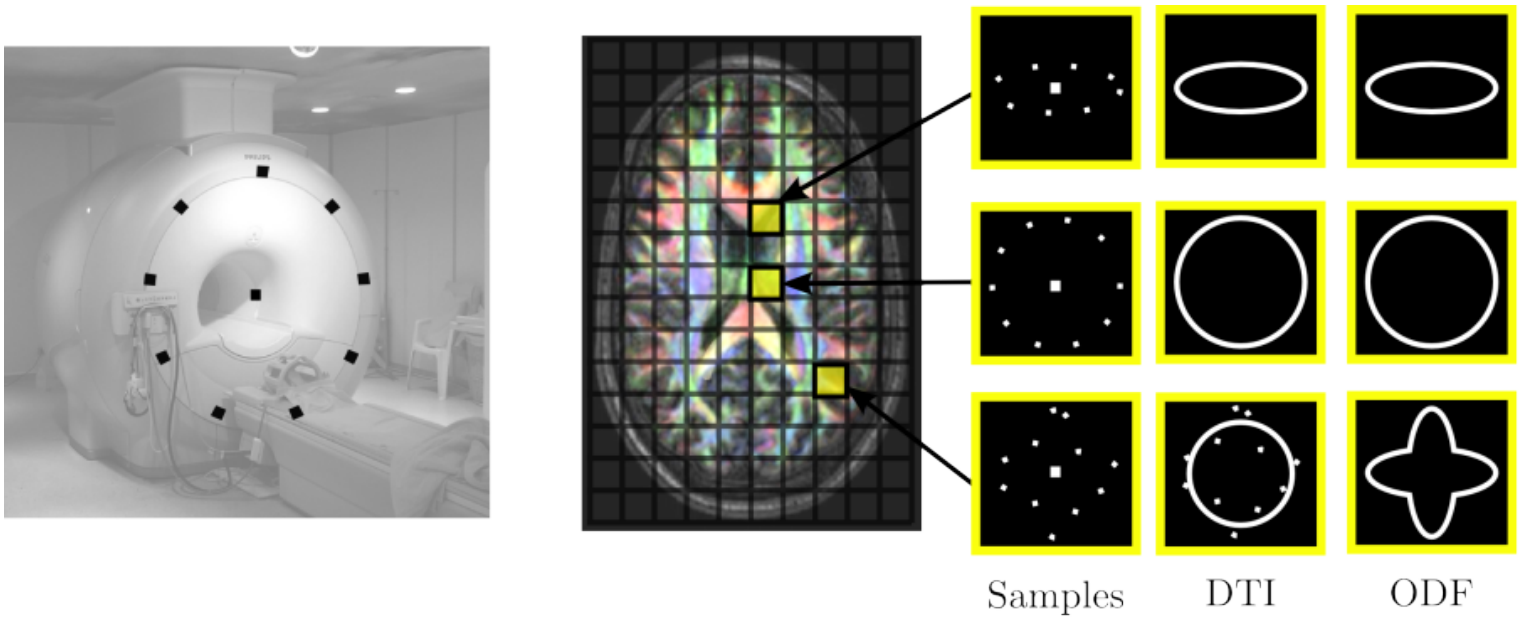

Figure: Diffusion MRI acquisition steps.

DTI versus higher order models

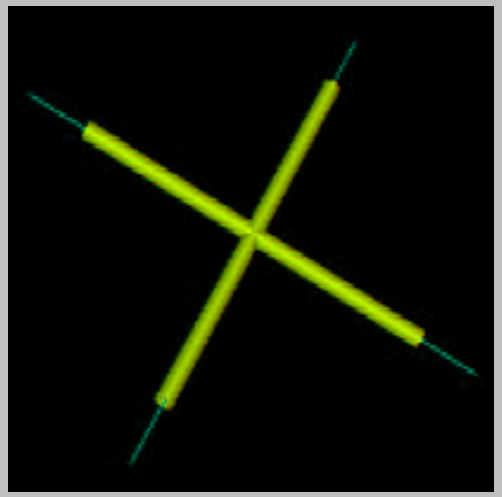

Fibers
Raw data

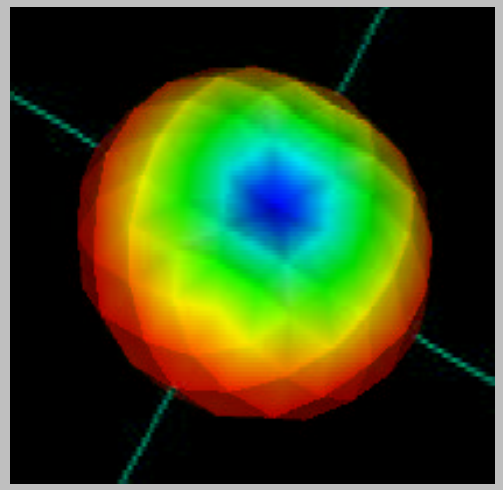

DTI
2nd-order tensor
[Basser94]

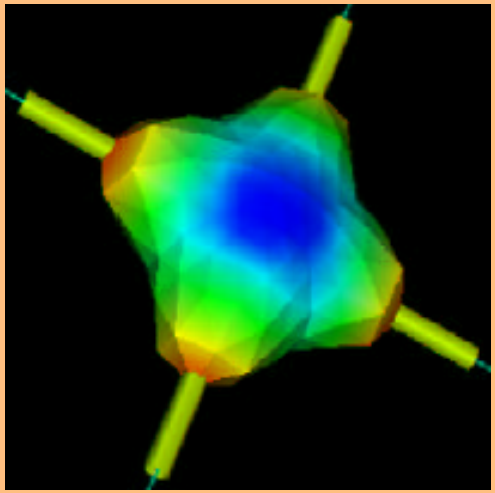

higher orders
approaches

Numerous approaches exist: GDTI [Liu03], PASMRI [Jansons03], HODT / DOT [Özarslan03,06], Spherical Deconvolution [Tournier04], ODF [Tuch04, Descoteaux-etal05], etc.

Spherical Harmonics: Definition

Spherical harmonics are a basis for complex functions on the unit sphere. We use a modified basis constrained to be real and symmetric (imaginary and non-symmetric parts = noise)

$$\forall(\theta_q, \phi_q) \in \Omega_S = [0, \pi] \times [0, 2\pi), S : \Omega_S \rightarrow \mathbb{R}$$

$$S(\theta_q, \phi_q) = \sum_{j=0}^{N} c_j Y_j(\theta_q, \phi_q) = \tilde{B} C_j(\theta_q, \phi_q), \quad (1)$$

$$\text{with } \tilde{B} = \begin{bmatrix} Y_1(\theta_1, \phi_1) & \dots & Y_N(\theta_1, \phi_1) \\ \vdots & \ddots & \vdots \\ Y_1(\theta_{n_s}, \phi_{n_s}) & \dots & Y_N(\theta_{n_s}, \phi_{n_s}) \end{bmatrix}$$

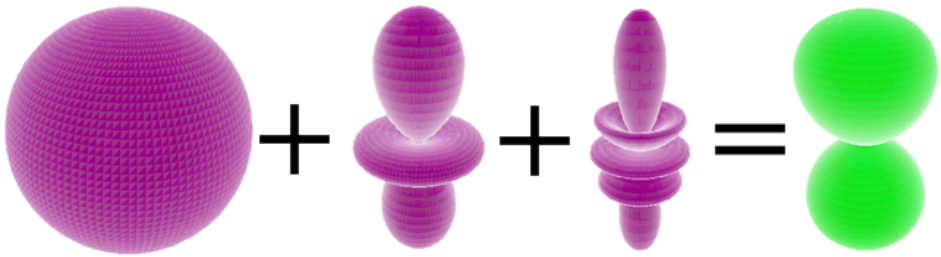

Angular Atoms

$$y_l^m = \begin{cases} \sqrt{2}\,\mathbb{R}(Y_l^m) & \text{if} \quad 0 < m \leq l \\ Y_l^0, & \text{if} \quad m = 0 \\ \sqrt{2}\,\Im(Y_l^{|m|}) & \text{if} \quad -l \leq m < 0 \end{cases} \qquad \text{with } l \in 2\mathbb{N} \qquad (2)$$

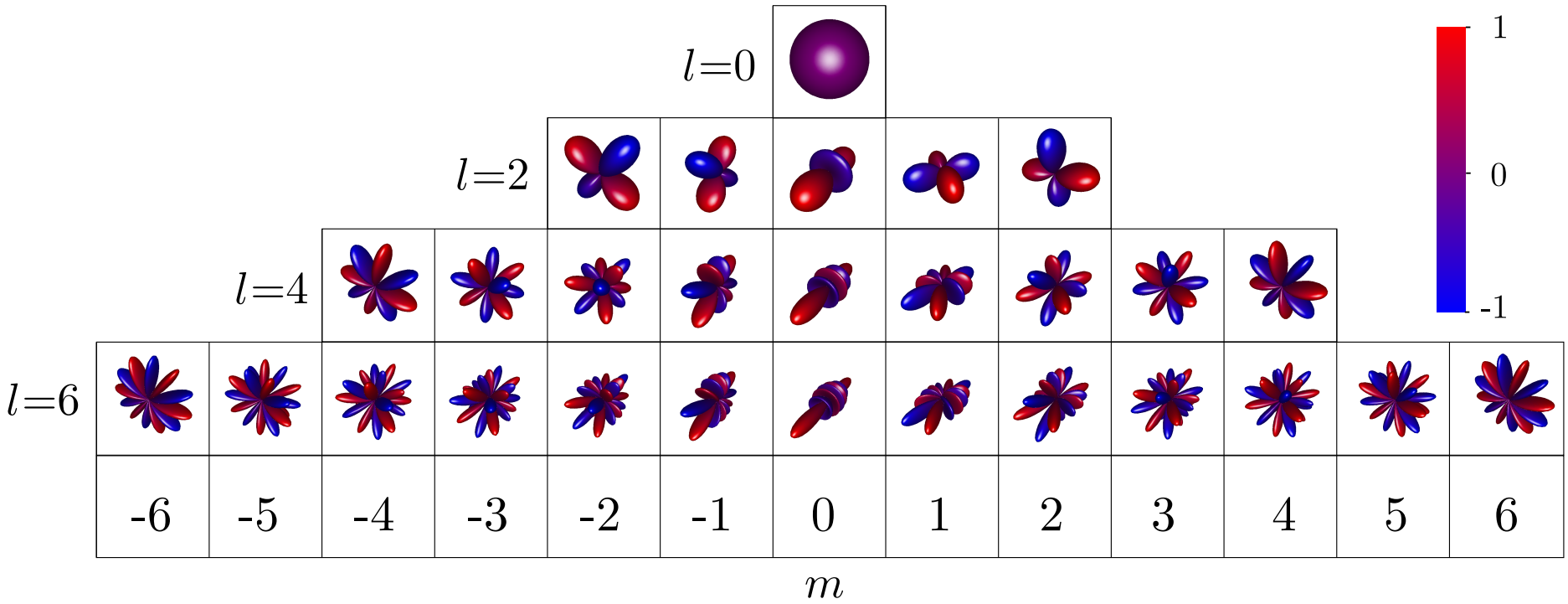

Figure: Real and symmetric spherical harmonics: first orders $l = 0, 2, 4, 6$. Blue indicates a negative value, whereas indicates red a positive value.

Angular profile using Spherical Harmonics

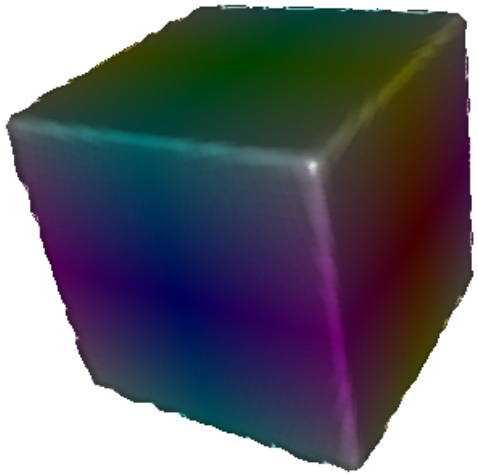

(a)

Figure: Square sampled along a 5-subdivided icosahedron.

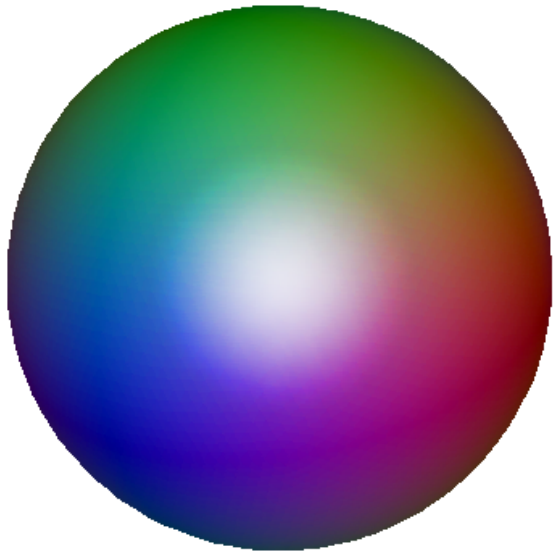

(a) 6 coefficients

Figure: Angular reconstruction along with increasing truncation order L.

Angular profile using Spherical Harmonics

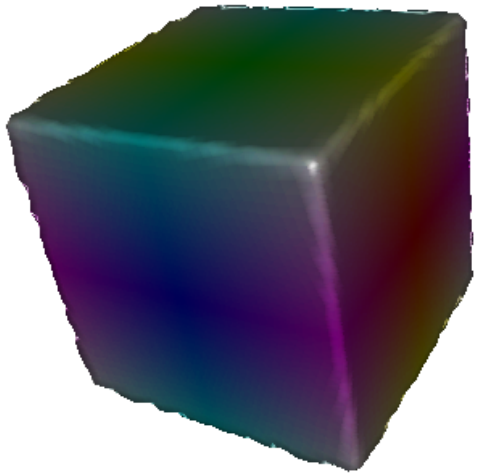

(a)

Figure: Square sampled along a 5-subdivided icosahedron.

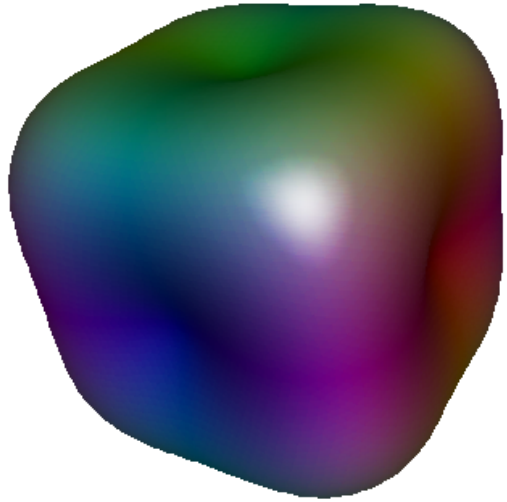

(a) 15 coefficients

Figure: Angular reconstruction along with increasing truncation order L.

Angular profile using Spherical Harmonics

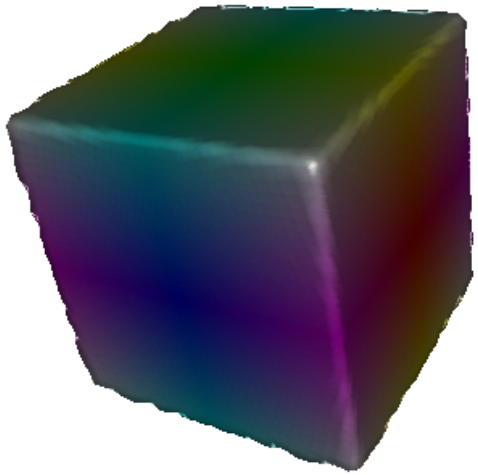

(a)

Figure: Square sampled along a 5-subdivided icosahedron.

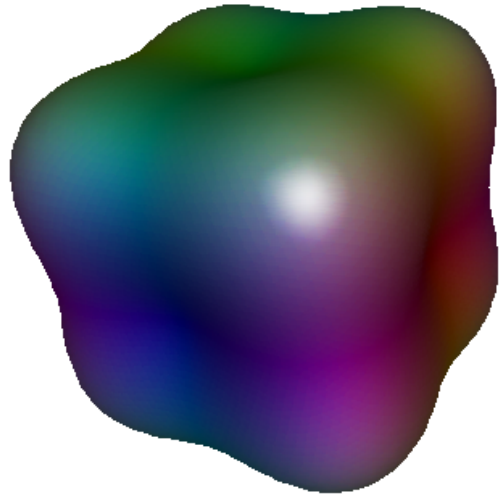

(a) 28 coefficients

Figure: Angular reconstruction along with increasing truncation order L.

Angular profile using Spherical Harmonics

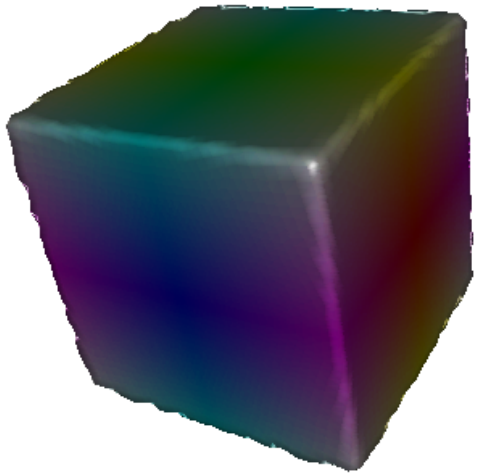

(a)

Figure: Square sampled along a 5-subdivided icosahedron.

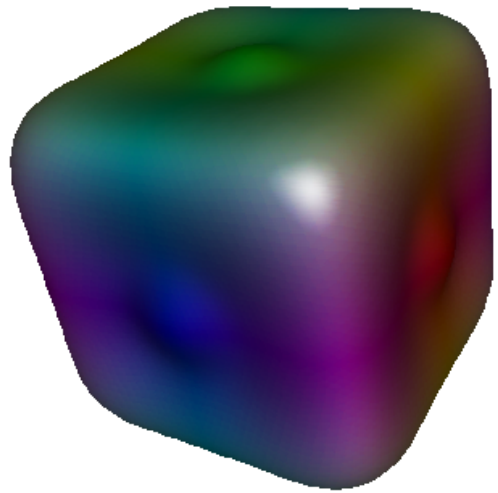

(a) 45 coefficients

Figure: Angular reconstruction along with increasing truncation order L.

Angular profile using Spherical Harmonics

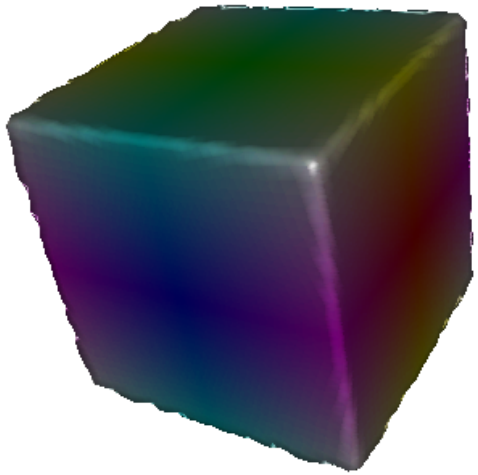

(a)

Figure: Square sampled along a 5-subdivided icosahedron.

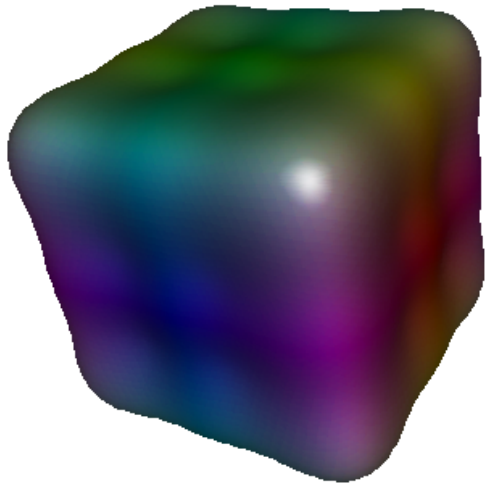

(a) 66 coefficients

Figure: Angular reconstruction along with increasing truncation order L.

Angular profile using Spherical Harmonics

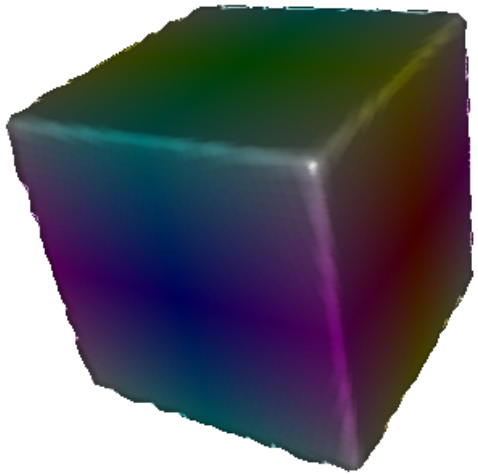

(a)

Figure: Square sampled along a 5-subdivided icosahedron.

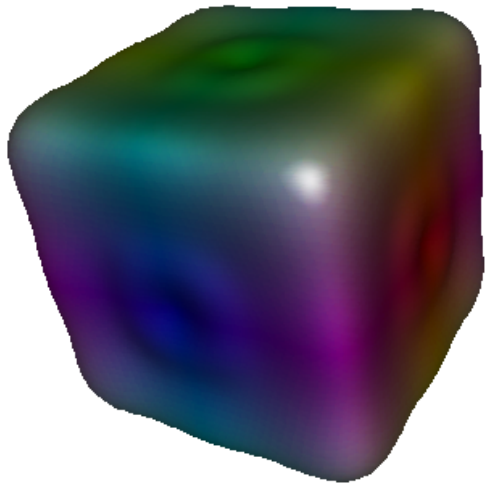

(a) 91 coefficients

Figure: Angular reconstruction along with increasing truncation order L.

Angular profile using Spherical Harmonics

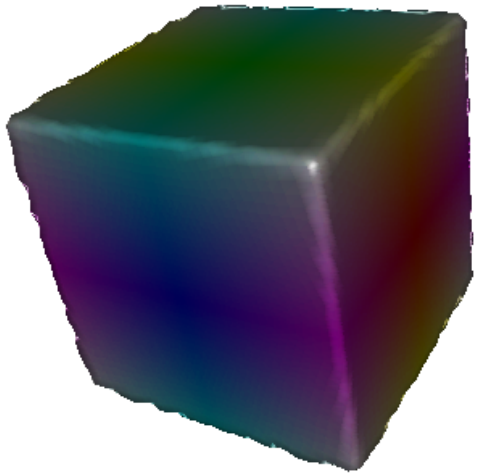

(a)

Figure: Square sampled along a 5-subdivided icosahedron.

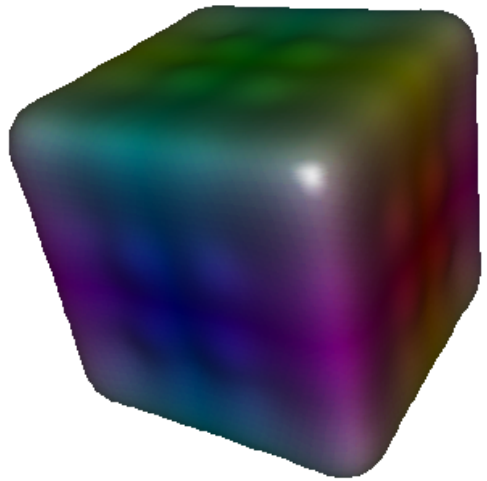

(a) 120 coefficients

Figure: Angular reconstruction along with increasing truncation order L.

Angular profile using Spherical Harmonics

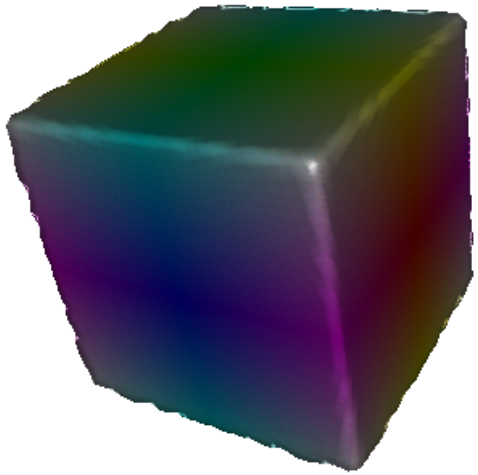

(a)

Figure: Square sampled along a 5-subdivided icosahedron.

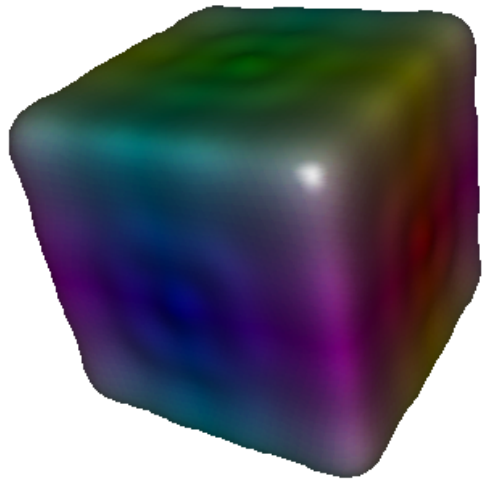

(a) 153 coefficients

Figure: Angular reconstruction along with increasing truncation order L.

Orientation Density Function (ODF)

The ODF Ψ at direction $\mathbf{u}$ is defined as the radial projection of the diffusion PDF

$$\begin{aligned}\Psi(\mathbf{u}) &= \int_o^\infty P(\alpha\mathbf{u})d\alpha \\ &= \int P(r,\theta,z)\delta(\theta,z)rdrd\theta dz\end{aligned} \tag{3}$$

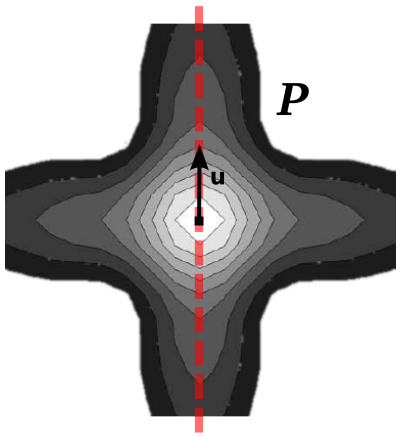

ODF

Problem: How to get the PDF ?

Funk-Radon Transform (FRT)

The FRT (4) is a smoothed estimation of the true ODF (3) [Tuch04]

$$\mathcal{G}_{q'}(\mathbf{u}) = 2\pi q' \int P(r,\theta,z) J_0(2\pi q' r) r dr d\theta dz \tag{4}$$

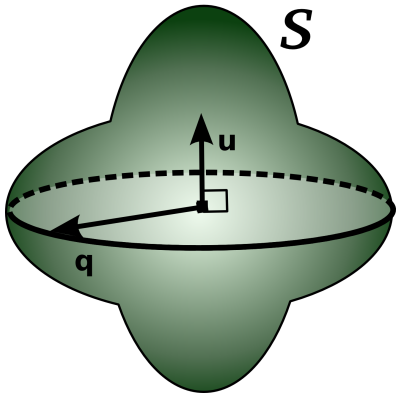

FRT

Besides, the ODF can be directly expressed from diffusion signal in spherical harmonics by a Least Square minimization [Descoteaux06]

$$ODF \approx \mathcal{G}_{q'} = \tilde{P}\tilde{B}\mathbf{C} = \sum_j 2\pi P_{l_j}(0) c_j Y_j \tag{5}$$

Least Square ODF estimation

Least Square ODF estimation :

- Enables resolution of any specific local structure (crossing fibers)
- Model-free method: no assumption on macroscopic diffusion
- Light matrix computations

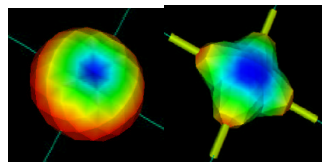

But...

- Least Square method not adapted to Rice noise model [Sijbers98]
- No guaranty on spatial coherence of the ODF field

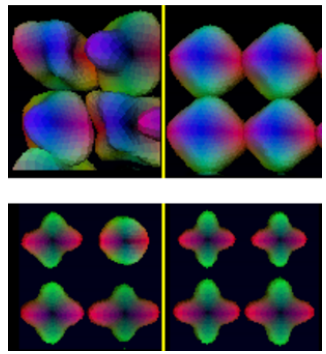

Variational estimation of ODF

$$\min_{\mathbf{C}:\Omega_C \to \mathbb{R}^N} \left\{ E(\mathbf{C}) = \int_{\Omega_S} \left[\sum_k^{n_s} \psi(|\mathbf{D}_k|) \right] + \alpha\varphi(||\nabla \mathbf{C}||) d\Omega_S \right\},$$
$$\text{with } \mathbf{D}_{k_{(\mathbf{p})}} = \mathbf{S}_{k_{(\mathbf{p})}} - \sum_j \tilde{B}_{k,j} \tilde{P}_j^{-1} \mathbf{C}_{j_{(\mathbf{p})}} \tag{6}$$

The best fitting coefficients are computed with a gradient descent coming from the Euler-Lagrange derivation of the energy E. This leads to a set of *multi-valued* partial derivate equation.

$$\begin{cases} \mathbf{C}_{t=0} & = \mathcal{U}_0 \\ \\ \frac{\partial \mathbf{C}_j}{\partial t} & = \sum_q \psi'(|\mathbf{D}_q|) \operatorname{sign}(\mathbf{D}_q) P_j^{-1} \tilde{B}_{q,j} + \alpha \operatorname{div}\left(\frac{\varphi'(||\nabla \mathbf{C}||)}{||\nabla \mathbf{C}||} \nabla \mathbf{C} \right) \end{cases} \tag{7}$$

Advantages: regularity

- Ensure a global regularity of the ODF field: $\varphi(||\nabla \mathbf{C}_{(\mathbf{p})}||)$

Spherical harmonics coefficients characterize anistropy [Frank02]

$l = 0$
Isotropic diffusion

$l = 2$
Single fibers orientation

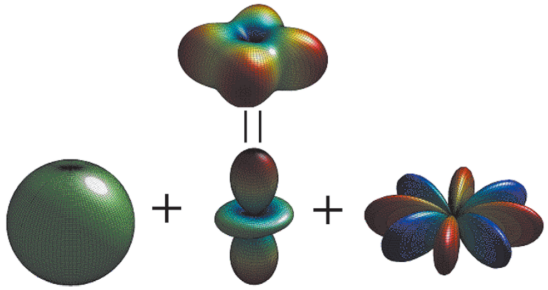

$l = 4$
Several fibers orientation

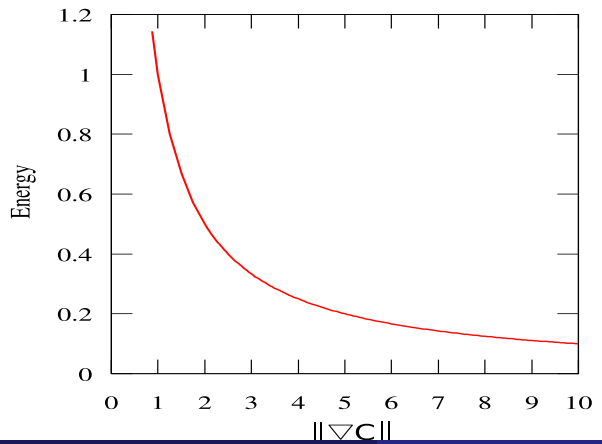

Example of possible regularization function φ

Advantages: adaptive to noise distribution

- ψ-likelihood function adapted to MRI noise law:

The best ψ function is the one specific to MR scanners, ie. Rice distribution
We seek $\mathbf{S}_r$ which maximizes a posteriori (MAP) the log-posterior probability

$$\log p(\mathbf{S}_r|\mathbf{S}) = \log p(\mathbf{S}|\mathbf{S}_r) + \log p(\mathbf{S}_r) - \log p(\mathbf{S}) \tag{8}$$

Consequently the pointwise likelihood is

$$\psi(\mathbf{S}_r) = \log p(\mathbf{S}|\mathbf{S}_r, \sigma) = \log \frac{\mathbf{S}}{\sigma^2} - \frac{(\mathbf{S}^2 + \mathbf{S}_r^2)}{2\sigma^2} + \log I_0\left(\frac{\mathbf{S} \cdot \mathbf{S}_r}{\sigma^2}\right) \tag{9}$$

[Basu,2006]

Simulation: influence of Rice model

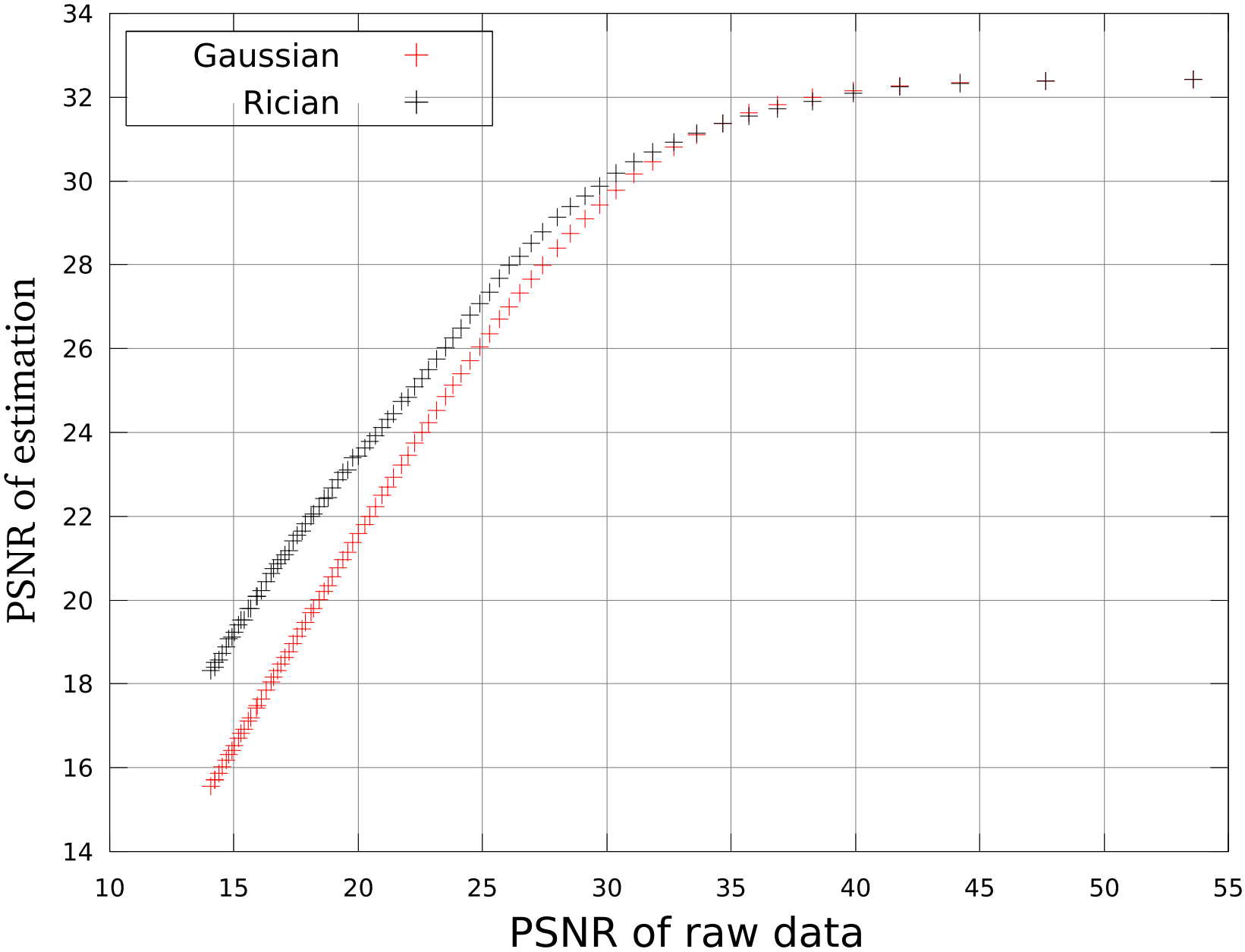

Results on synthetical data

DTI field

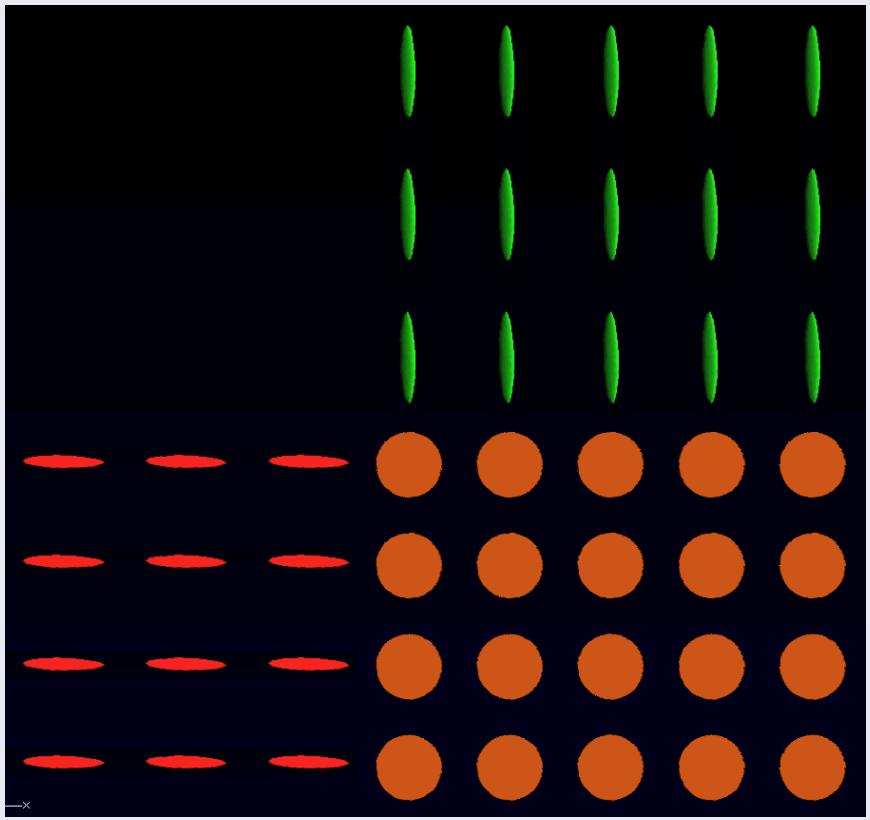

ODF field

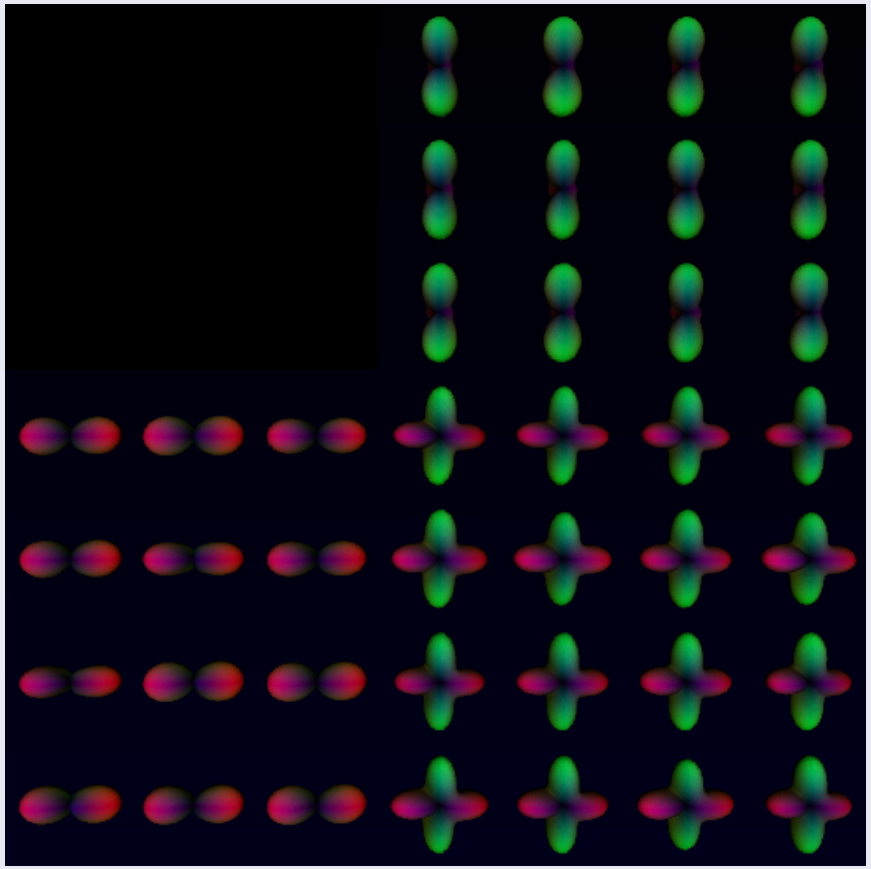

Results are good on perfect datasets, what about MRI acquisition noise ?

Results on human brain hardi data

GFA

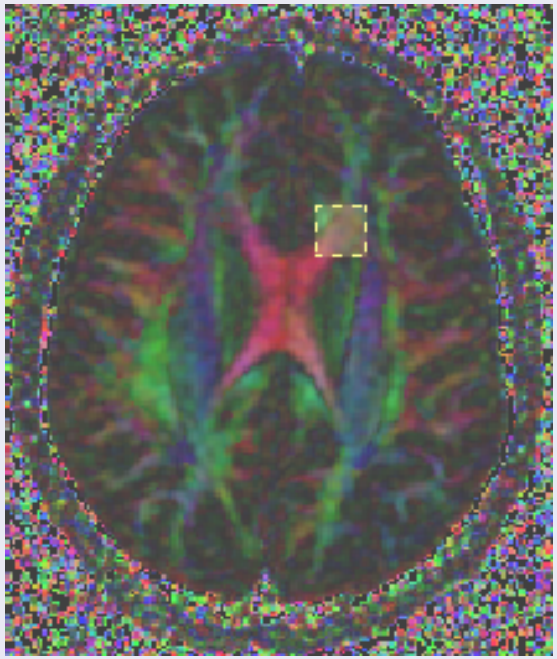

DTI field

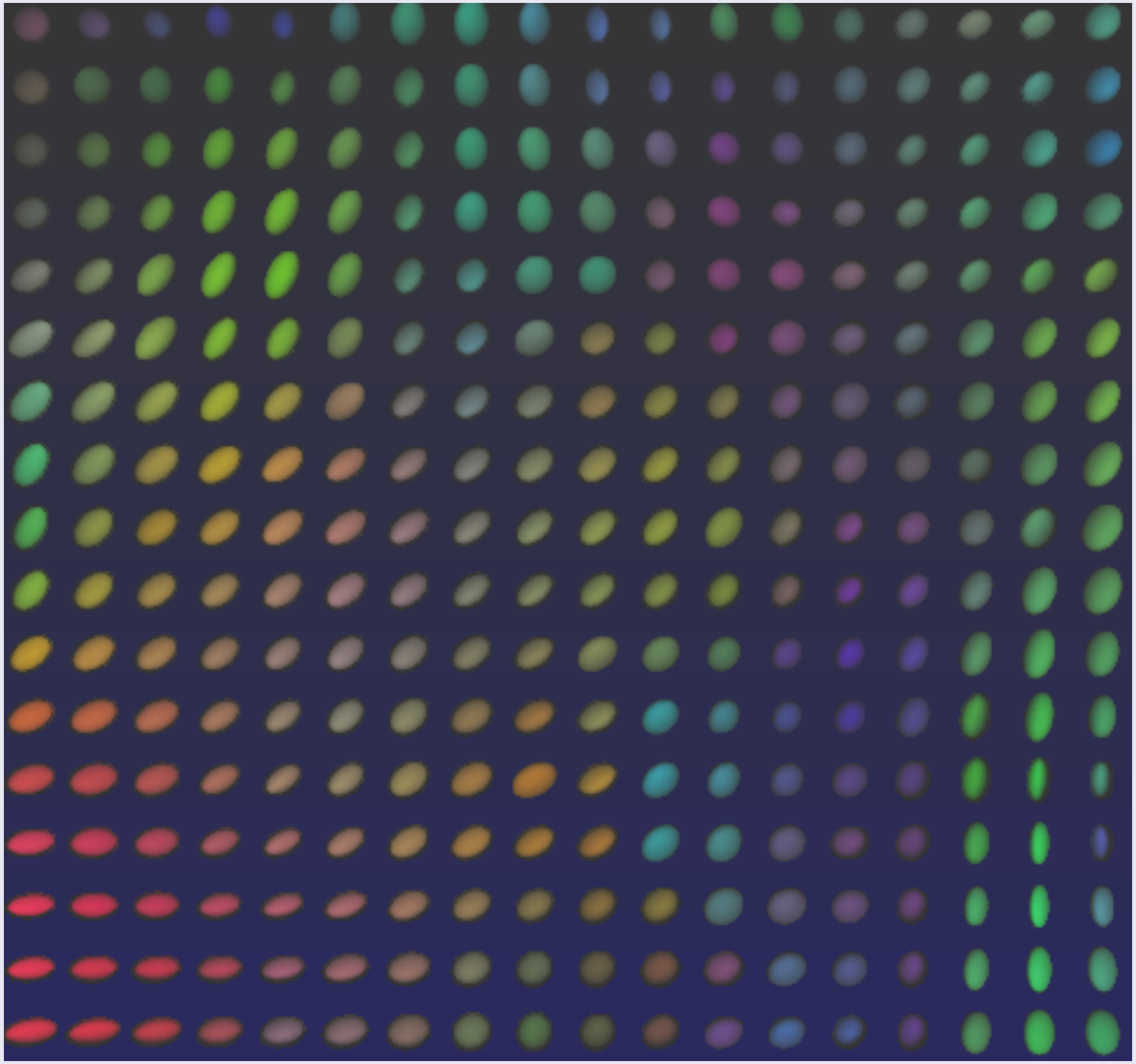

Results on human brain hardi data

GFA

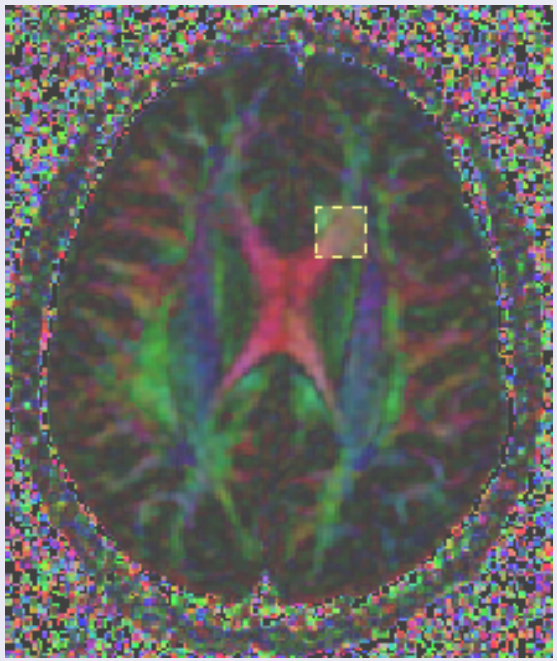

ODF field

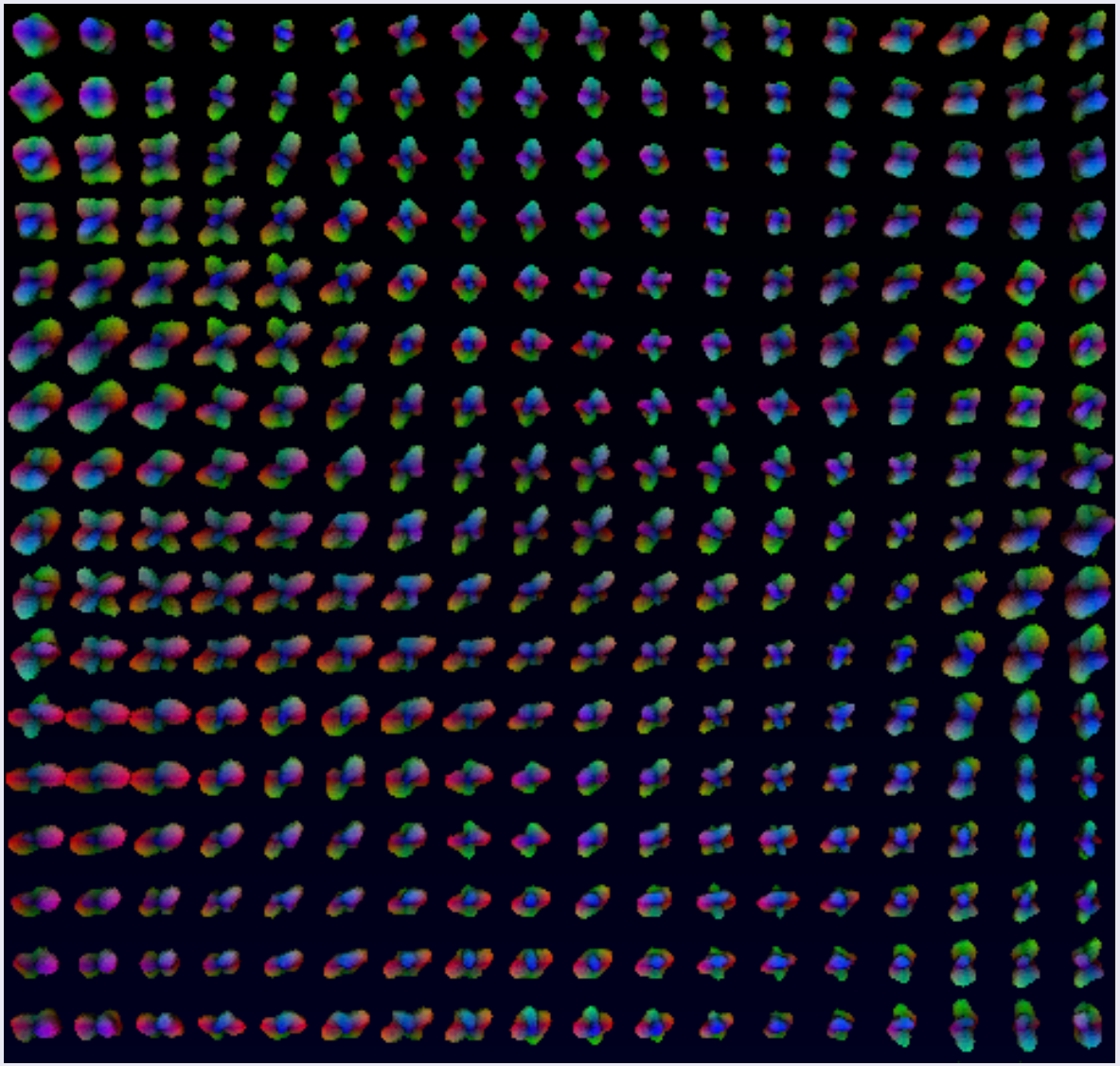

Simulation: energy minimization

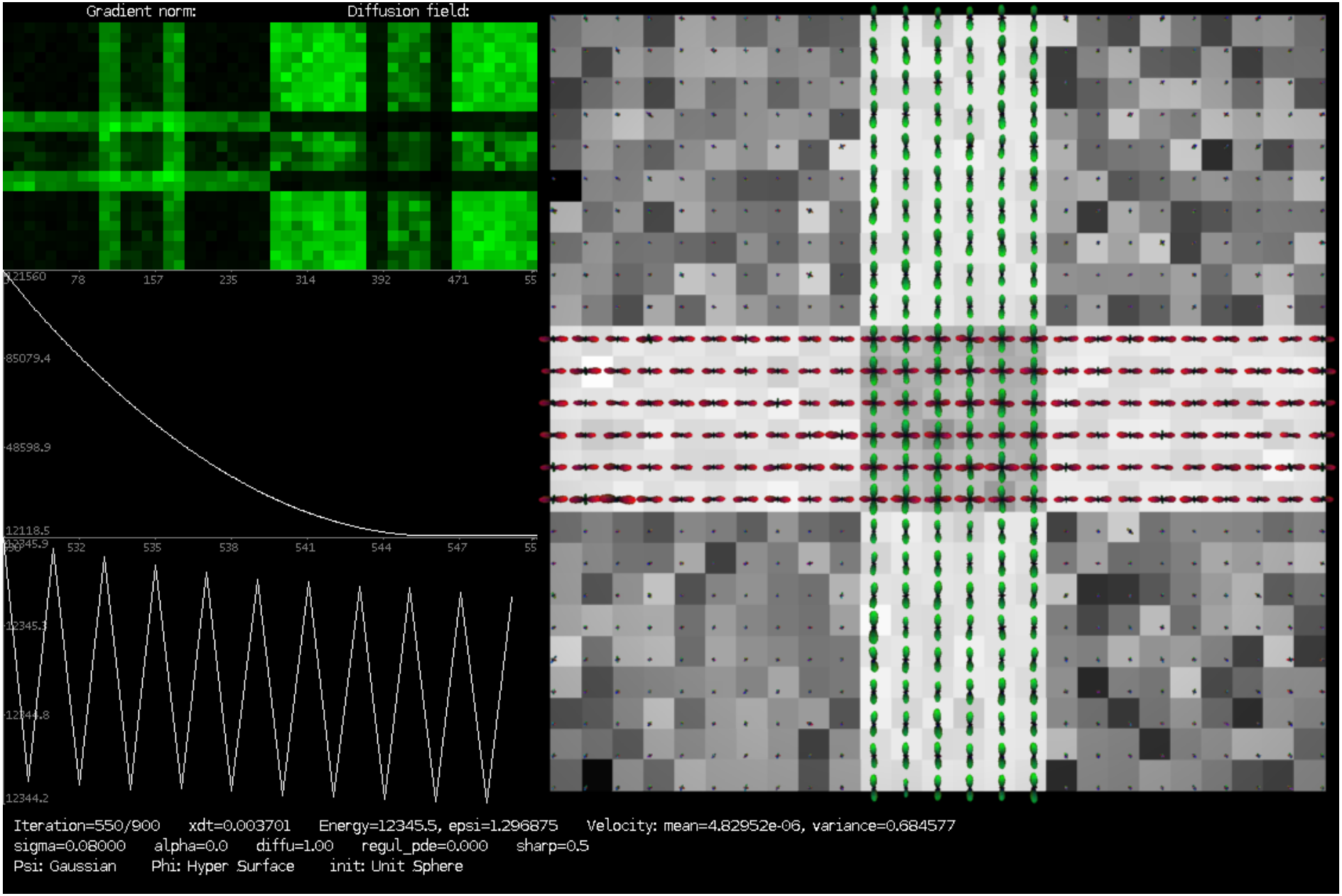

Simulation: regularization

without

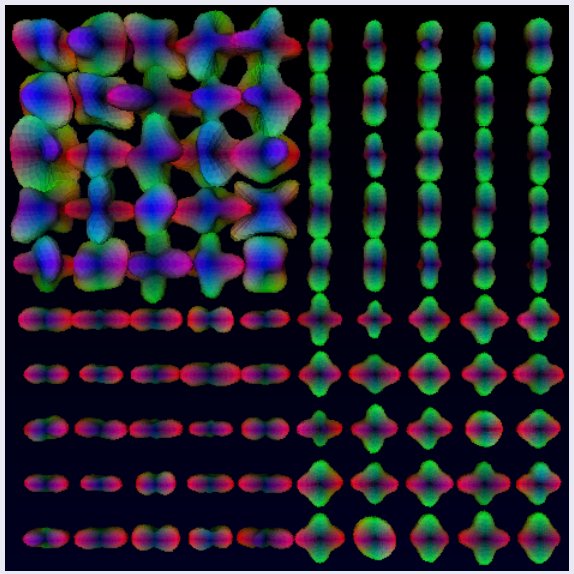

with

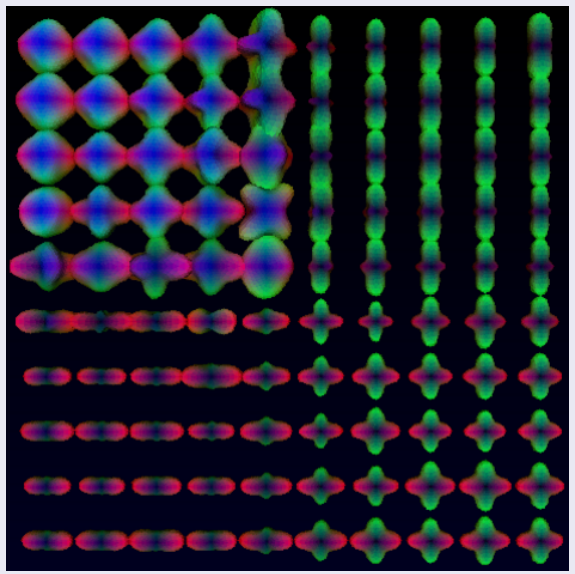

zoom

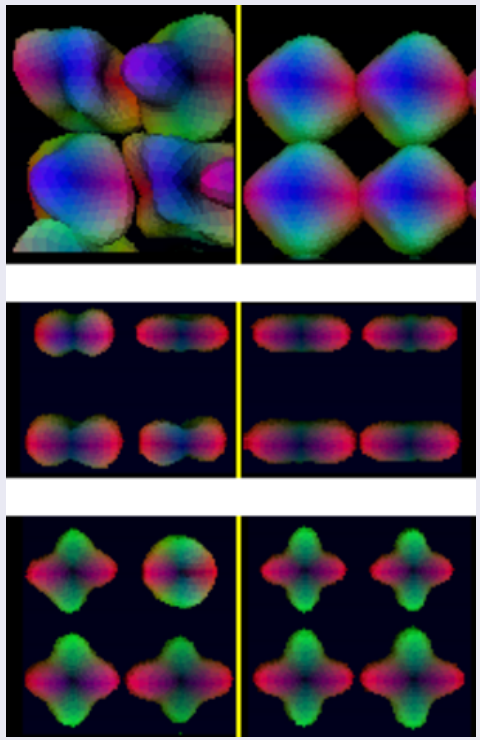

GFA

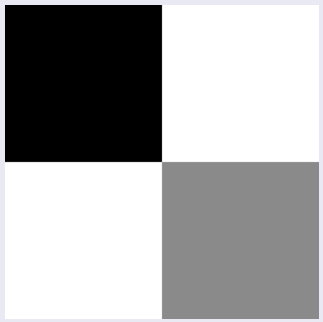

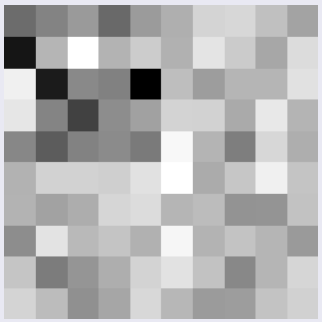

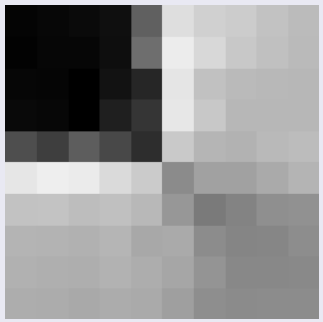

GFA

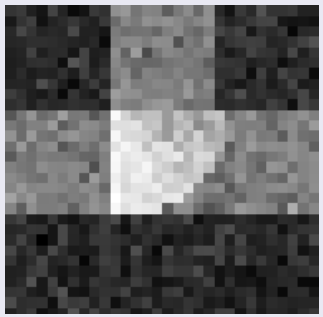

DTI

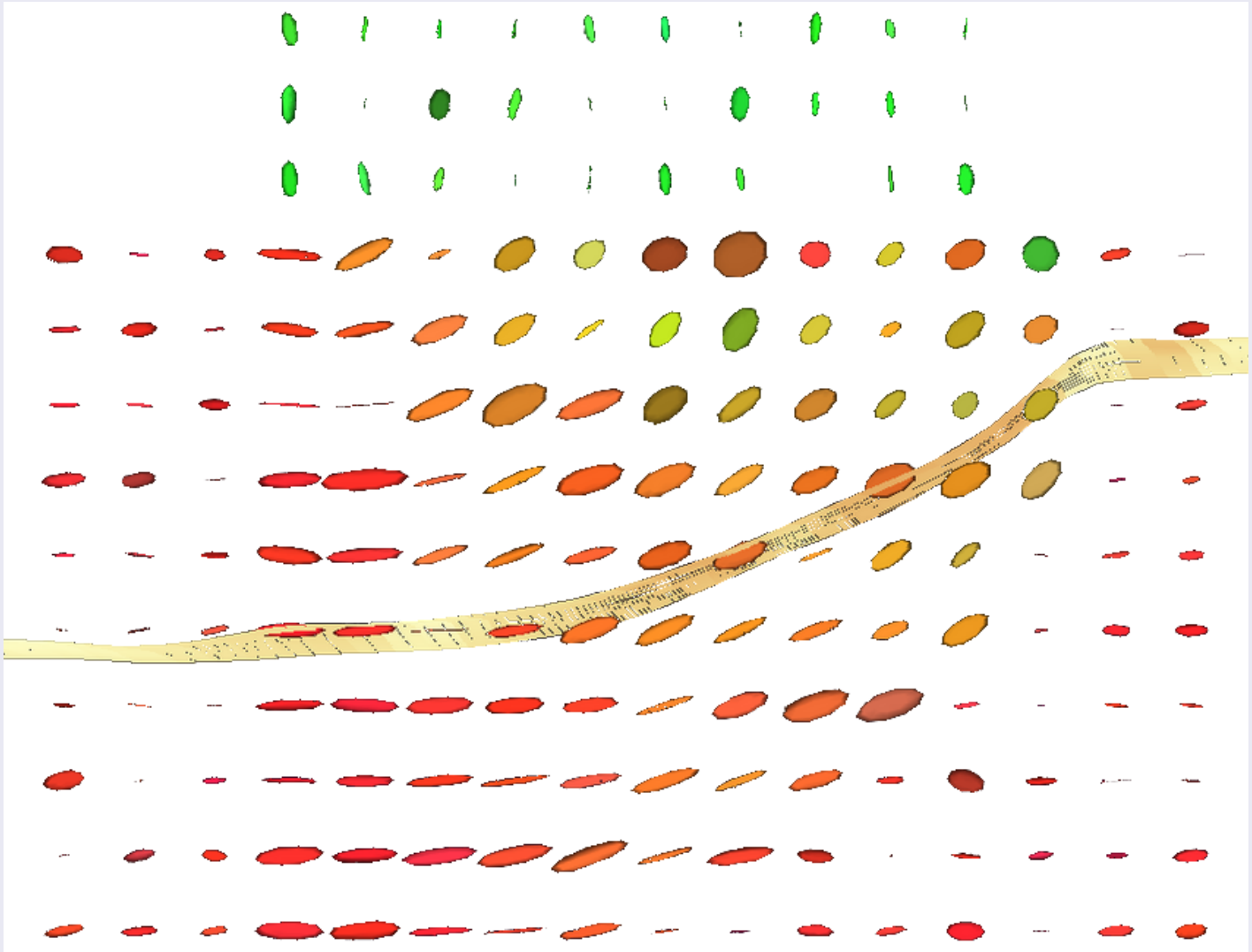

Consequences on fiber-tracking

GFA

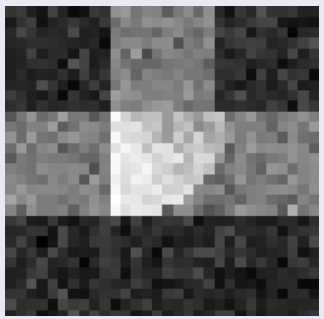

LS

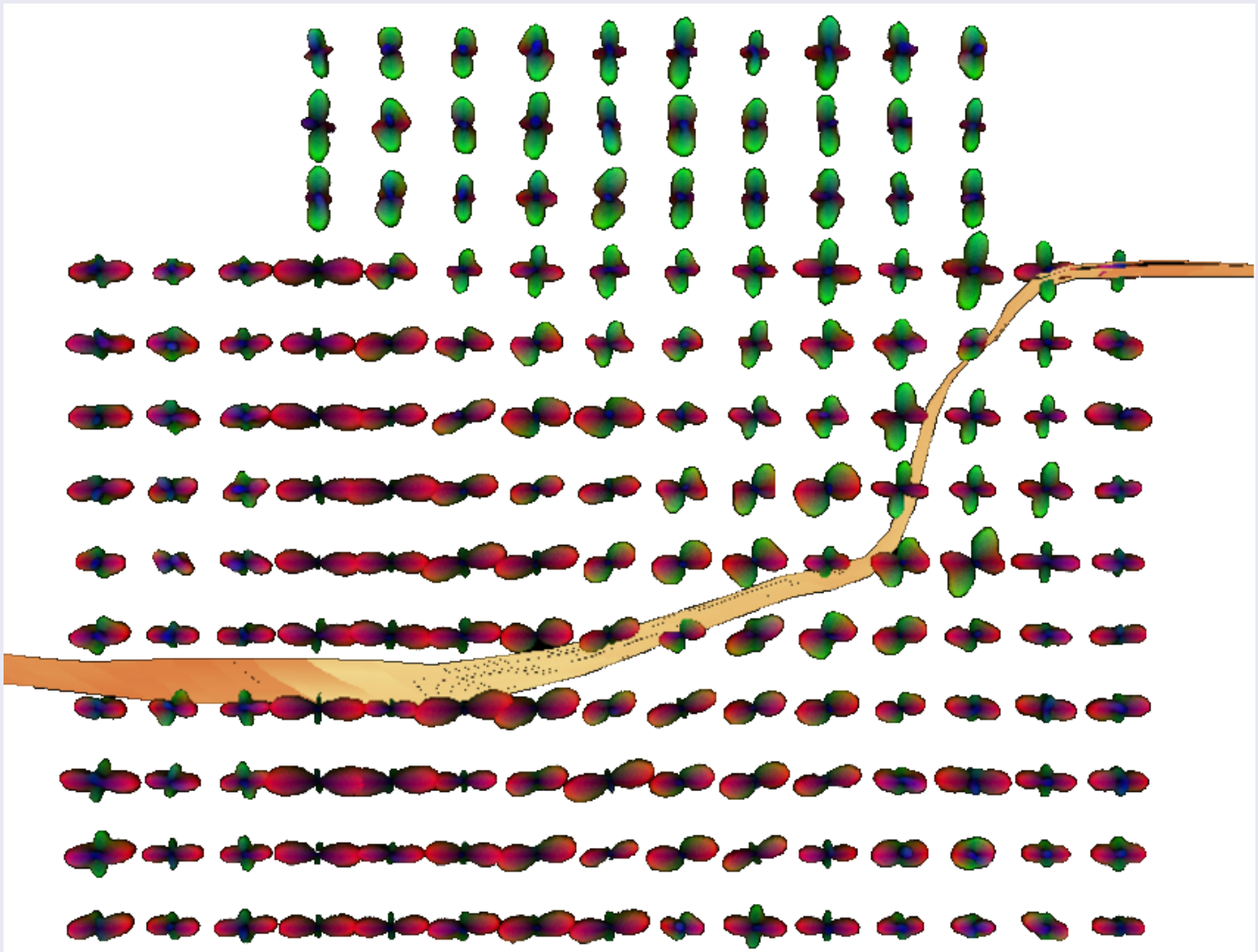

Consequences on fiber-tracking

GFA

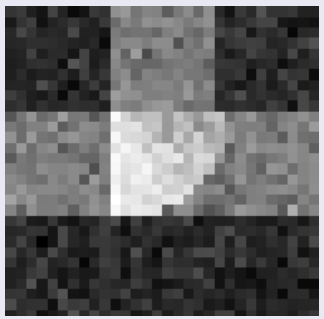

LS

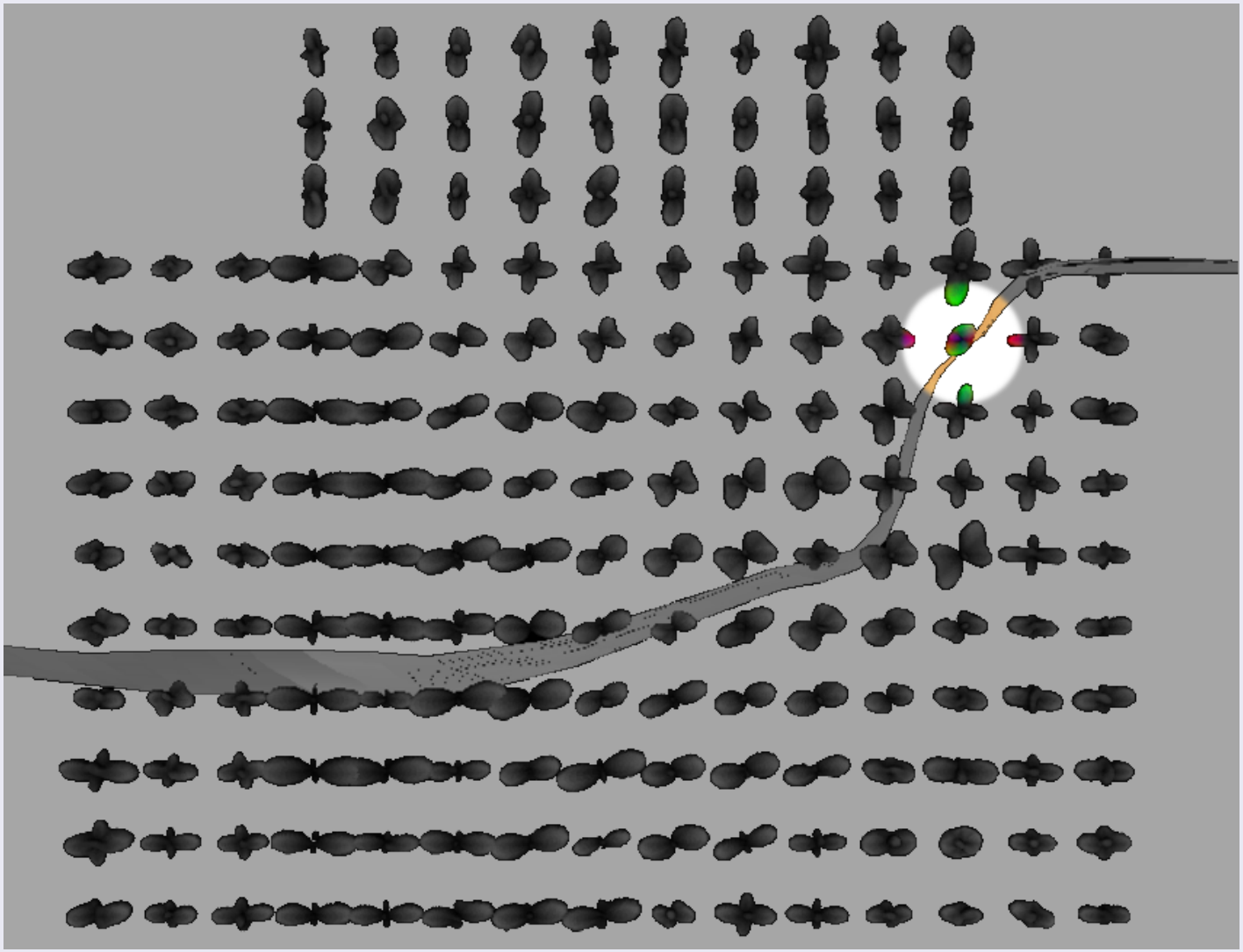

Consequences on fiber-tracking

GFA

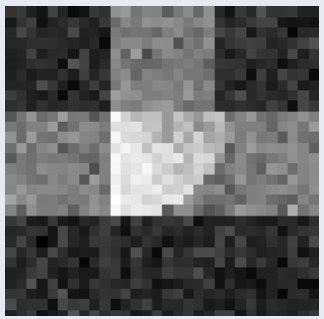

PDE

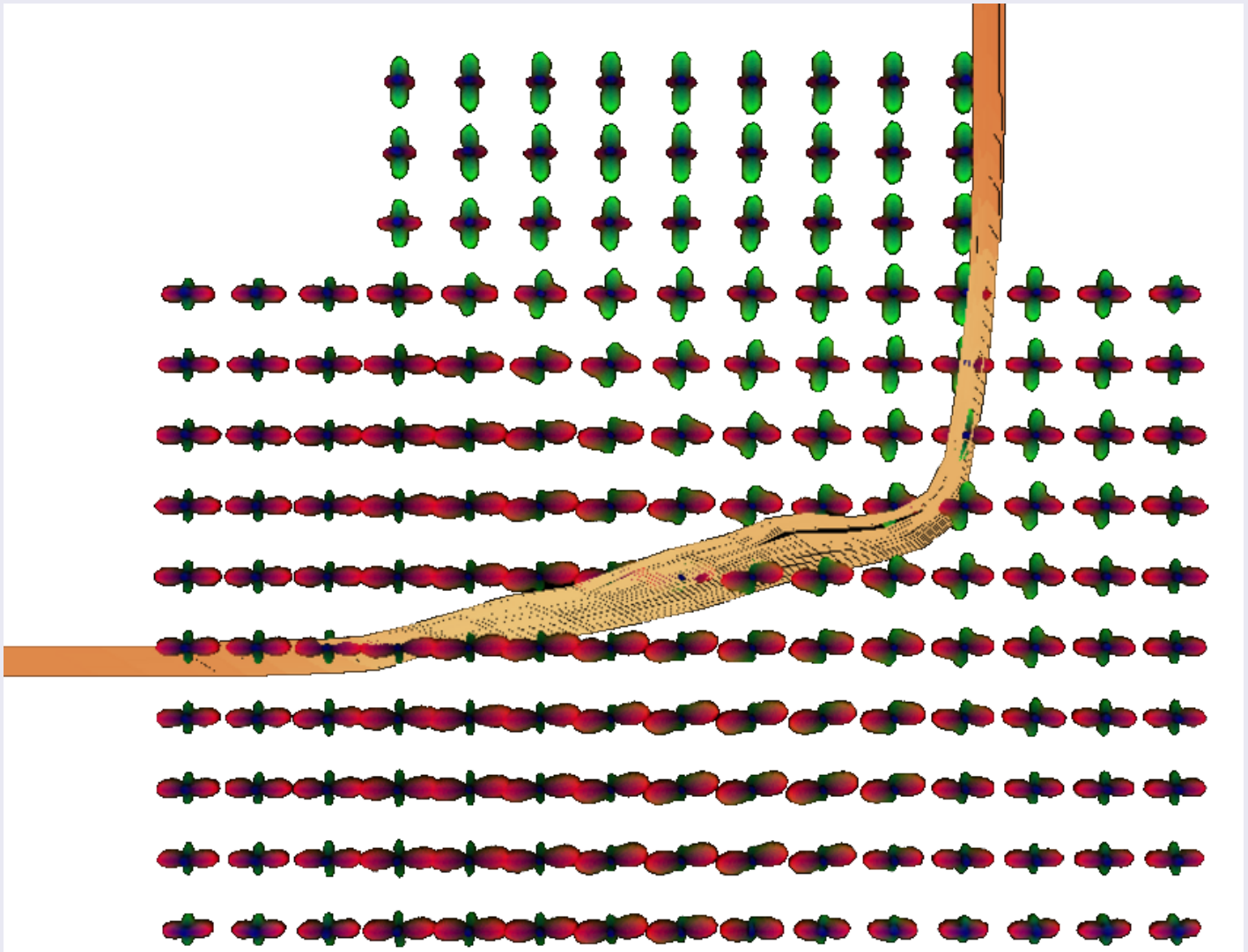

Fibertracking: regularization

As for DTI models, ODF fibertracking is very sensitive to noise.

without regularization

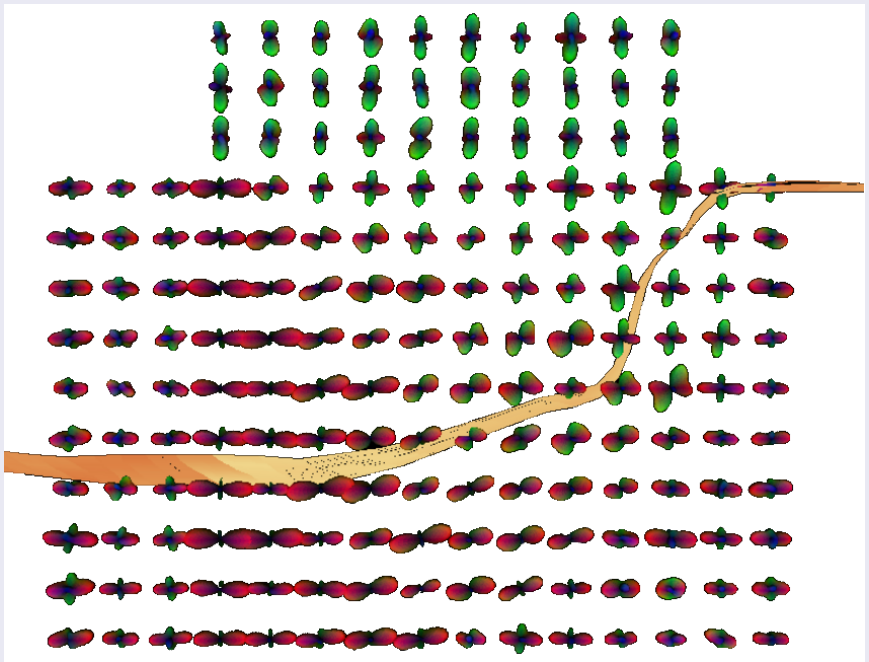

with regularization

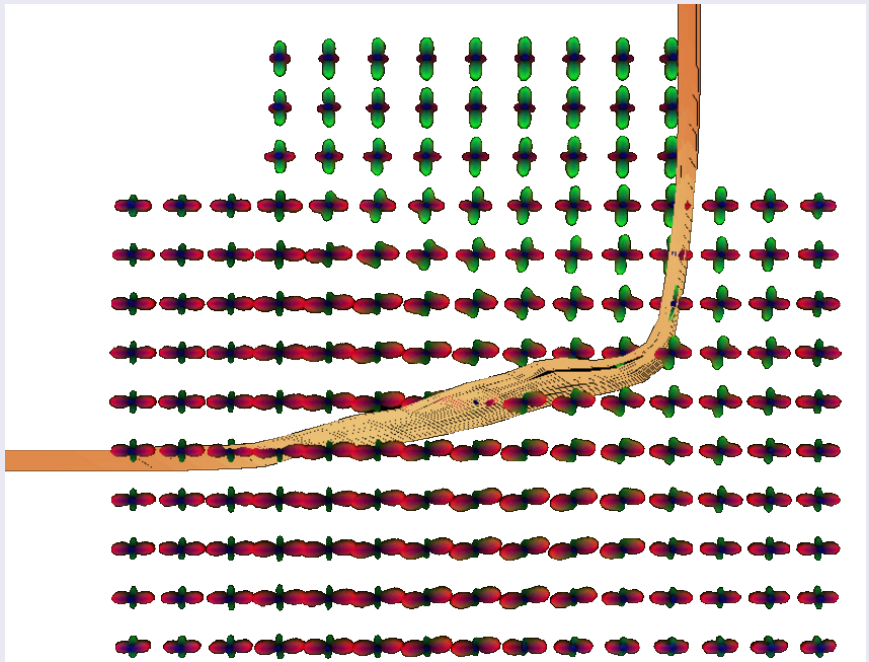

1 Context

2 DTI model : Diffusion Tensor Imaging

3 QBI model : Q-Ball Imaging

4 Measuring the PDF : DSI and Multi Q-Ball

5 Conclusions & Perspectives

Signal acquisition

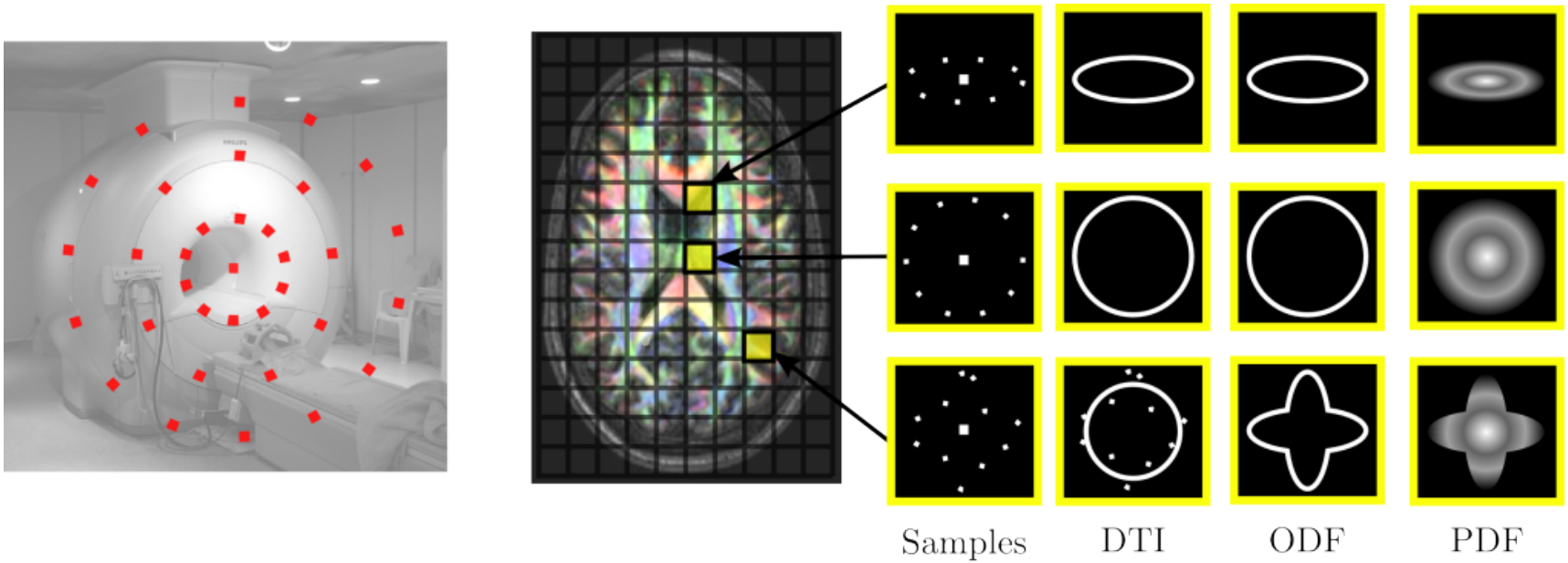

Figure: Diffusion MRI acquisition steps.

Why measuring the PDF ?

The PDF brings new important *radial* information.

Interest of Radial part of the PDF

- Information on cells micro-structure that composed the organic tissue. Ex: axon diameter, number of compartments.

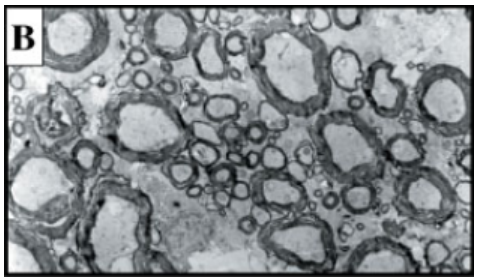

Spinal cord
[Cohen02]

- May increase detection of anomalies such as demyelinization, a symptom of multiple sclerosis.

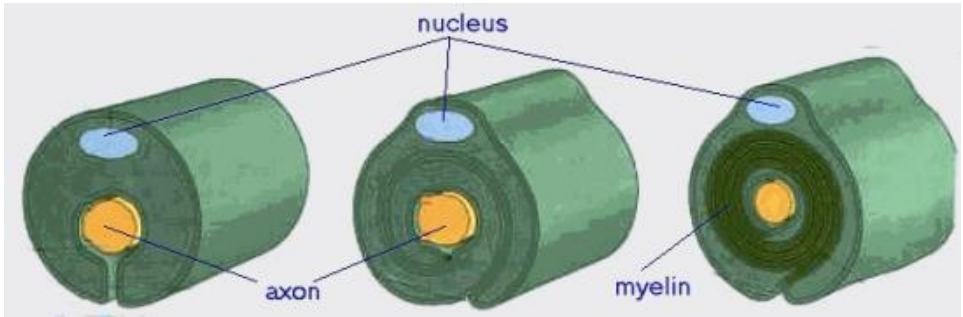

Figure: Myelination of an axone [www.jdaross.cwc.net]

Diffusion in a bi-homogeneous environment

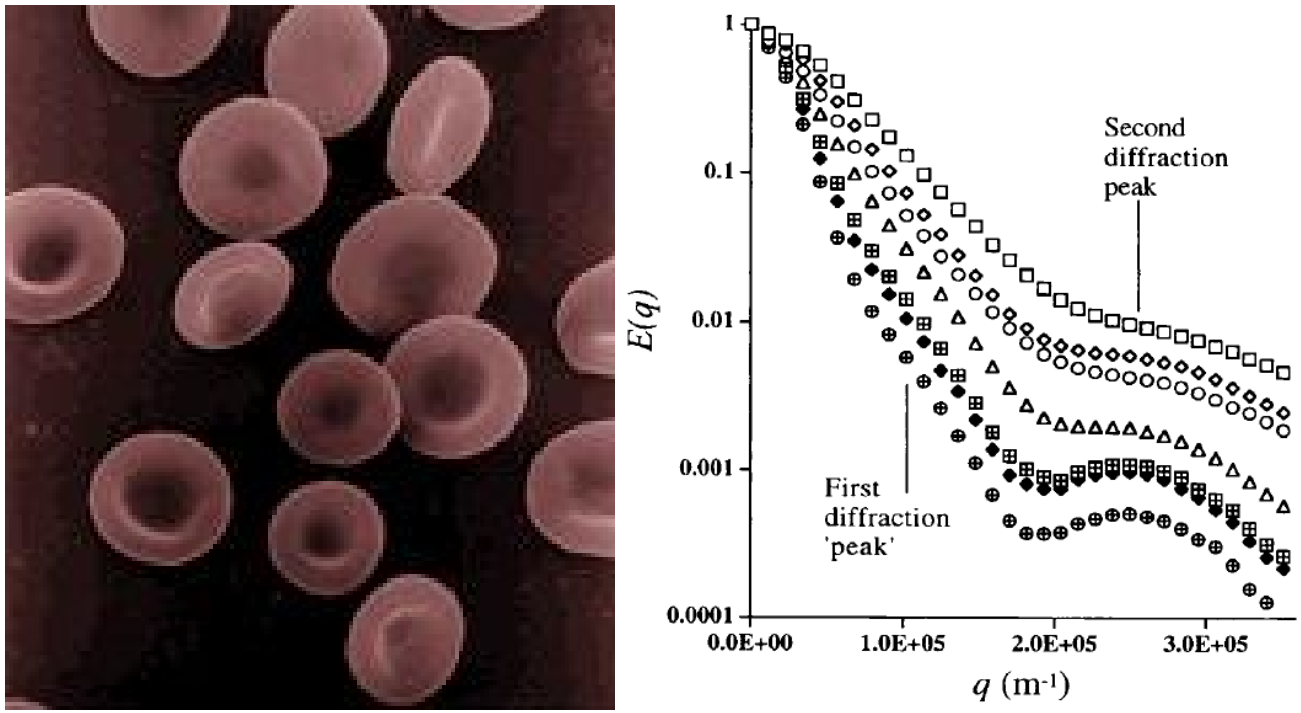

Figure: Experimental graph: human erythocytes rate for decreasing values of hematocrites. [Kuchel97]

Empirical approximation of signal by a bi-exponential function (compartiments: intra/extra diffusion).

Diffusion in a complex environment

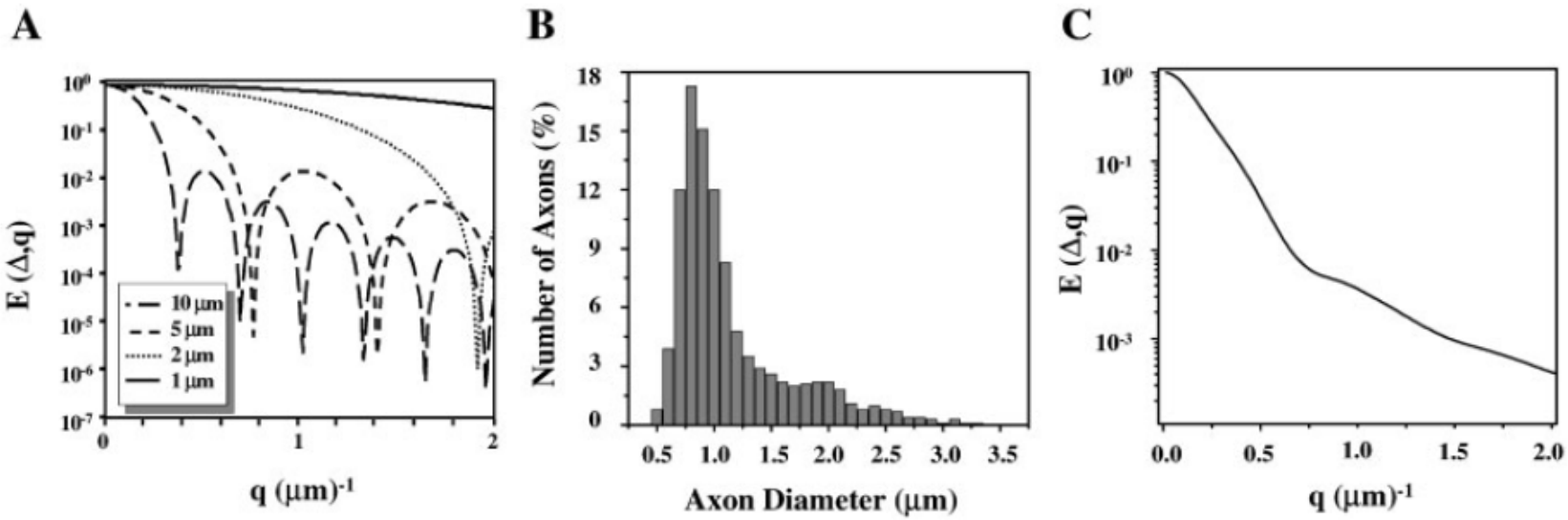

Figure: Simulation plot: fibers set of various diameters. [Cohen02]

Observations

Important information are found in the *radial* diffusion profile.

High Angular Resolution Diffusion Imaging

The Fourier Transform

$PDF(\mathbf{p}) = \int_{\mathbf{q}} E(\mathbf{q}) \exp(-2\pi i \mathbf{q}^T \mathbf{p}) d\mathbf{q}$ [Cory90,Callaghan91]

DSI: Fourier transform [Wedeen00]

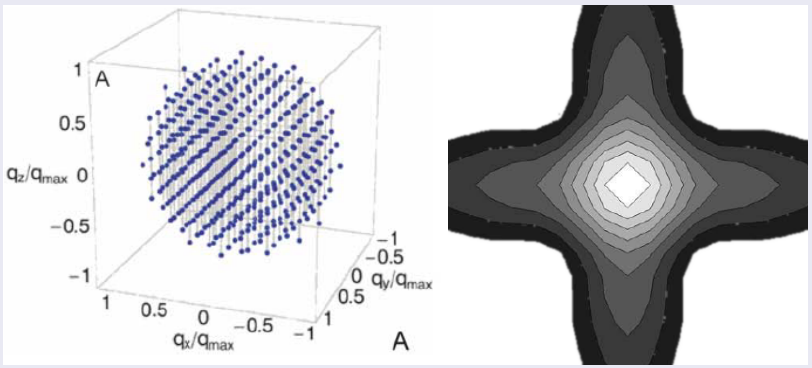

- Very long acquisition time
- Needs high gradients ⇒ Magnetic field distortion

High Angular Resolution Diffusion Imaging

The Fourier Transform

$PDF(\mathbf{p}) = \int_{\mathbf{q}} E(\mathbf{q}) \exp(-2\pi i \mathbf{q}^T \mathbf{p}) d\mathbf{q}$ [Cory90,Callaghan91]

DSI: Fourier transform [Wedeen00]

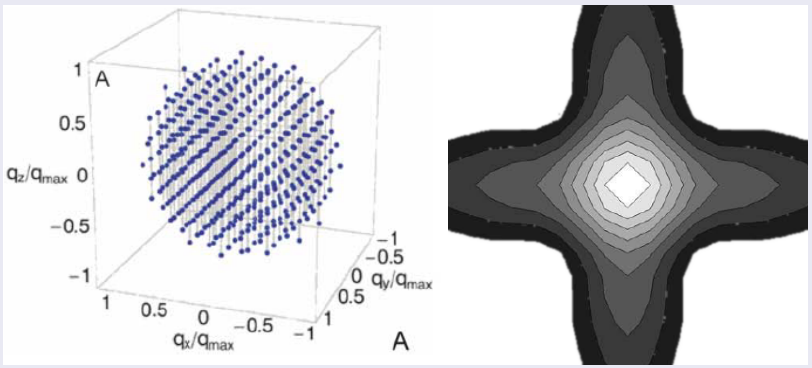

- Very long acquisition time
- Needs high gradients ⇒ Magnetic field distortion

Problem

The DSI is not clinical-compliant.

High Angular Resolution Diffusion Imaging

The Funk-Radon Transform

$$ODF(\mathbf{k}) = \int_{\mathbf{u} \perp \mathbf{k}} E(\mathbf{u}) d\mathbf{u}$$

HARDI: High Angular Diffusion Imaging [Tuch02]

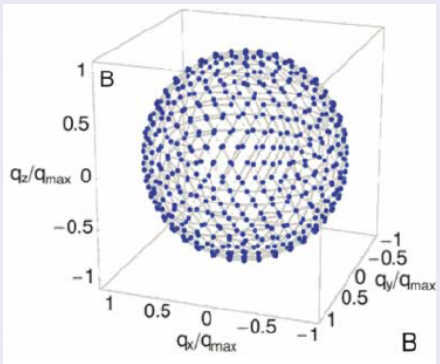

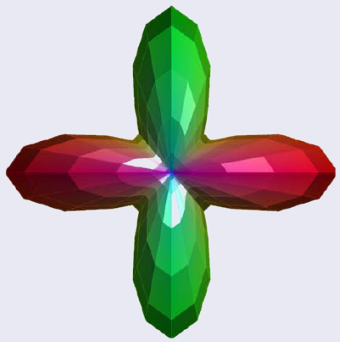

- Reduced acquisition time
- Lack of radial information

High Angular Resolution Diffusion Imaging

The Funk-Radon Transform

$ODF(\mathbf{k}) = \int_{\mathbf{u} \perp \mathbf{k}} E(\mathbf{u}) d\mathbf{u}$

HARDI: High Angular Diffusion Imaging [Tuch02]

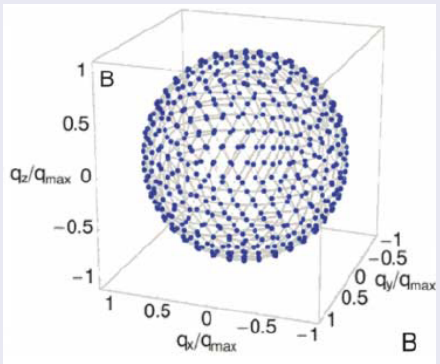

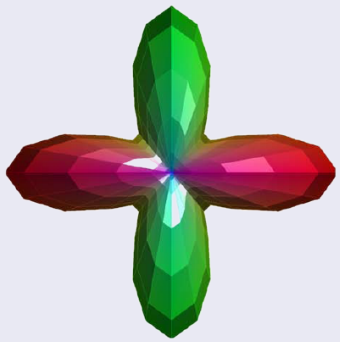

- Reduced acquisition time
- Lack of radial information

Problem

The ODF does not give any radial information.

HARDI Extension: multi-sphere imaging

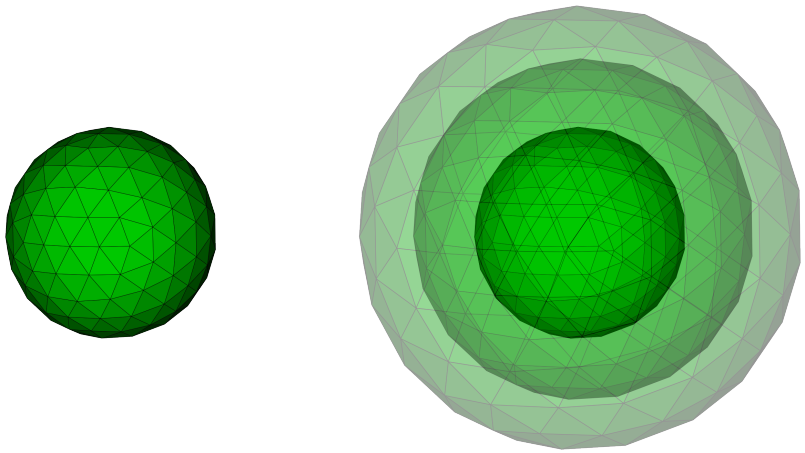

Figure: Example of HARDI extension [Assaf05, Özarslan06, Wu07, Khachaturian07, Assemlal-et.al08, Assemlal-et.al09].

Better distribution of samples on the Q-Space.

HARDI Extension: multi-sphere imaging

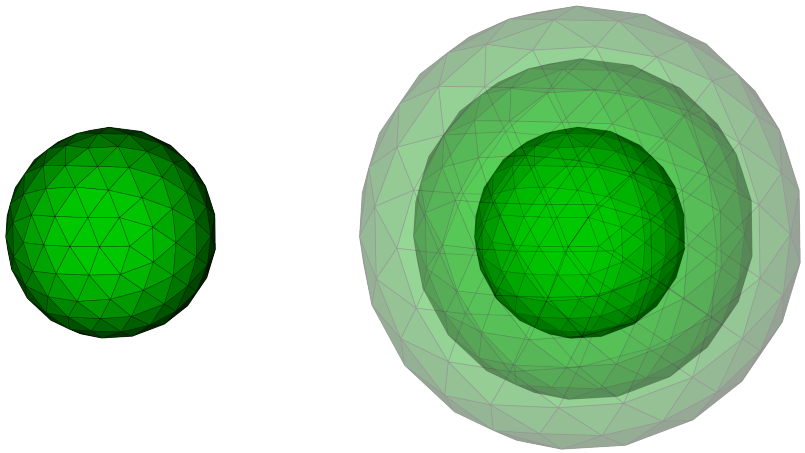

Figure: Example of HARDI extension [Assaf05, Özarslan06, Wu07, Khachaturian07, Assemlal-et.al08, Assemlal-et.al09].

Better distribution of samples on the Q-Space.

Problem

Still insufficient number of samples for a Fourier transform. Which mathematical tool for the signal estimation ?

Continuous representation of the signal

Continuous representation of the MR signal E in the following basis (Spherical Polar Fourier SPF):

$$E(\mathbf{q}) = \sum_{n=0}^{\infty} \sum_{l=0}^{\infty} \sum_{m=-l}^{l} a_{nlm} R_n(||\mathbf{q}||) y_l^m \left(\frac{\mathbf{q}}{||\mathbf{q}||} \right) \tag{10}$$

where a_{nlm} expansion coefficients, R_n and y_l^m are respectively are radial and angular atoms.
The basis is *orthonormal* in spherical coordinates:

$$\int_{\mathbf{q} \in \mathbb{R}^3} \left[R_n(||\mathbf{q}||) y_l^m \left(\frac{\mathbf{q}}{||\mathbf{q}||} \right) \right] \cdot \left[R_{n'}(||\mathbf{q}||) y_{l'}^{m'} \left(\frac{\mathbf{q}}{||\mathbf{q}||} \right) \right] d\mathbf{q} = \delta_{nn'll'mm'} \tag{11}$$

Radial Atoms

$$R_n\left(||\mathbf{q}||\right) = \left[\frac{2}{\gamma^{3/2}\,\Gamma\left(n+3/2\right)}\right]^{1/2} \exp\left(-\frac{||\mathbf{q}||^2}{2\gamma}\right) L_n^{1/2}\left(\frac{||\mathbf{q}||^2}{\gamma}\right) \qquad (12)$$

Radial Atoms

$$R_n\left(||\mathbf{q}||\right) = \left[\frac{2}{\gamma^{3/2}}\frac{n!}{\Gamma\left(n+3/2\right)}\right]^{1/2} \exp\left(-\frac{||\mathbf{q}||^2}{2\gamma}\right) L_n^{1/2}\left(\frac{||\mathbf{q}||^2}{\gamma}\right) \qquad (12)$$

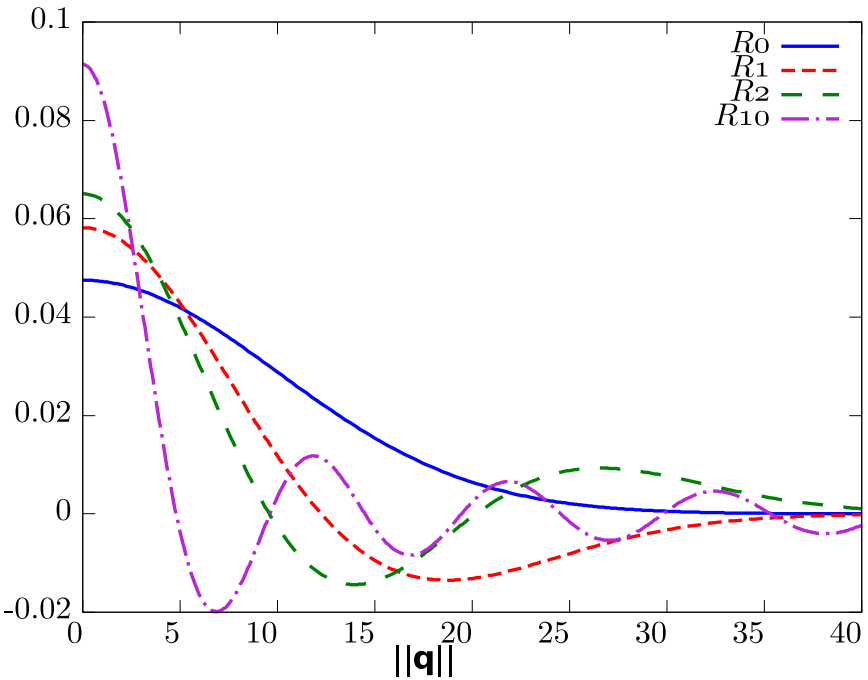

Figure: Some radial atoms R_n, $\gamma = 100$

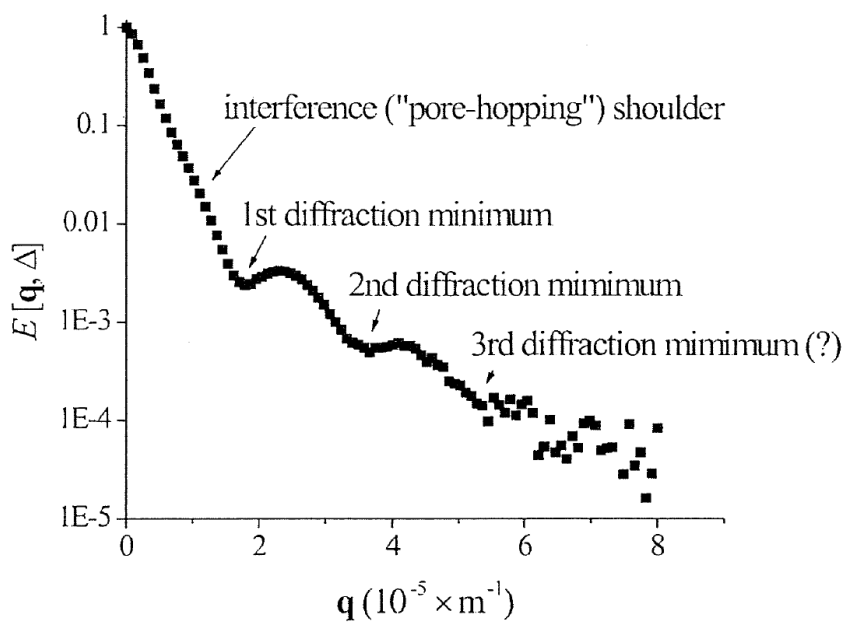

Figure: Experimental plot [Regan06]

Radial Atoms

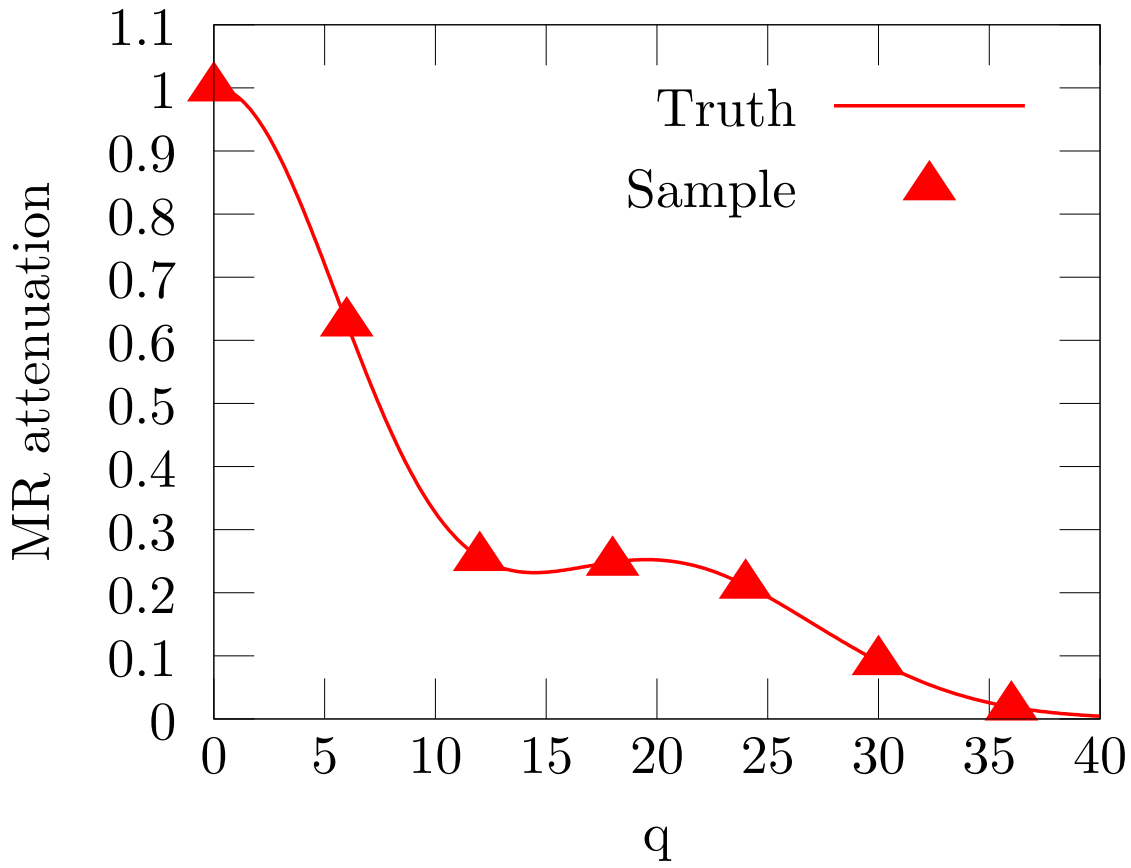

(a) Signal de diffusion

Figure: Radial reconstruction along with increasing truncation order N.

Radial Atoms

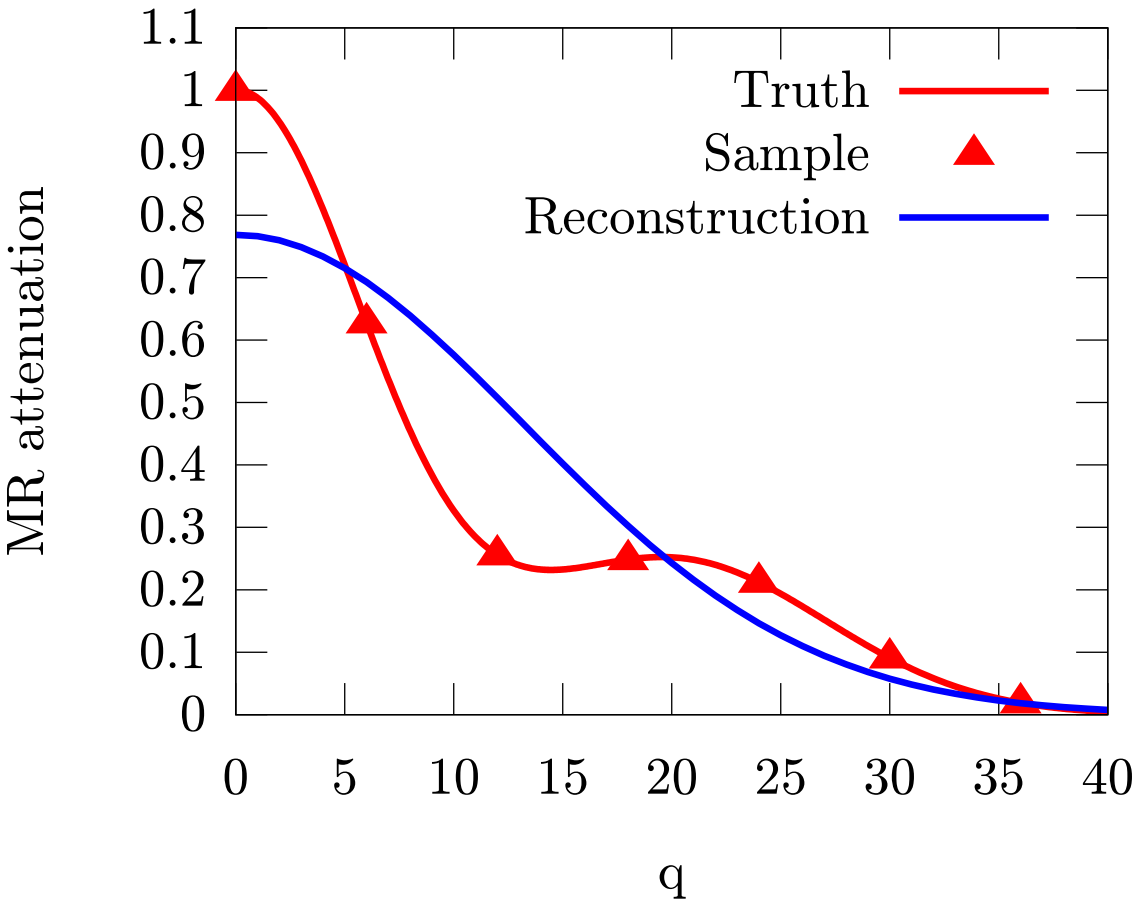

(a) 1 Coefficient

Figure: Radial reconstruction along with increasing truncation order N.

Radial Atoms

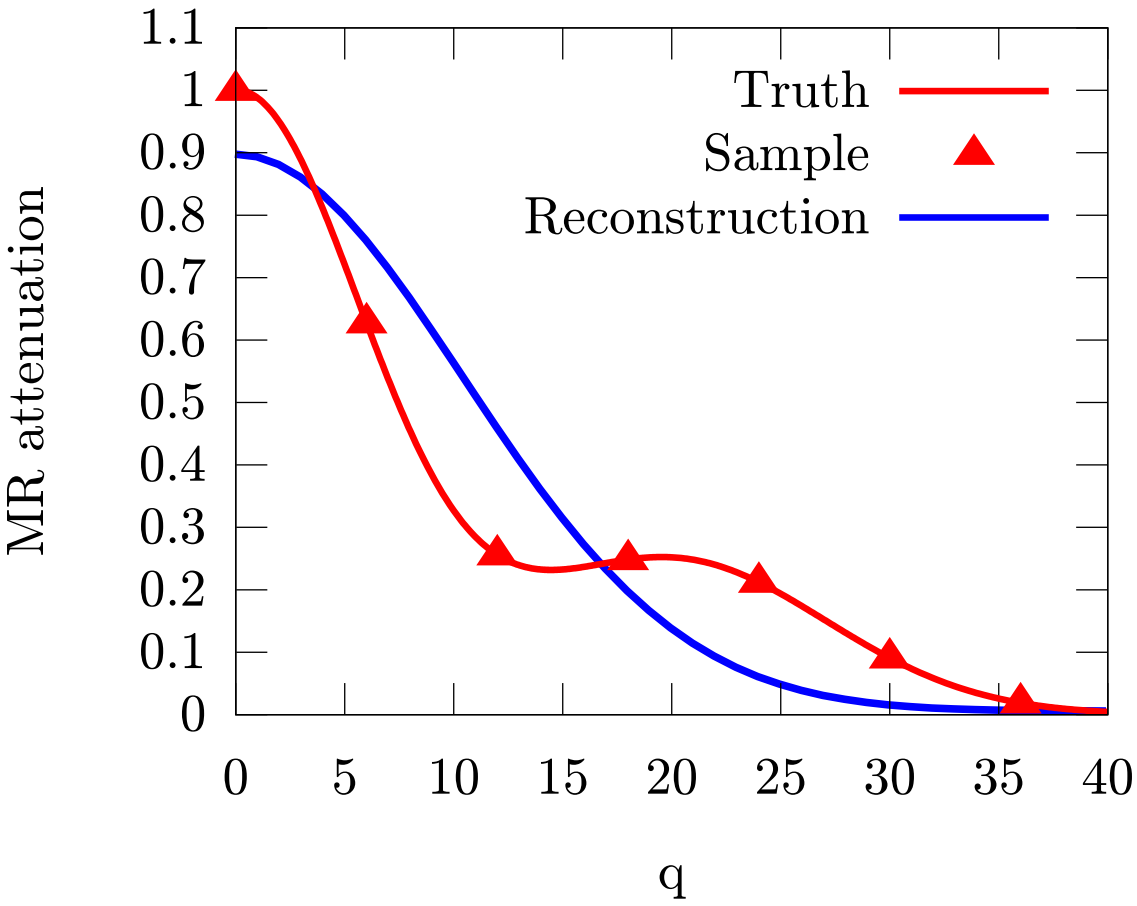

(a) 2 Coefficients

Figure: Radial reconstruction along with increasing truncation order N.

Radial Atoms

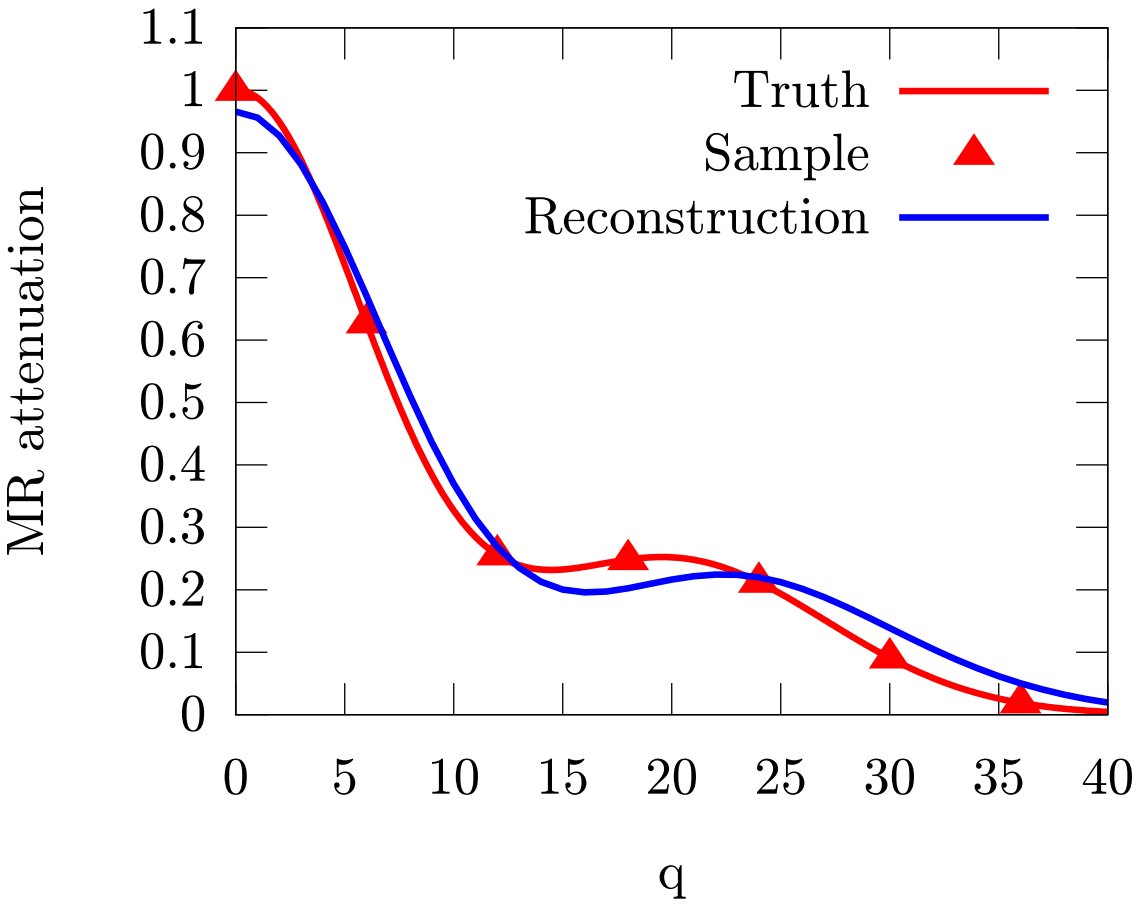

(a) 3 Coefficients

Figure: Radial reconstruction along with increasing truncation order N.

Radial Atoms

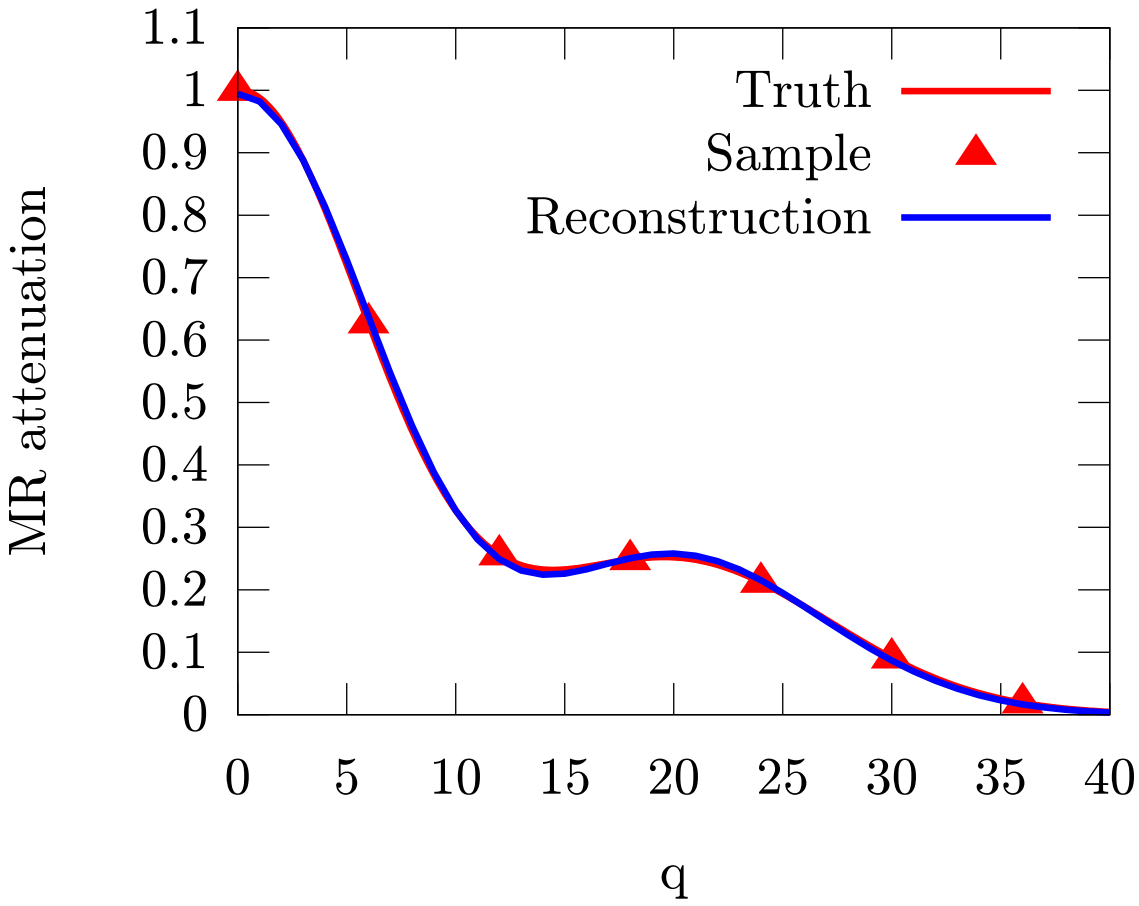

(a) 4 Coefficients

Figure: Radial reconstruction along with increasing truncation order N.

Radial Atoms

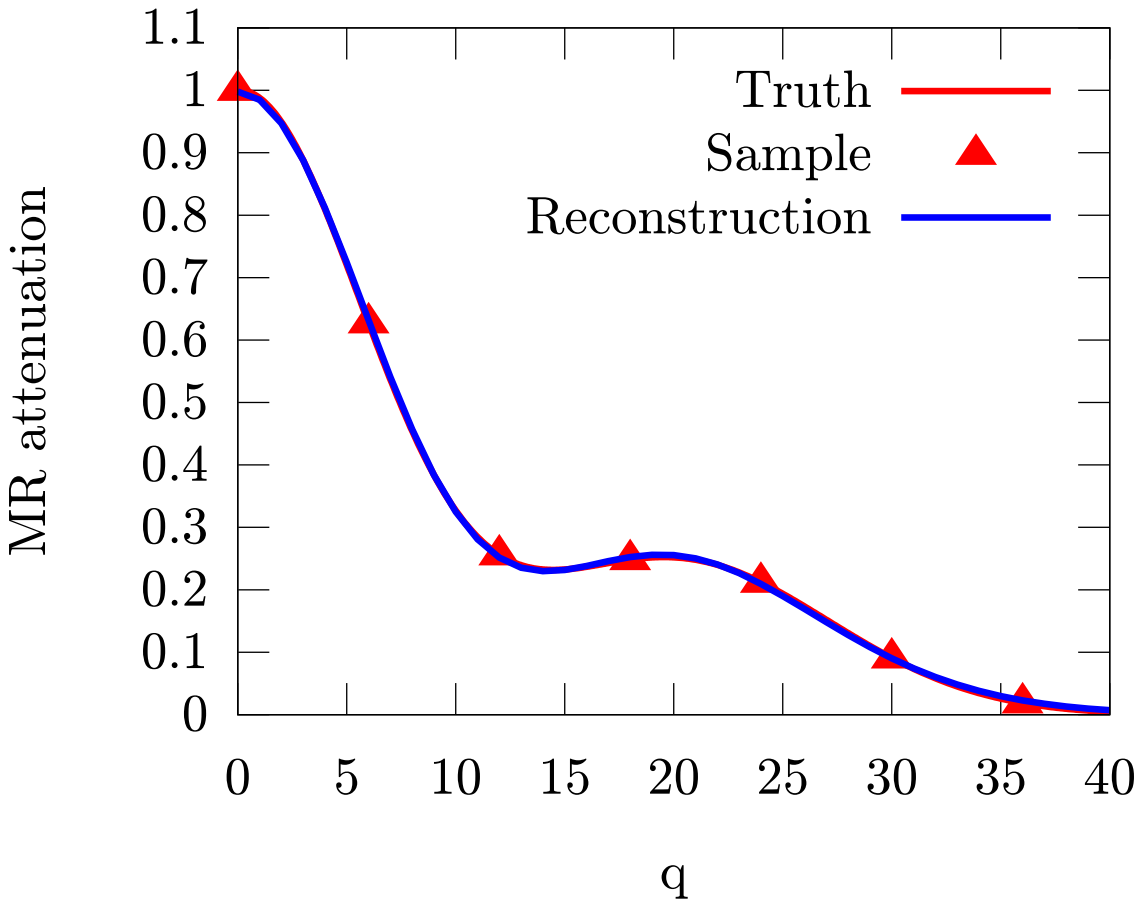

(a) 5 Coefficients

Figure: Radial reconstruction along with increasing truncation order N.

Fitting the data

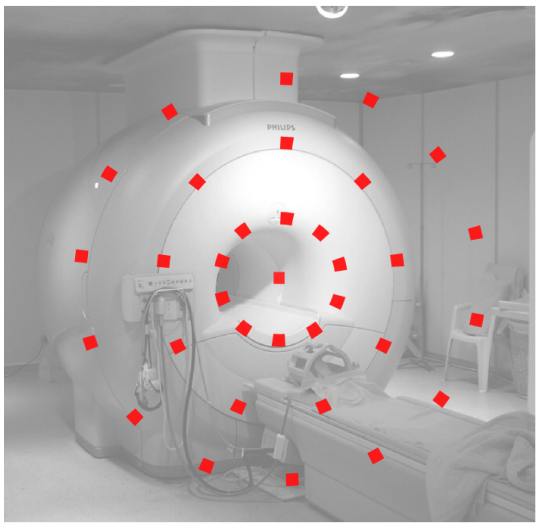

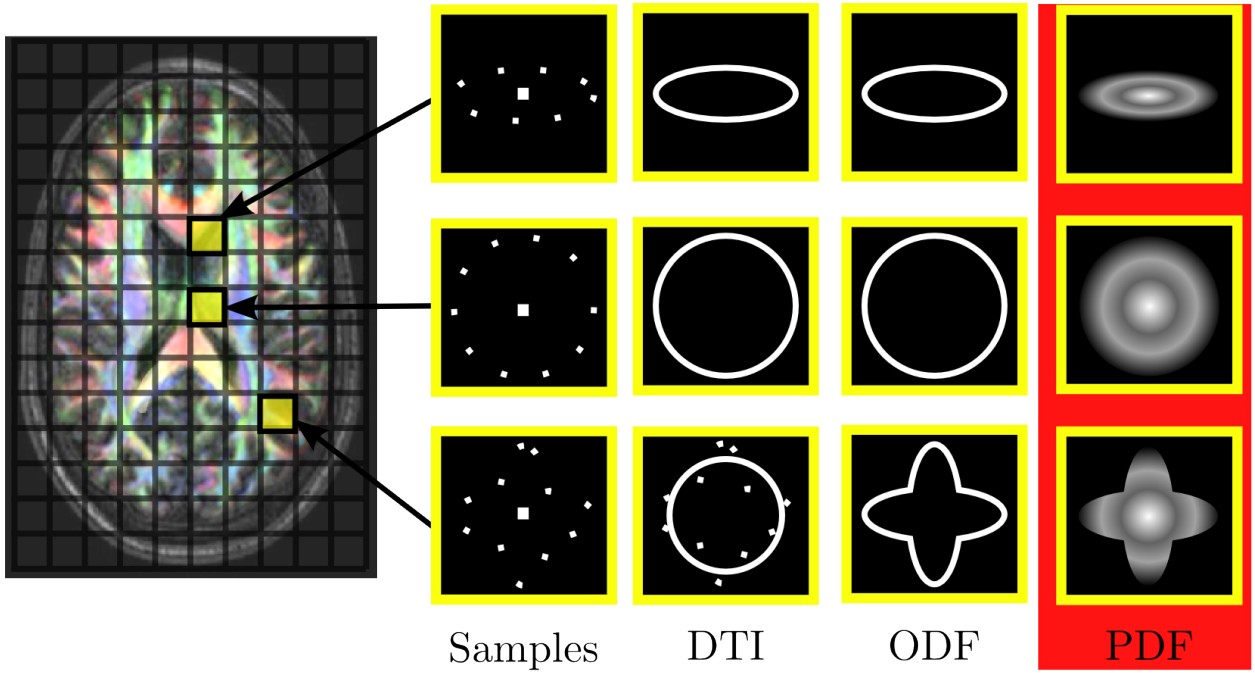

How to fit the data

From the diffusion samples, how do we retrieve the SPF coefficients ?

?

Linear signal estimation

The coefficient estimation is computed by the linear damped least square method:

$$\mathbf{A} = \arg\min_{\mathbf{A}} ||\mathbf{E} - \mathbf{M}\mathbf{A}||^2 + \lambda_l ||\mathbf{L}||^2 + \lambda_n ||\mathbf{N}||^2 \tag{13}$$

$$= (\mathbf{M}^T\mathbf{M} + \lambda_l \mathbf{L}^T\mathbf{L} + \lambda_n \mathbf{N}^T\mathbf{N})^{-1}\mathbf{M}^T\mathbf{E} \tag{14}$$

where $\mathbf{M}$ is the basis matrix, $\mathbf{E}$ is the MR signal vector and $\mathbf{A}$ is the coefficient vector:

$$\mathbf{M} = \begin{bmatrix} R_0(||\mathbf{q}_1||)y_0^0\left(\frac{\mathbf{q}_1}{||\mathbf{q}_1||}\right) & \dots & R_N(||\mathbf{q}_1||)y_L^L\left(\frac{\mathbf{q}_1}{||\mathbf{q}_1||}\right) \\ \vdots & \ddots & \vdots \\ R_0(||\mathbf{q}_{ns}||)y_0^0\left(\frac{\mathbf{q}_{ns}}{||\mathbf{q}_{ns}||}\right) & \dots & R_N(||\mathbf{q}_{ns}||)y_L^L\left(\frac{\mathbf{q}_{ns}}{||\mathbf{q}_{ns}||}\right) \end{bmatrix}, \tag{15}$$

$$\mathbf{E} = (E(\mathbf{q}_1), \dots, E(\mathbf{q}_{ns}))^T \tag{16}$$

$$\mathbf{A} = (a_{000}, \dots, a_{NLL})^T \tag{17}$$

Simulation: linear least square reconstruction

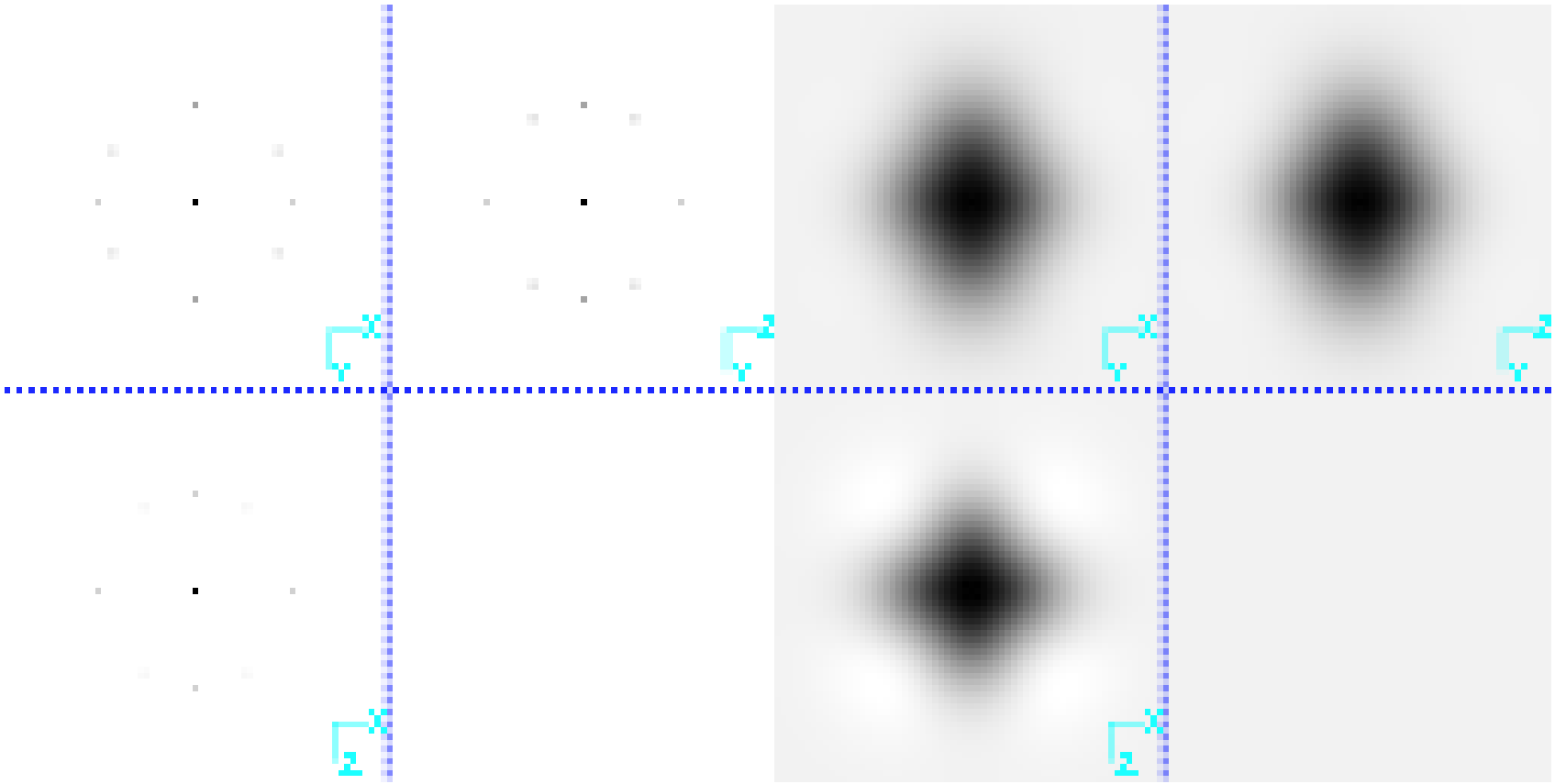

Figure: $N = 0$, $L = 4$, $\gamma = 100$,
1 sphere – 42 directions,
PSNR: 33.337902, 30 Coefficients

Simulation: linear least square reconstruction

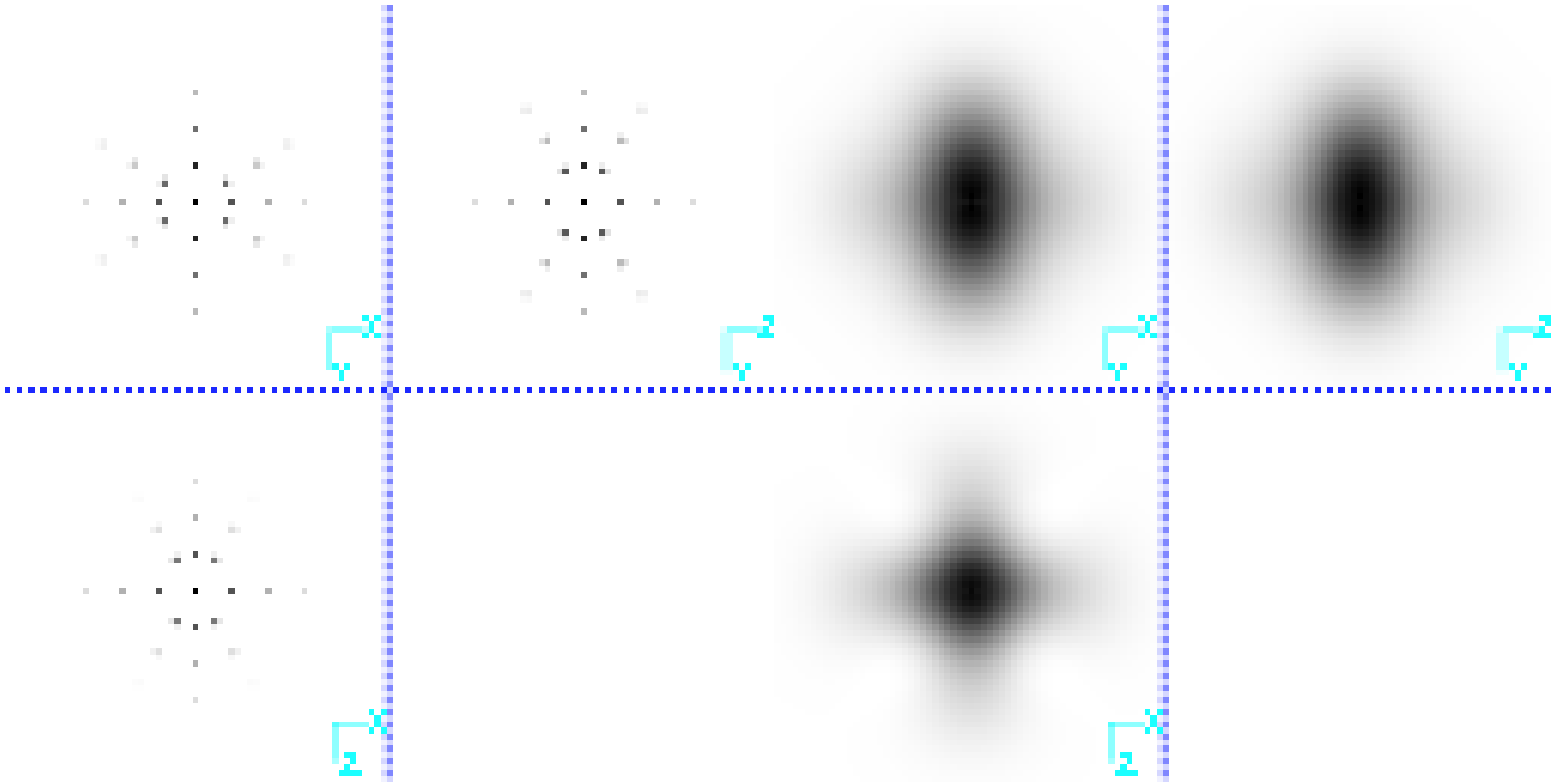

Figure: $N = 3$, $L = 4$, $\gamma = 70$,
3 spheres – 42 directions,
PSNR: 45.172752, 45 Coefficients

Simulation: linear least square reconstruction

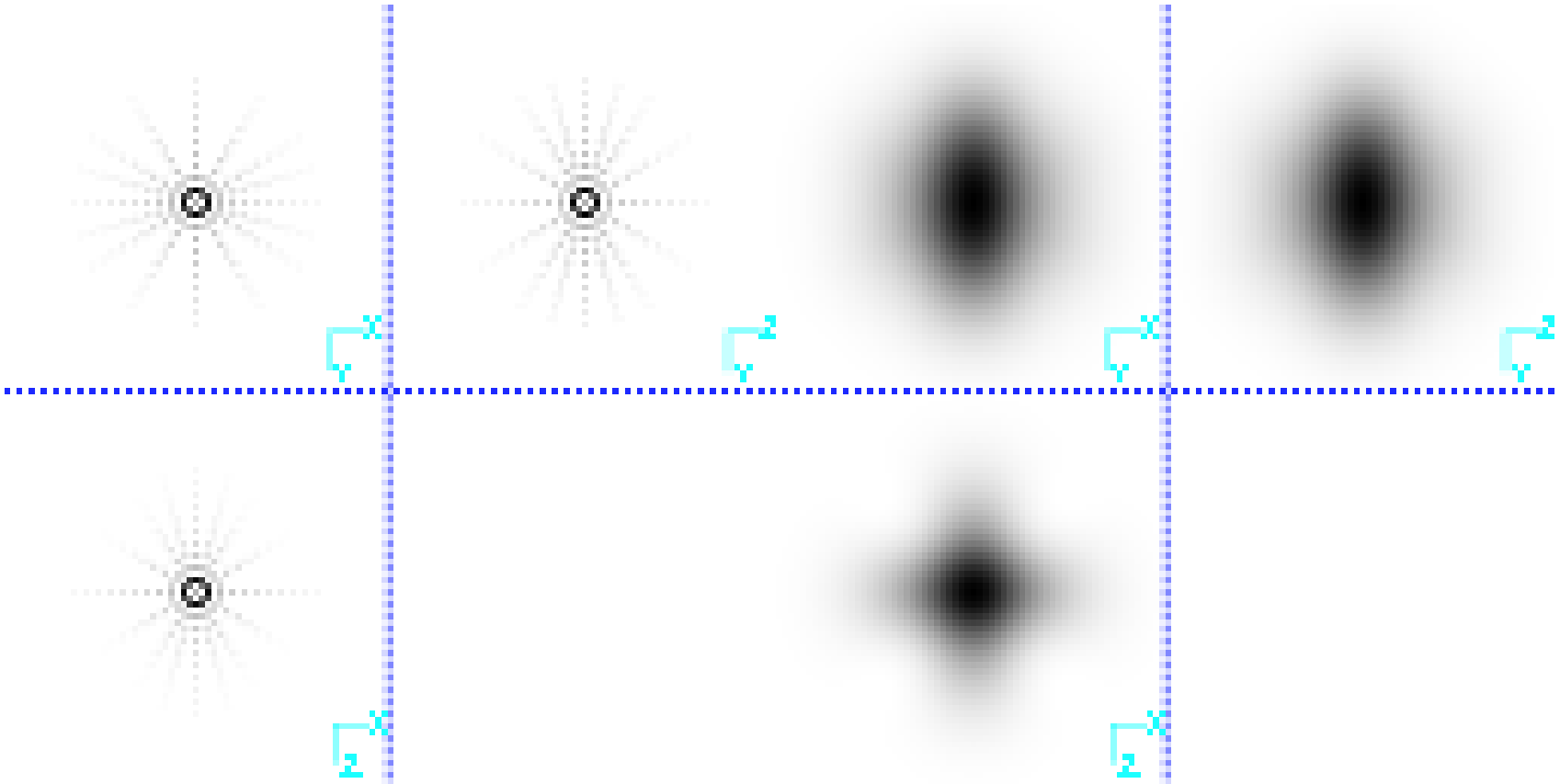

Figure: $N = 5$, $L = 6$, $\gamma = 50$,
10 spheres – 162 directions,
PSNR: 50.255381, 168 Coefficients

Features of the PDF

Now that we have a continuous reconstruction of the diffusion signal E, how do we compute the PDF ?

Features of the PDF

Now that we have a continuous reconstruction of the diffusion signal E, how do we compute the PDF ?

We don't. This would require a lot of computation. Besides, the PDF is cumbersome to display.

Features of the PDF

Now that we have a continuous reconstruction of the diffusion signal E, how do we compute the PDF ?

We don't. This would require a lot of computation. Besides, the PDF is cumbersome to display.

We are interesting in a data reduction suitable to display: *features* of the PDF.

$$\mathcal{G}(\mathbf{k}) = \int_{p \in \mathbb{R}^3} PDF(\mathbf{p})\, H_{\mathbf{k}}(\mathbf{p}) d\mathbf{p} \tag{18}$$

Features of the PDF: projection

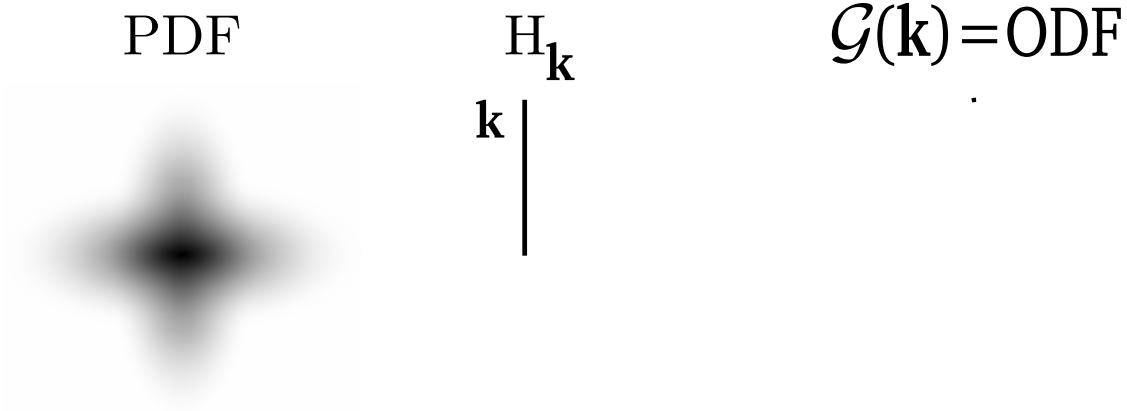

Figure: Example: ODF feature.

$$\mathcal{G}(\mathbf{k}) = \int_{p \in \mathbb{R}^3} PDF(\mathbf{p})\, H_{\mathbf{k}}(\mathbf{p}) d\mathbf{p} \tag{19}$$

Features of the PDF: projection

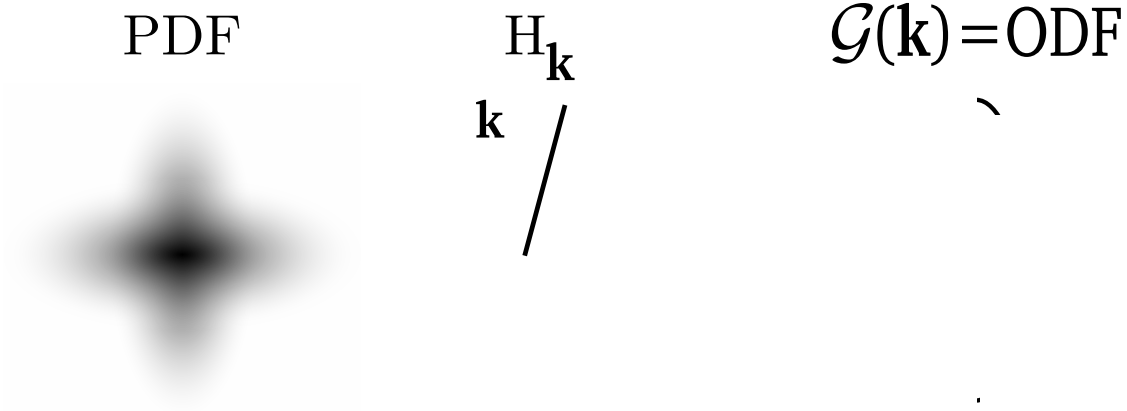

Figure: Example: ODF feature.

$$\mathcal{G}(\mathbf{k}) = \int_{p \in \mathbb{R}^3} PDF(\mathbf{p})\, H_{\mathbf{k}}(\mathbf{p}) d\mathbf{p} \tag{19}$$

Features of the PDF: projection

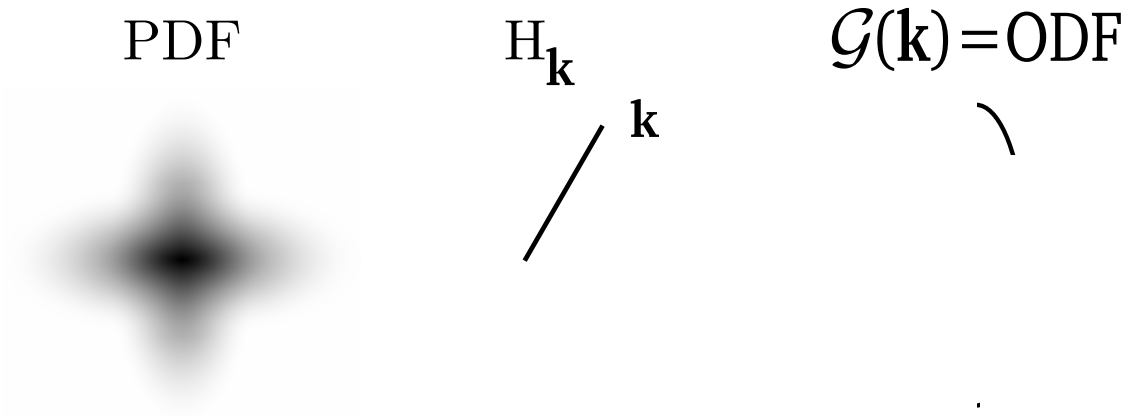

Figure: Example: ODF feature.

$$\mathcal{G}(\mathbf{k}) = \int_{p \in \mathbb{R}^3} PDF(\mathbf{p})\, H_{\mathbf{k}}(\mathbf{p}) d\mathbf{p} \tag{19}$$

Features of the PDF: projection

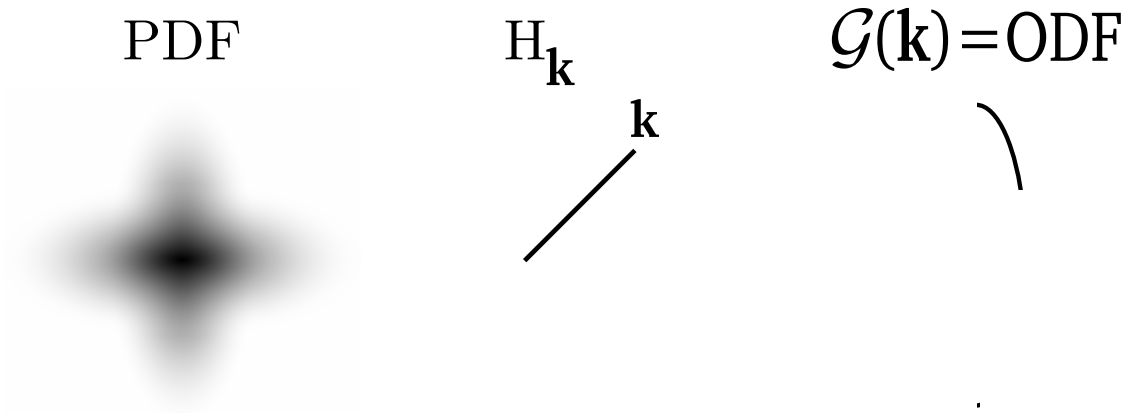

Figure: Example: ODF feature.

$$\mathcal{G}(\mathbf{k}) = \int_{p \in \mathbb{R}^3} PDF(\mathbf{p})\, H_{\mathbf{k}}(\mathbf{p}) d\mathbf{p} \tag{19}$$

Features of the PDF: projection

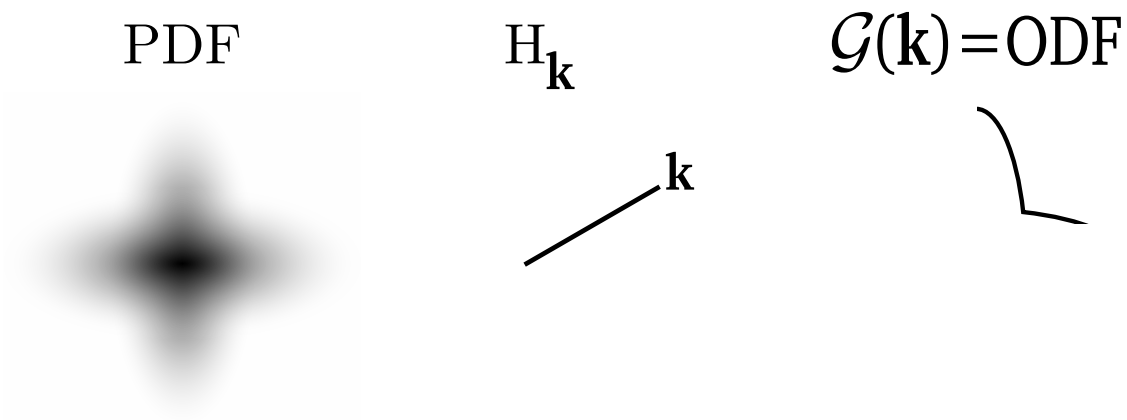

Figure: Example: ODF feature.

$$\mathcal{G}(\mathbf{k}) = \int_{p\in\mathbb{R}^3} PDF(\mathbf{p})\, H_{\mathbf{k}}(\mathbf{p}) d\mathbf{p} \tag{19}$$

Features of the PDF: projection

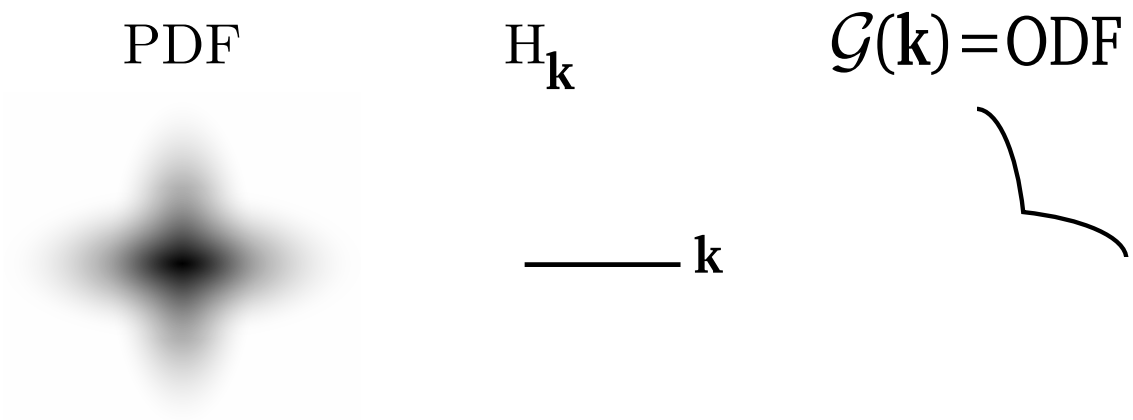

Figure: Example: ODF feature.

$$\mathcal{G}(\mathbf{k}) = \int_{p \in \mathbb{R}^3} PDF(\mathbf{p})\, H_{\mathbf{k}}(\mathbf{p}) d\mathbf{p} \tag{19}$$

Features of the PDF: projection

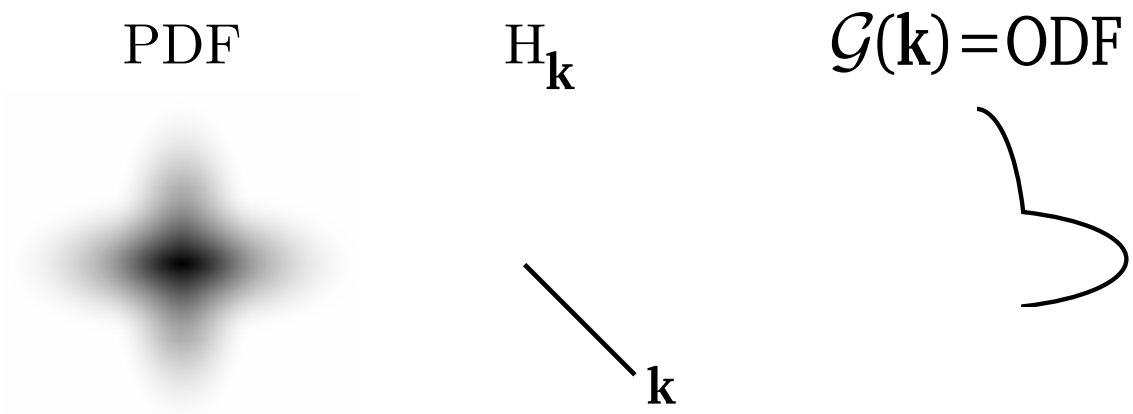

Figure: Example: ODF feature.

$$\mathcal{G}(\mathbf{k}) = \int_{p\in\mathbb{R}^3} PDF(\mathbf{p})\, H_{\mathbf{k}}(\mathbf{p}) d\mathbf{p} \tag{19}$$

Features of the PDF: projection

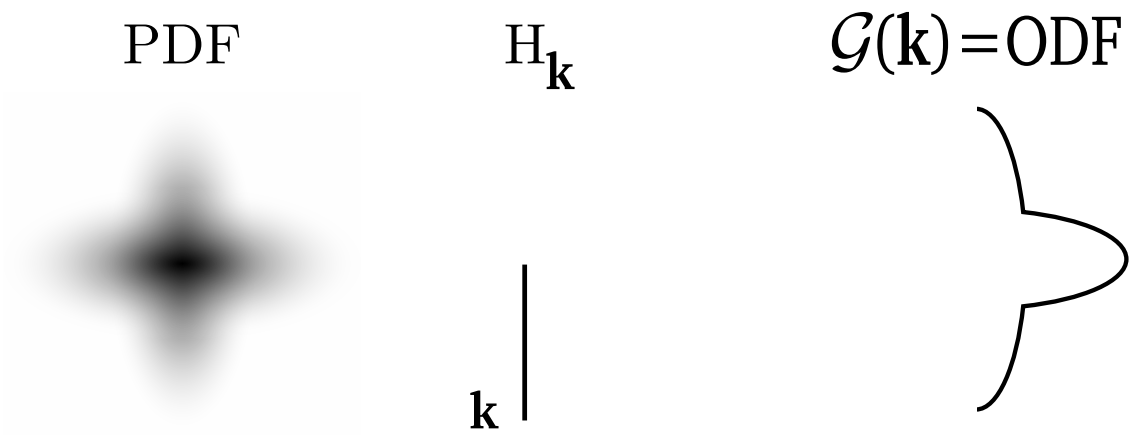

Figure: Example: ODF feature.

$$\mathcal{G}(\mathbf{k}) = \int_{p\in\mathbb{R}^3} PDF(\mathbf{p})\, H_{\mathbf{k}}(\mathbf{p}) d\mathbf{p} \tag{19}$$

Features of the PDF: projection

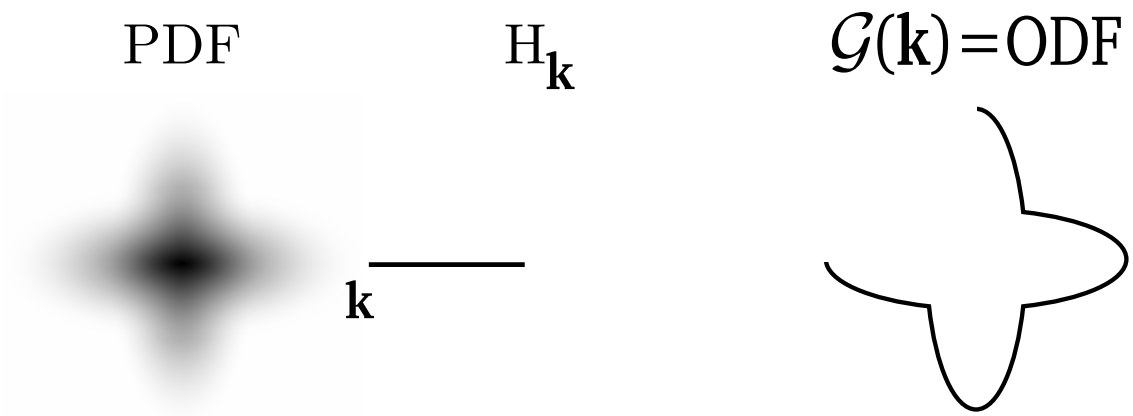

Figure: Example: ODF feature.

$$\mathcal{G}(\mathbf{k}) = \int_{p\in\mathbb{R}^3} PDF(\mathbf{p})\, H_{\mathbf{k}}(\mathbf{p}) d\mathbf{p} \tag{19}$$

Features of the PDF: projection

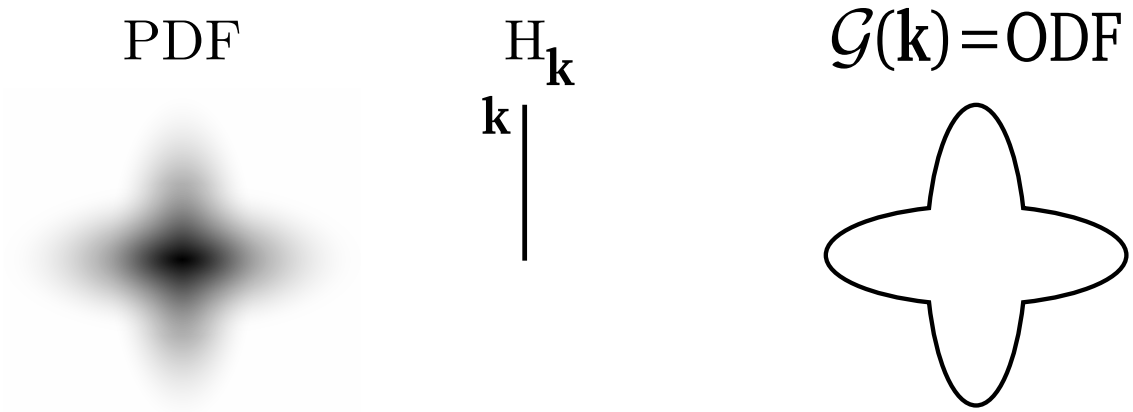

Figure: Example: ODF feature.

$$\mathcal{G}(\mathbf{k}) = \int_{p\in\mathbb{R}^3} PDF(\mathbf{p})\, H_{\mathbf{k}}(\mathbf{p}) d\mathbf{p} \tag{19}$$

Features of the PDF: projection

$$\mathcal{G}(\mathbf{k}) = \int_{p \in \mathbb{R}^3} PDF(\mathbf{p})\, H_{\mathbf{k}}(\mathbf{p}) d\mathbf{p} \tag{20}$$

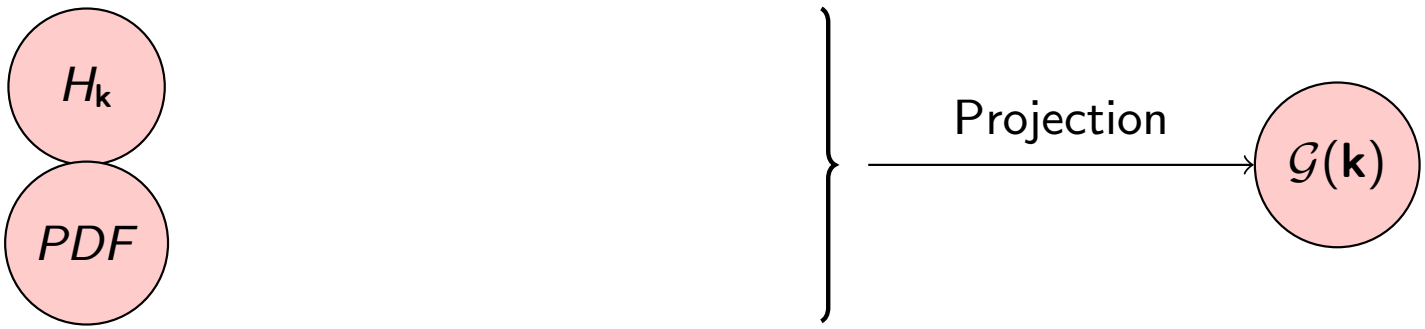

Figure: Overview of the algorithm for the *fast computation* of a PDF feature $\mathcal{G}$ at point $\mathbf{k}$

Features of the PDF: projection

$$\mathcal{G}(\mathbf{k}) = \int_{p \in \mathbb{R}^3} PDF(\mathbf{p})\, H_{\mathbf{k}}(\mathbf{p}) d\mathbf{p} \tag{20}$$

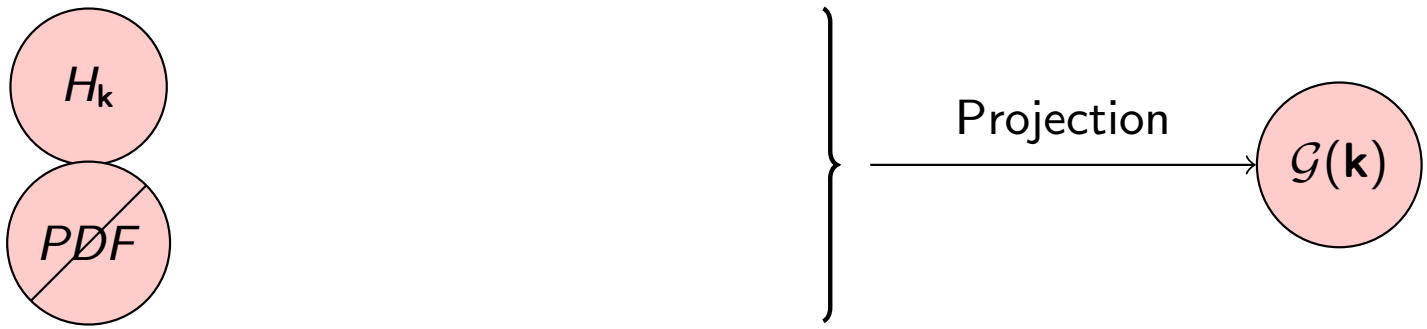

Figure: Overview of the algorithm for the *fast computation* of a PDF feature $\mathcal{G}$ at point $\mathbf{k}$

Features of the PDF: projection

$$\mathcal{G}(\mathbf{k}) = \int_{q \in \mathbb{R}^3} E(\mathbf{q})\, h_{\mathbf{k}}(\mathbf{q}) d\mathbf{q} \tag{20}$$

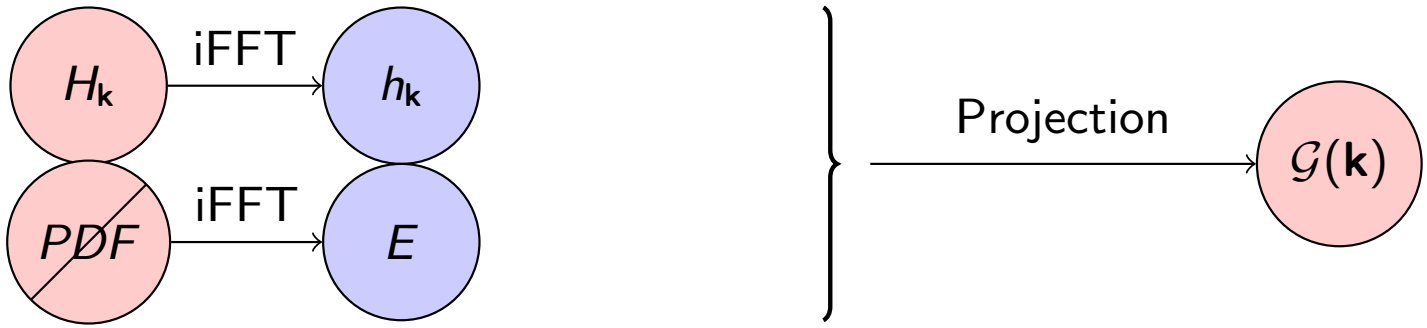

Figure: Overview of the algorithm for the *fast computation* of a PDF feature $\mathcal{G}$ at point $\mathbf{k}$

Features of the PDF: projection

$$\mathcal{G}(\mathbf{k}) = \sum_{n,l,m}^{\infty} a_{nlm}^{\mathbf{k}} b_{nlm} \tag{20}$$

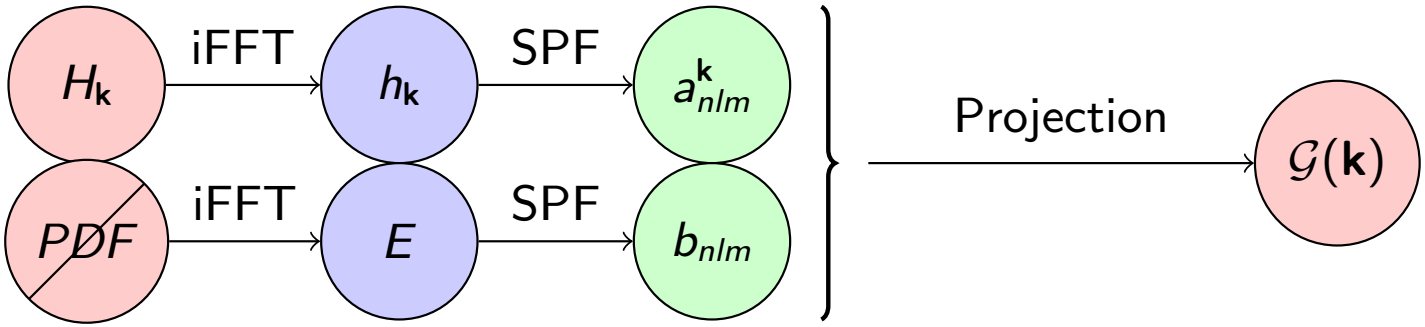

Figure: Overview of the algorithm for the *fast computation* of a PDF feature $\mathcal{G}$ at point $\mathbf{k}$

Features of the PDF

$\mathcal{G}$	ODF	FRT	ISO	P(0)
$H_{\mathbf{k}}(\mathbf{p})$	$\delta(1-\frac{\lvert\mathbf{p}\cdot\mathbf{k}\rvert}{\lvert\mathbf{p}\rvert\lvert\mathbf{k}\rvert})$	$2\pi q' J_0(2\pi q'\lvert\mathbf{p}\rvert(1-\frac{\lvert\mathbf{p}\cdot\mathbf{k}\rvert}{\lvert\mathbf{p}\rvert\lvert\mathbf{k}\rvert}))$	$\delta(\lvert\mathbf{p}-\mathbf{k}\rvert)+\delta(\lvert\mathbf{p}+\mathbf{k}\rvert)$	$\delta(\mathbf{p})$
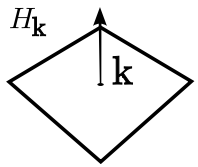		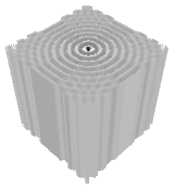		
$h_{\mathbf{k}}(\mathbf{q})$	$\delta(\frac{\mathbf{q}\cdot\mathbf{k}}{\lvert\mathbf{q}\rvert\lvert\mathbf{k}\rvert})$	$\delta(\lvert\mathbf{q}\rvert-\lvert\mathbf{q}'\rvert)\delta(\frac{\mathbf{q}\cdot\mathbf{k}}{\lvert\mathbf{q}\rvert\lvert\mathbf{k}\rvert})$	$\cos(2\pi\mathbf{q}\cdot\mathbf{k})$	$\frac{1}{Z^3}$
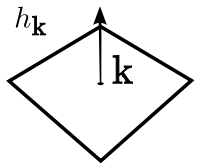	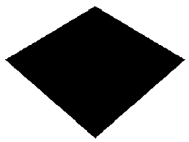	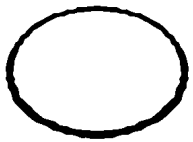	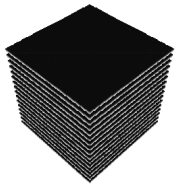	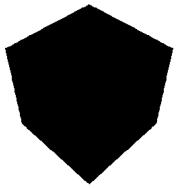

Simulation: features of the PDF (ODF)

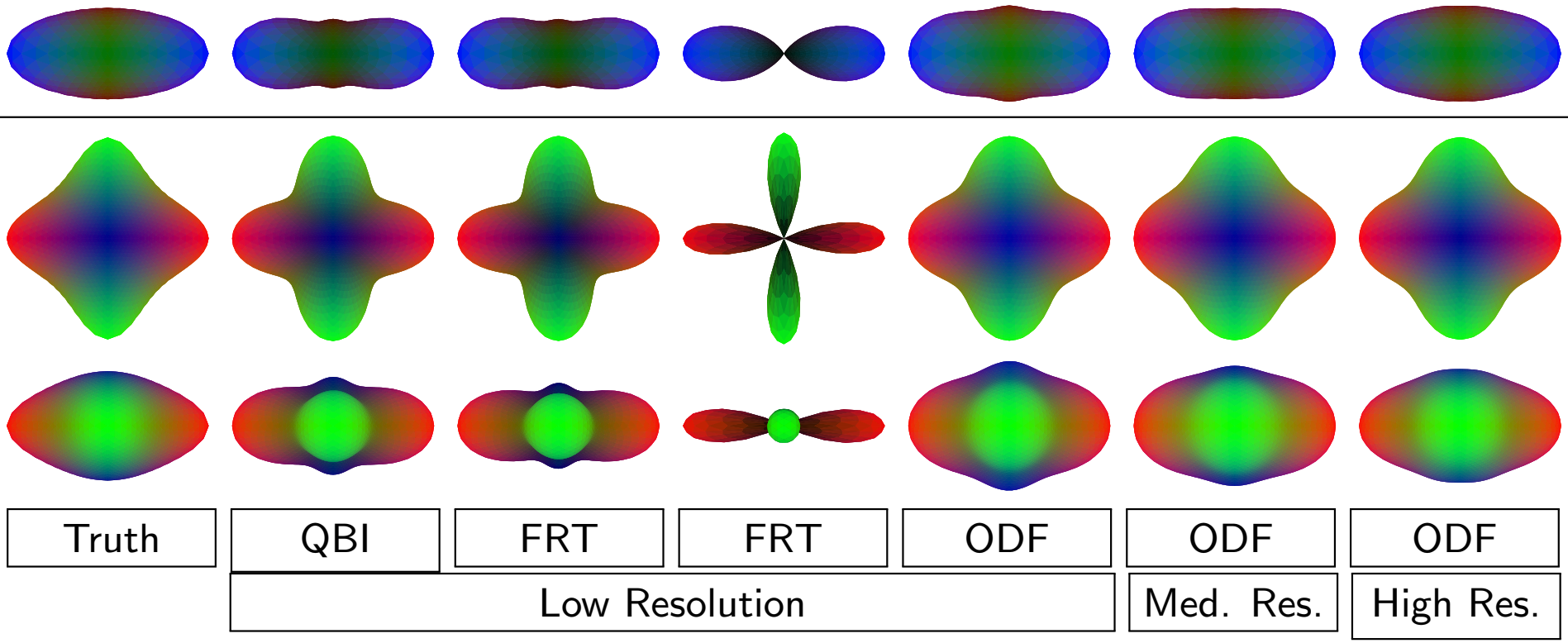

Figure: ODF comparisons.
1st line: single fiber.
2nd, 3rd lines: crossing fibers (face and profile view)

Variational framework

Robustly estimate and regularize the SPF coefficients by minimizing the functional energy:

$$\min_{A} \left\{ \int_{\Omega_E} \left[\sum_{k}^{n_s} \psi(\hat{\mathbf{E}}_k) \right] + \alpha_r \varphi(||\nabla \mathbf{A}||) d\Omega_E \right\}, \text{ with } \hat{\mathbf{E}} = \mathbf{MA} \tag{21}$$

The best fitting coefficients A are computed with a gradient descent coming from the Euler-Lagrange derivation of the energy. This leads to a set of *multi-valued* partial derivate equation.

$$\begin{cases} \mathbf{A}_{t=0} & = U_0 \\ \\ \frac{\partial \mathbf{A}_j}{\partial t} & = \sum_k^{n_s} \mathbf{M}_{k,j} \psi'(\hat{\mathbf{E}}_k) + \alpha_r \operatorname{div}\left(\frac{\varphi'(||\nabla \mathbf{A}||)}{||\nabla \mathbf{A}||} \nabla \mathbf{A} \right) \end{cases} \tag{22}$$

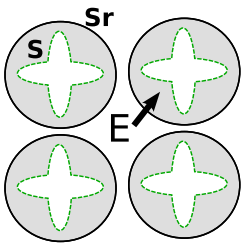

iteration 0

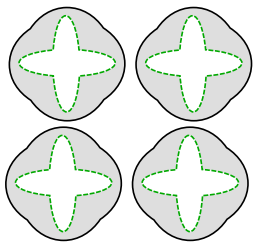

iteration 1

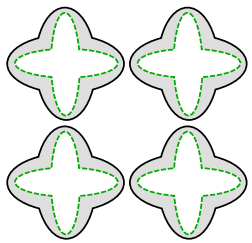

...

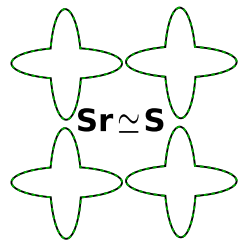

iteration n

Simulation: Rician vs Gaussian likelihood function

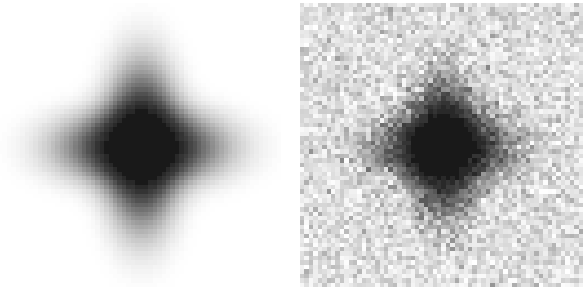

a) Truth b) Noisy

c) Gaussian d) Rician

$|Gauss - Truth|$ $|Rice - Truth|$

Simulation: validation on synthetical data (likelihood)

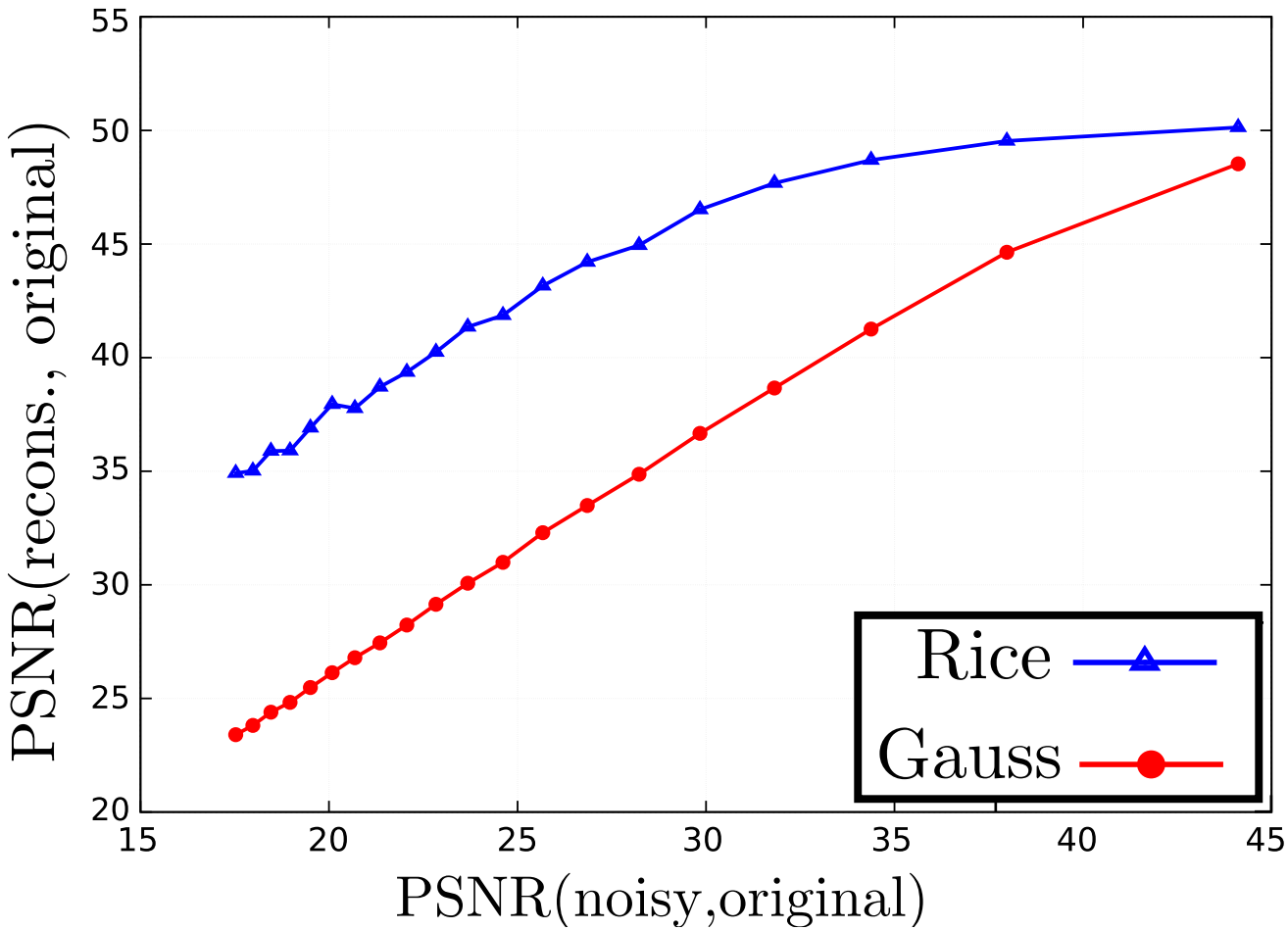

Figure: Synthetic phantom of networks of crossing fibers. Performances of likelihood functions on increasing levels of noise.

Simulation: regularization vs no regularization

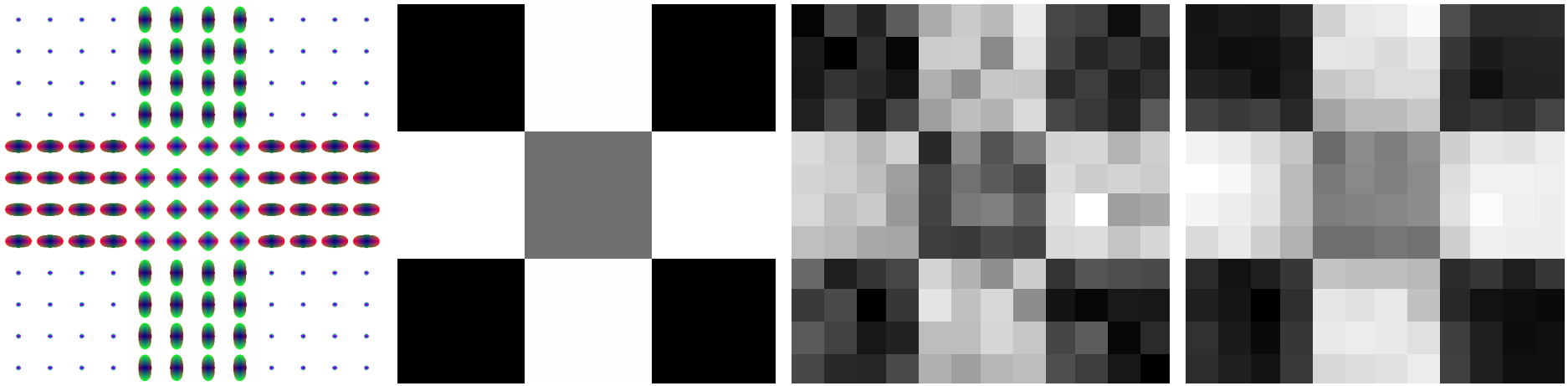

a) Phantom b) Original data PSNR: ∞ c) Without regul. PSNR: 12.8 d) With regul. PSNR: 16.6

Figure: Effects of spatial regularization on the GFA. Isotropic area are black, anisotropic area are white. PSNR(noisy,original)=18.5.

1 Context

2 DTI model : Diffusion Tensor Imaging

3 QBI model : Q-Ball Imaging

4 Measuring the PDF : DSI and Multi Q-Ball

5 Conclusions & Perspectives

Conclusions & Perspectives

Diversity of estimation algorithms

- **Before estimation :** Sensitivity to image registration.
- **During estimation :** Algorithms with few parameters miss often important signal features (rice noise model, regularity constraints).
- **After estimation :** There are at least as far as many fibertracking algorithms as estimation techniques.

Conclusions & Perspectives

Diversity of estimation algorithms

- **Before estimation :** Sensitivity to image registration.
- **During estimation :** Algorithms with few parameters miss often important signal features (rice noise model, regularity constraints).
- **After estimation :** There are at least as far as many fibertracking algorithms as estimation techniques.

Do not trust your algorithms !

Conclusions & Perspectives

Modern estimation methods are trying to reconstruct the PDF

- Estimation of the PDF or PDF characteristics from a minimal set of images, sampled in the Q-space.
- **Generic approach :** The same method is able to compute different diffusion characteristics.
- **Flexible approach :** The more number of samples you get, the more precise characteristic you compute.

Conclusions & Perspectives

Modern estimation methods are trying to reconstruct the PDF

- Estimation of the PDF or PDF characteristics from a minimal set of images, sampled in the Q-space.
- **Generic approach :** The same method is able to compute different diffusion characteristics.
- **Flexible approach :** The more number of samples you get, the more precise characteristic you compute.

Thank you for your attention.